

Establishment of Total Liquid Ventilation System with Oxygen Fine  
Bubble Dispersion and Application to Acute Lung Injury Model Rats  
酸素ファインバブル分散液を用いた完全液体換気システムの  
構築および急性肺障害モデルラットへの応用

February 2021

**Kenta KAKIUCHI**

垣内 健太

Establishment of Total Liquid Ventilation System with Oxygen Fine  
Bubble Dispersion and Application to Acute Lung Injury Model Rats  
酸素ファインバブル分散液を用いた完全液体換気システムの  
構築および急性肺障害モデルラットへの応用

February 2021

Waseda University  
Graduate School of Advanced Science and Engineering  
Department of Life Science and Medical Bioscience  
Research on Biomolecular Assembly

**Kenta KAKIUCHI**

垣内 健太

Principal Referee: Prof. Dr. Shinji TAKEOKA  
Referees: Prof. Dr. Nobuhito GODA  
Prof. Dr. Haruko TAKEYAMA

## *Preface*

More than five decades ago, it was reported that mice and cats could spontaneously breathe in atmospheric pressure perfluorocarbon liquids (PFCs), which are artificial organic compounds. Since then, research on “liquid ventilation (LV)” with PFCs were widely conducted, and techniques were developed to perform accurate respiratory management. Valuable outcomes of safe and therapeutic effects were confirmed in several animal experiments. Partial LV (PLV), which is one of the liquid ventilation techniques, has proceeded to clinical trials in humans. Positive effects were obtained in newborns, however, the clinical trials in adult humans were not fruitful. Moreover, PFCs are expensive for extensive use both in animal research and in clinical fields. Thus, the number of studies on PLV has been decreasing yearly. Although total LV (TLV), which is another LV technique, is expected to be a more effective treatment method than PLV, issues with PFCs and the necessity of technical devices hinder the advancement of TLV research.

TLV has not been studied thoroughly enough, although it has the potential to be a causative treatment as total alveolar lavage (TAL) for several lung diseases because 1) TLV can re-expand collapsed alveolar and 2) TLV can directly eliminate causative substances. Oxygen fine bubble dispersion (FB dispersion) was used as an alternative for PFCs in this research. The FB dispersion is supersaturated water which can be prepared in large quantities in a short amount of time. A novel oxygen measurement method for FB dispersions was established and the property of FBs as oxygen carrier was examined in this study. Although it was a great challenge to establish a TLV system using liquids other than PFCs, a TLV system with FB dispersion was developed and its promising possibility was demonstrated. This study aims to show the efficacy of the 5-min TAL with the TLV system for acute lung injury model rats. It is expected that the TLV system efficiently removes the causative substances and can alleviate lung inflammation.

This thesis consists of five chapters. Chapter 1 reviews the background of the research. Chapter 2 describes the development of the method for oxygen content measurement and examination of the property of FB as oxygen carrier. Chapter 3 describes the improvement and evaluation of the TLV system. Chapter 4, which is the core section, describes the efficacy of the TAL with the TLV system as a preventive treatment for acute lung injury. Chapter 5 concludes this thesis and proposes prospects.

Kenta Kakiuchi

## *Contents*

### *Preface*

### *Chapter 1: Introduction*

#### **1.1. Purpose and strategy of this study**

#### **1.2. Background of this study.....4**

1.2.1. Lung lavage for intratracheal therapy.....4

1.2.2. History of liquid ventilation.....5

1.2.3. Partial liquid ventilation vs. total liquid ventilation.....9

1.2.4. Physical properties of fine bubbles.....11

1.2.5. Stability of fine bubbles.....14

1.2.6. Applications of fine bubbles.....17

#### **References.....21**

### *Chapter 2: Studies on fine bubble dispersion as oxygen carrier using a novel oxygen measurement method*

#### **2.1. Background of this chapter.....32**

2.1.1. Measurement method for oxygen content in water.....32

2.1.2. Measurement method for oxygen content in fine bubble dispersion.....34

2.1.3. Fine bubble dispersion as an oxygen carrier.....35

#### **2.2. Development of novel oxygen measurement method for oxygen fine bubble dispersion.....37**

2.2.1. Purpose.....37

2.2.2. Materials and experimental procedures.....37

2.2.3. Results and discussion.....41

<b>2.3. Evaluation of properties of oxygen fine bubbles as an oxygen carrier.....</b>	<b>46</b>
2.3.1. Purpose.....	46
2.3.2. Materials and experimental procedures.....	46
2.3.3. Results and discussion.....	50
<b>2.4. Conclusions of this chapter.....</b>	<b>61</b>
<b>References.....</b>	<b>62</b>
<i>Chapter 3: Evaluation and improvement of total liquid ventilation system with oxygen fine bubble dispersion</i>	
<b>3.1. Background of this chapter.....</b>	<b>66</b>
3.1.1. Total liquid ventilation system with perfluorocarbons.....	66
3.1.2. Total liquid ventilation system with oxygen fine bubble dispersion.....	67
<b>3.2. Short-time total liquid ventilation test with oxygen fine bubble dispersion and gas liposome dispersion.....</b>	<b>69</b>
3.2.1. Purpose.....	69
3.2.2. Materials and experimental procedures.....	69
3.2.3. Results and discussion.....	74
<b>3.3. Improvement of the total liquid ventilation system with oxygen fine bubble dispersion.....</b>	<b>85</b>
3.3.1. Purpose.....	85
3.3.2. Materials and experimental procedures.....	85
3.3.3. Results and discussion.....	88
<b>3.4. Conclusions of this chapter.....</b>	<b>91</b>
<b>References.....</b>	<b>92</b>

*Chapter 4: Efficacy of total alveolar lavage with a total liquid ventilation system using fine bubble dispersion on acute lung injury models*

<b>4.1. Background of this chapter</b> .....	<b>96</b>
4.1.1. Acute respiratory distress syndrome.....	96
4.1.2. Acute respiratory distress syndrome model.....	97
4.1.3. Treatment for acute respiratory distress syndrome.....	98
<b>4.2. Efficacy of total alveolar lavage with a total liquid ventilation system using oxygen fine bubble dispersion in a severe lung injury model</b> .....	<b>100</b>
4.2.1. Purpose.....	100
4.2.2. Materials and experimental procedures.....	100
4.2.3. Results and discussion.....	106
<b>4.3. Efficacy of total alveolar lavage with a total liquid ventilation system using oxygen fine bubble dispersion in a lethal lung injury model</b> .....	<b>115</b>
4.3.1. Purpose.....	115
4.3.2. Materials and experimental procedures.....	115
4.3.3. Results and discussion.....	117
<b>4.4. Conclusions of this chapter</b> .....	<b>124</b>
<b>References</b> .....	<b>125</b>

*Chapter 5: Conclusions and Prospects*

<b>5.1. Conclusions</b> .....	<b>130</b>
<b>5.2. Prospects</b> .....	<b>132</b>
<b>References</b> .....	<b>137</b>

*Academic achievement*

*Acknowledgement*

## **Chapter 1: Introduction**

### **1.1. Purpose and strategy of this study**

### **1.2. Background of this study**

1.2.1. Lung lavage for intratracheal therapy

1.2.2. History of liquid ventilation

1.2.3. Partial liquid ventilation vs. total liquid ventilation

1.2.4. Physical properties of fine bubbles

1.2.5. Stability of fine bubbles

1.2.6. Applications of fine bubbles

### **References**

### **1.1. Purpose and strategy of this study**

Liquid ventilation (LV) is a type of artificial respiration performed in lungs filled with liquid. By using a liquid, some advantages can be obtained, such as 1) the lungs can be expanded with lower pressure, 2) collapsed alveoli can be re-expanded, 3) debris and exudates can be removed by washing, and 4) oxygenation of blood can be improved due to an increased functional area. These features are suitable for lung disease treatments<sup>1,2</sup>. LV contains two techniques: partial LV (PLV) and total LV (TLV). Most research on LV adopts PLV, which performs mechanical gas ventilation (MGV) wherein the lungs are filled with liquid. This is because PLV requires a conventional gas ventilator and a smaller dosage of expensive liquid materials<sup>3</sup>. However, clinical studies on PLV in adult humans did not show any beneficial outcomes, even though good results were obtained in newborns and children<sup>4</sup>.

Perfluorocarbon liquids (PFCs), which are artificial organic compounds, have been used as the liquid material in LV research for more than 50 years<sup>5</sup>. PFCs have unique characteristics: 1) high oxygen dissolving capacity (40–50 vol% at 37°C)<sup>6</sup> and 2) low surface tension (14–18 dyne/cm)<sup>7</sup>. This is adequate for LV, and no other material has been used since PFCs were developed. However, some of them have been discontinued due to environmental issues<sup>8,9</sup>. Furthermore, their cost has increased.

TLV has the potential to improve certain lung diseases and is considered superior to PLV. However, some issues, such as the necessity of an exclusive system, requirement of a copious amount of PFCs, and failure in PLV clinical trials, hindered further development of TLV research<sup>10</sup>. Thus, there was no growth similar to PLV development in TLV research, even though the usefulness of TLV has been confirmed<sup>11–13</sup>.

Following this background, I attempted to use saline containing oxygen fine bubbles (FB dispersion) as an alternative to PFCs and constructed a novel TLV system,

with FB dispersion<sup>14</sup>. FB dispersion is a simple, inexpensive, and safe oxygen carrier; thus, FB dispersion may be an excellent candidate for dissemination to clinical fields. However, some physical properties of FB remain unclear, especially that of FB as an oxygen carrier. In a previous study, I reported the feasibility of the TLV system with FB dispersion by showing that anesthetized rats survived over 40 min during TLV<sup>14</sup>. However, I have yet to demonstrate its efficacy to treat lung disease.

I hypothesized that short-time total alveolar lavage (TAL) with the TLV system was effective for the direct removal of pathogens and other aspirated substances from the lungs. Then, I examined TAL efficacy on a lipopolysaccharide (LPS)-induced lung injury model. Whole lung lavage (WLL), which washes the lungs one by one with saline, has been adopted as a standard treatment for a specific lung disease (pulmonary alveolar proteinosis)<sup>15</sup>. The TLV system can wash both lungs simultaneously; thus, the treatment time and easiness of operation are superior to WLL. If I can develop a TLV system with a saline-based liquid material, it is expected to enormously contribute not only to LV research but also to lung lavage research.

The purpose of this study is to show the efficacy of short-time TAL with the TLV system, using the FB dispersion in an acute lung injury model in rats as a preventive treatment. For that purpose, firstly, I developed a novel method for oxygen content measurement and examined the FB dispersion property as an oxygen carrier. Secondly, I evaluated and improved the TLV system, which I established previously<sup>14</sup>. Finally, I examined the efficacy of short-time TAL for the lung injury model.

## **1.2. Background of this study**

### **1.2.1. Lung lavage for intratracheal therapy**

#### ***Concept of lung lavage (pulmonary irrigation)***

After World War I, research on lung lavage for poisonous gas inhalation was conducted by introducing saline into the lungs. The idea of introducing liquid into the lungs to wash (lung lavage) was proposed by Winternitz and Smith in 1919<sup>16</sup>. They showed that pre-installed India ink, starch paste, and non-pathogenic bacteria could be removed by lung lavage in dogs. For bacteria, 90% was washed out of the lungs<sup>16</sup>. They also confirmed that the remaining liquid inside the lungs after lavage was absorbed into the body within a few days and the dog could return to full health within 10 days<sup>17</sup>. However, the progress of viral pneumonia was not prevented completely, although parts of the virus were removed from the lungs. The authors suggested a necessity of the combination of drugs for the disease<sup>17</sup>.

#### ***Lung lavage with a combination of gas ventilation***

In 1928, Vicente reported a technique for lung lavage in humans, which was to lavage the lungs one by one, using a catheter<sup>18</sup>. The patient simultaneously breathes atmospheric air into the other lung. He aggressively evaluated the efficacy of lung lavage for various lung diseases such as bronchiectasis, chronic bronchitis, asthma, and lung abscesses<sup>18</sup>. Based on this technique, Ramirez-R and Kylstra improved the lung lavage technique by introducing oxygen bags and transtracheal catheters. As a result, two significant advantages were obtained: 1) improvement of oxygen supply and 2) expansion of the washing area. This technique referred as whole lung lavage (WLL)<sup>18</sup>. Subsequently, Ramirez-R showed the efficacy of WLL on pulmonary alveolar proteinosis; that proteins (or protein-like substances) accumulate in the alveoli. It was then accepted as a therapy and is still applied<sup>19</sup>.

### ***Application of lung lavage (1920s–1970s)***

The feasibility of WLL was examined on lung diseases until the establishment of the LV technique. Although some reports were preliminary case studies, WLL was applied for some diseases, such as asthma, bronchitis, cystic fibrosis, chronic obstructive lung disease, bronchiectasis, and Goodpasture's syndrome. Positive effects could be obtained in several disorders; however, ventilatory impairment and fever occurred in patients with severe symptoms<sup>18,20–22</sup>. These reports summarized that WLL was suitable for symptoms induced by accumulation of secretions or alveoli blockage, but not for symptoms with structural failure (e.g., hypertrophy, bronchospasm, edema, and diminished elastic recoil)<sup>18,20</sup>.

### **1.2.2. History of liquid ventilation**

#### ***Liquid ventilation with saline***

In 1962, the original experiment of LV was performed by Kylstra *et al.*, who had engaged in lung lavage research for many years. They showed that the rats could breathe for 18 h in 20°C infusion solution with 0.1% tris buffer at 6 atm<sup>23</sup>. It suggested that gas exchange was possible in the buffer solution as long as it contained considerable oxygen. Subsequently, they conducted an LV experiment with dogs in a US Navy recompression chamber, where it was large enough to accommodate an experimental animal and two investigators. This research showed that 6 out of 16 dogs survived after LV without sequela and pulmonary damage<sup>24</sup>. However, these techniques had two problems that disrupted further evaluation. Firstly, it could not efficiently remove carbon dioxide (CO<sub>2</sub>). Secondly, it was required to be performed in a special environment with high-pressure (over 5–6 atm)<sup>23,24</sup>.

***Liquid ventilation with perfluorocarbon liquids***

In 1966, Clark and Gollan reported that mice were able to breathe in PFCs and survived for many hours in immersion. This phenomenon was attributable to PFCs' capacity to dissolve copious amounts of oxygen. They also tried the LV experiment with silicone oil, which can also dissolve substantial amounts of oxygen. However, they gave up due to its viscosity, no-volatility, and toxicity<sup>5</sup>. In 1974, Shaffer and Moskowitz developed a demand-regulated LV system and showed that it supplied adequate amount of oxygen and improved CO<sub>2</sub> elimination. They also confirmed that mechanical lung damage and pulmonary edema could be avoided by keeping the peak esophageal pressure as low as 10 mmHg (13.6 cmH<sub>2</sub>O)<sup>25</sup>. Schwieler *et al.* showed the utility of PFCs in oxygenation and surfactant-like properties on a lung surfactant deficient model in rabbits<sup>26</sup>. In 1989, the first clinical trial of LV was conducted in three preterm neonates who had severe respiratory disorders. Arterial oxygen partial pressure (PaO<sub>2</sub>) and arterial carbon dioxide partial pressure (PaCO<sub>2</sub>) were improved in two patients during LV treatment. Furthermore, lung compliance was elevated in all patients. However, after a few hours, the conditions worsened, and all babies died within 19 h<sup>27,28</sup>. In 1991, Fuhrman *et al.* constructed a hybrid technique with MGJV and LV, which they named "partial liquid ventilation (PLV)" or "perfluorocarbon associated gas exchange (PAGE)"<sup>29</sup>. Since PLV was established, the previous technique which uses only PFCs, came to be called "total/tidal liquid ventilation (TLV)." Research on PLV was actively performed in the 1990s<sup>30-33</sup>, and clinical trials on newborns and children were conducted in the late 1990s<sup>2,34,35</sup>. These studies showed that PLV improved gas exchange and lung compliance in both animal and human babies with respiratory distress syndrome. Moreover, there were no adverse events related to the technique<sup>2</sup>. However, clinical studies in adult humans did not show beneficial effects. There was no difference in ventilator-free days,

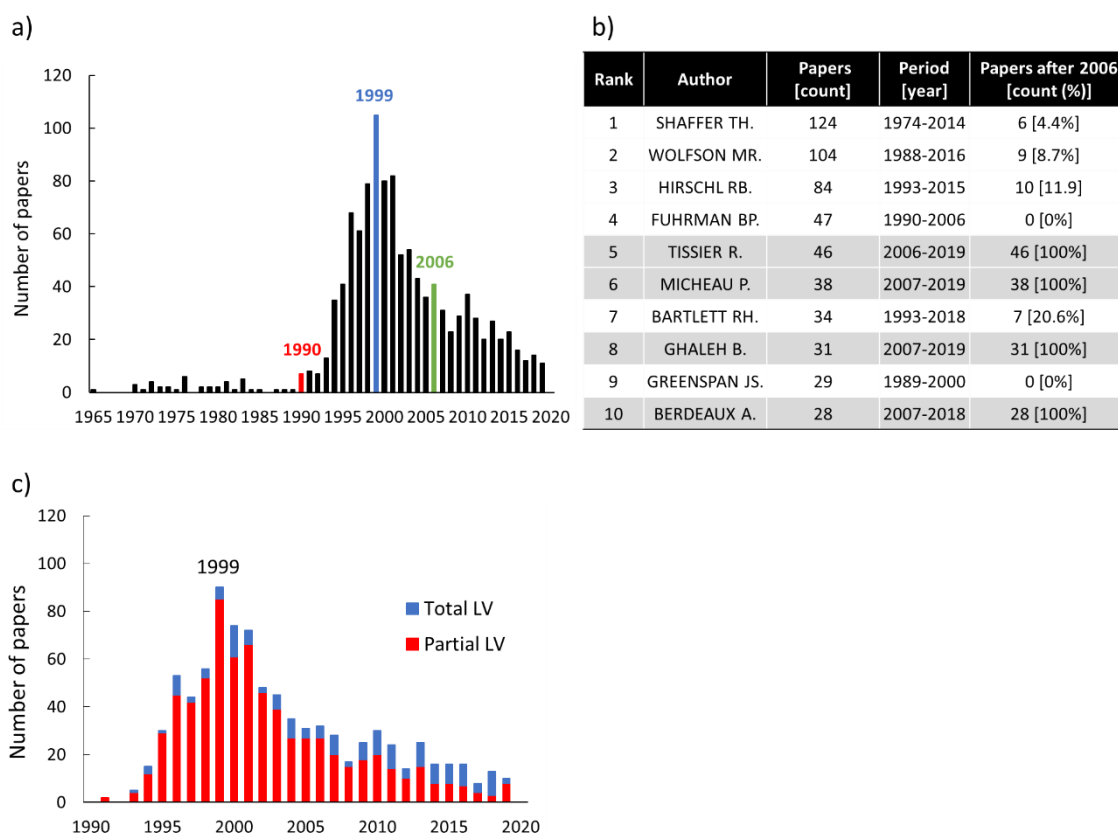
mortality, and oxygenation between the treatment groups of PLV and MGV. Furthermore, adverse events, such as pneumothoraxes, hypoxia, respiratory acidosis, and bradycardia, were observed more frequently in the PLV treatment group than those in the MGV treatment group<sup>4,36</sup>. They explained that there was an issue with the MGV settings during the PLV treatment. In fact, the respiratory management conditions used in that study may induce barotrauma, and it deviates from the current guidelines of respiratory management for patients with acute respiratory distress syndrome (ARDS).

Table 1.1 History of liquid ventilation

<b>Year</b>	<b>Achievement</b>
1919	Winternitz <i>et al.</i> washed the lungs with saline for the treatment of poisonous gas inhalation <sup>16</sup> .
1929	Von Neergaard showed the lung compliance of a saline-filled lung is higher than an air-filled lung <sup>37</sup> .
1962	Kylstra showed mice spontaneously breathed in oxygenated saline under hyperbaric conditions <sup>23</sup> .
1963	Ramirez-R <i>et al.</i> proposed lung irrigation as a treatment for pulmonary alveolar proteinosis <sup>38</sup> .
1974	Shaffer <i>et al.</i> developed a demand-controlled (total) liquid ventilator <sup>25</sup> .
1989	Greenspan <i>et al.</i> performed total liquid ventilation for three newborn babies and showed the feasibility of the technique <sup>39</sup> .
1991	Fuhrman <i>et al.</i> proposed partial liquid ventilation <sup>29</sup> .
2006	Kacmarek <i>et al.</i> reported a large clinical trial on PLV; however, it did not show expected results <sup>4</sup> .

***Decline in the partial liquid ventilation research population***

The decline in LV studies after the failure of PLV clinical trials was reflected in the number of academic papers. I investigated the number of reports using Web of Science, which is one of the largest databases. Fig. 1.1a shows the change in the number of papers, which included at least one of the following words as a topic: “liquid ventilation,” “liquid breathing,” “fluorocarbon ventilation,” or “perfluorocarbon associated gas exchange.” LV studies sharply increased after the establishment of PLV and peaked in 1999 (Fig. 1.1a). The reason why the studies of LV declined after 1999 maybe because the research stage had advanced to human clinical trials from earlier animal studies. Furthermore, some PFCs (less than six carbon chains) were enacted as greenhouse gases under the Kyoto Protocol in 1997. The emission of them was regulated in Europe, Canada, and Japan<sup>40</sup>. FC-77, which was widely used for LV studies, was discontinued in Japan. The ranking of the authors is summarized in Fig. 1.1b according to the number of reports. The authors can be divided into two groups by their active period. A division existed in 2006 when a large clinical trial of PLV was reported. The four authors, shown in gray color (Fig. 1.1b), reported their papers after 2006. The contents are mainly TLV for whole-body cooling as a cardioprotective strategy, not a treatment for acute lung injury<sup>41,42</sup>. This means that the purpose of LV studies changed from PLV as an acute lung injury treatment to TLV for whole-body cooling. While the number of TLV study populations is small, its percentage against all LV studies has increased (Fig. 1.1c), and its research has been continued persistent.



**Fig. 1.1. The transition of the number of studies on liquid ventilation (LV).** a) The transition of papers on LV research. b) Top 10 ranking of authors in LV research. c) The transition of papers on partial LV and total LV research. (survey date: 2020/01/14)

### 1.2.3. Partial liquid ventilation vs. total liquid ventilation

#### *Partial liquid ventilation*<sup>1-3</sup>

PLV is the respiratory method that uses both liquid and a conventional mechanical gas ventilator (CMV) (Fig. 1.2). Firstly, PFCs are introduced into the lungs, and PFCs expand the collapsed alveoli. Secondly, MGV is performed against lungs filled with PFCs. The respiratory conditions were managed by CMV. Finally, PFCs are removed from the lungs, and PLV treatment is completed. The advantages of PLV (against TLV) are: 1) no special equipment is required, 2) usage of expensive PFCs can be minimized (10–20 mL/kg<sup>4</sup>), 3) influence on the cardiovascular system is stable, and 4) several respiratory

conditions can be applied (e.g., high-frequency oscillatory ventilation [HFOV]). As shown in the previous section, several examinations have explored not only animals but also humans.

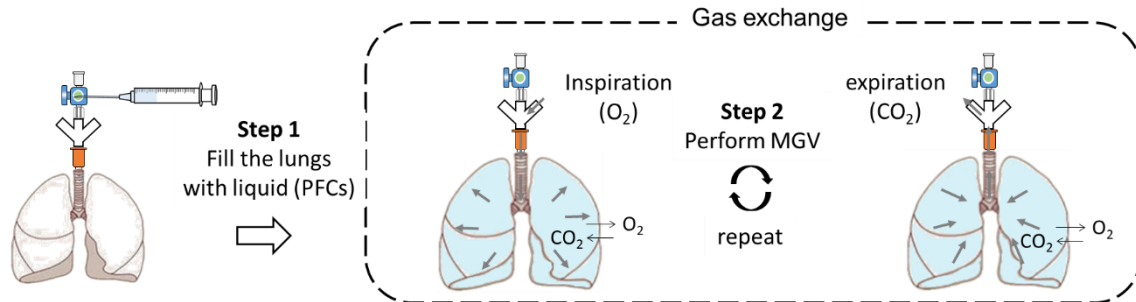


**Fig. 1.2. Schematic illustration of partial liquid ventilation**

**Total liquid ventilation<sup>3,43</sup>**

TLV is a respiratory method using only tidal liquid (Fig. 1.3). Gas exchange is performed by continuous PFCs replacement. TLV can expand the lungs with lower pressure due to the increased lung compliance and remove alveolar exudates and debris efficiently. Although TLV has several advantages on therapeutic effects over PLV, TLV requires a large amount of PFCs and an exclusive TLV system. These issues hinder further development; thus, research was limited compared to that of PLV. However, the efficacy of TLV has been confirmed in some lung injury models, such as the lung surfactant deficient model, meconium aspiration injury model, and ARDS model<sup>11,44-46</sup>.

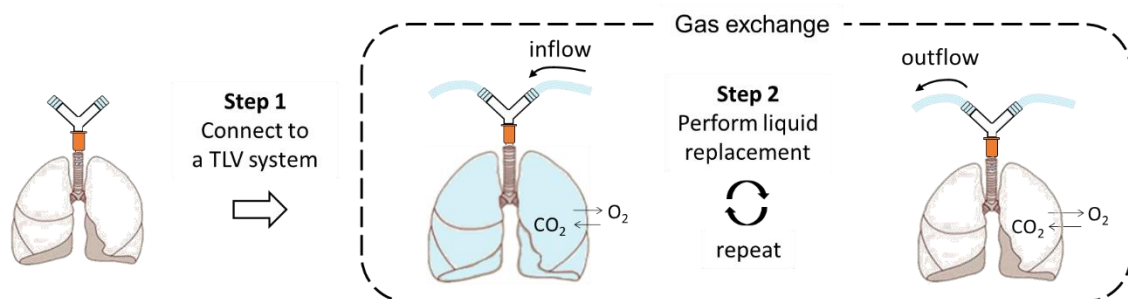


**Fig. 1.3. Schematic illustration of total liquid ventilation**

### ***Partial liquid ventilation vs. total liquid ventilation***

In 1997, Foust *et al.* examined the efficacy of PLV and TLV on newborn lambs with meconium aspiratory injury. They showed that both PLV and TLV were effective in terms of improving hemodynamics, pulmonary function, and arterial blood gas parameters compared to exogenous surfactant therapy and non-treatment groups. Regarding pulmonary compliance, only the TLV group improved. It was explained that the TLV process eliminated the air-liquid interface and kept the alveoli in an expanded state<sup>45</sup>.

In 2012 and 2013, Yao-bin *et al.* published two papers that separately showed the effect of TLV and PLV on the same animal model. They used immature piglets with oleic acid-induced lung injury and evaluated an LV treatment group compared to an MGV treatment group. Their results showed that the rats in the PLV group did not recover from a severe lung injury, even though there were significant differences in cardiopulmonary variables, blood gas parameters, and tumor necrosis factor (TNF- $\alpha$ ) levels between the PLV and MGV groups<sup>47</sup>. Meanwhile, TLV improved not only lung function and gas ventilation, but also biochemical and histologic factors compared to the MGV group<sup>48</sup>. These studies suggest that TLV is more curative than PLV in the ARDS model.

#### **1.2.4. Physical properties of fine bubbles<sup>49</sup>**

“Bubble” means a ball of gas in a liquid or solid, and there was no critical definition of sizes until the 1990s. However, it is necessary to classify in detail by size because tiny bubbles have extraordinary characteristics. The tiny bubbles were described as “microbubbles (MB)” and “nanobubbles (NB),” and were later internationally standardized as “fine bubbles (FB)” by the Union of Fine Bubble Science and Engineers in 2013. Furthermore, NB changed its name to “ultrafine bubbles (UFB),” and size definitions of MB and UFB were set as 1–100  $\mu\text{m}$  and less than 1  $\mu\text{m}$ , respectively. MBs

remain stable for a few minutes in water and gradually rise to the surface while shrinking in size. Meanwhile, UFBs hardly rise and remain in the liquid for a long time (Fig. 1.4). It was reported that UFBs exist in saturated water for over one month<sup>50,51</sup>.

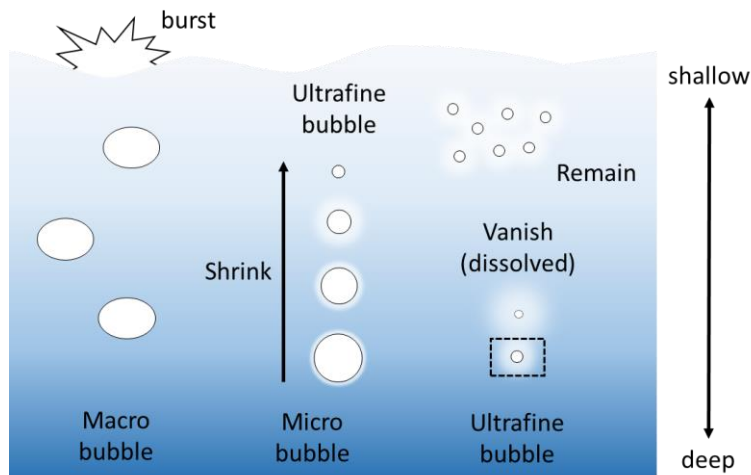


**Fig. 1.4. Behavior of macro bubbles and fine bubbles in water**

### *Floating speed*

FBs remain stable in water for a long time because they rise very slowly, whereas macro bubbles rise rapidly with an increment of size and burst at the liquid surface (Fig. 1.4). This property is explained with Stokes' law (Formula 1.1) and experimentally confirmed by Takahashi<sup>52</sup>.

$$V_{ST} = \frac{g(P_s - P_l)d^2}{18\mu} \quad (1.1)$$

where  $V_{ST}$  is the sedimentation velocity [cm/s],  $g$  is the gravitational acceleration [cm/s<sup>2</sup>],  $P_s$  is the density of the particles [g/cm<sup>3</sup>],  $P_l$  is the density of the liquid,  $d$  is the diameter of the particles [cm],  $\mu$  is the coefficient of viscosity [g/cm/s]. Although Stokes' law is the formula to calculate the sedimentation velocity, the value becomes a floating velocity when  $P_s > P_l$ . From this formula, the rising speed of 50  $\mu\text{m}$ , 10  $\mu\text{m}$ , and 1  $\mu\text{m}$  MB are estimated as 1.36 mm/s, 54.5  $\mu\text{m/s}$ , and 0.54  $\mu\text{m/s}$ , respectively<sup>53</sup>. However, Takahashi examined the above relationship for the range of 10–55  $\mu\text{m}$ . According to a Japanese

Industry Standard (JIS; Z8820-1:2002), the upper and lower size limits of the formula are determined by the Reynolds coefficient ( $Re < 0.25$ ) and the ratio of Brownian and floating movement, respectively. Assuming the internal gas in MBs is oxygen, the application range of the size is calculated as 1.37–77  $\mu\text{m}$ . Parkinson *et al.* studied the terminal rise velocity of 10–100  $\mu\text{m}$  bubbles in water. They showed that the actual velocity was higher than the predicted velocity by Stokes' law, especially for bubbles larger than 50  $\mu\text{m}$ . Moreover, they concluded that Hadamard-Rybczynski (H-R) equation (Formula 1.2.) was better to predict the floating velocity of MBs than Stokes' law<sup>54</sup>.

$$V_{H-R} = \frac{2\Delta\rho gr^2}{3\mu} \frac{\mu - \mu'}{2\mu + 3\mu'} \approx \frac{3}{2} V_{ST} \quad (\mu' \ll \mu) \quad (1.2)$$

where  $V$  is the terminal rise velocity [cm/s],  $\Delta\rho$  is density difference between the bubble and ambient fluid [g/cm],  $g$  is the gravitational acceleration [cm/s<sup>2</sup>],  $r$  is the radius of bubble [cm],  $\mu$  is the viscosity of the ambient fluid [g/cm/s],  $\mu'$  is the viscosity of the bubble [g/cm/d]. They also said that additives in water caused reduction of the floating velocity, and the value got close to the value predicted by Stokes' law<sup>54</sup>. Thus, cleanliness is important to predict the floating velocity of MBs.

### **Gas solubility**

According to Henry's law, gas solubility depends on the pressure difference between the two phases. Therefore, the internal gas pressure and surrounding hydraulic pressure are important to estimate the gas solubility in water containing FBs. The pressure difference is determined by the Young-Laplace equation (Formula 1.3.)<sup>55</sup>.

$$\Delta P = P - P_o = \frac{2\sigma}{r} \quad (1.3.)$$

where  $P$  is the internal gas pressure [mN/m<sup>2</sup>],  $P_o$  is the surrounded hydraulic pressure [mN/m<sup>2</sup>],  $\sigma$  is the surface tension [mN/m], and  $r$  is the radius of a bubble [m]. Formula 1.2. shows that  $\Delta P$  increases as the radius decreases. Assuming the surface tension is 72.8 mN/m, and the diameters of the MB are 50  $\mu\text{m}$ , 10  $\mu\text{m}$ , and 1  $\mu\text{m}$ ,  $P$  is calculated as

1013.06 hPa ( $\approx 1.05$  atm), 1304 hPa ( $\approx 1.29$  atm), and 3925 hPa ( $\approx 3.87$  atm), respectively. Takahashi *et al.* proposed the hypothesis that “dissolved gas condensed region” was formed around FB due to the high pressure<sup>55</sup>. I will propose a different theory about the oxygen state in FB dispersion in Chapter 2.

### ***Negative charge surfaces***

FBs have negative charge in water. The negative charge is due to hydroxide ions ( $\text{OH}^-$ ), derived from the slight ionization of water molecules. In general, there are three types of OH orientation in water molecules; 1) symmetrical stretch, tetrahedrally hydrogen-bonded water molecules (ice-like bond); 2) asymmetrically stretch, hydrogen-bonded water molecules (liquid-like bond); and 3) dangling  $\text{OH}^-$  stretch: free from hydrogen-bonding (gas-like bond). It was reported that dangling  $\text{OH}^-$  was arranged at the gas-water interface and created negative charges on the liquid surface<sup>56</sup>. Ohgaki *et al.* reported that the surface of NBs have similar orientation of water molecules to the air-water surface<sup>57</sup>. Therefore, it is considered that the negative charges on the FBs' surface occur for the same reason as the gas-liquid interface. Indeed, the domination of  $\text{OH}^-$  on the FBs' surface was confirmed by some experiments<sup>51,52,58</sup>. The negative charge affects the stability of the FBs by preventing their aggregation. Furthermore, it was found that the charges could be controlled by surfactants, inner gas type, and salt concentrations<sup>49,58</sup>.

### **1.2.5. Stability of fine bubbles**

#### ***Mechanism of stability of fine bubbles***

FBs are said to be stable, but it is necessary to consider the stability of FBs separately from MBs and UFBs. Regarding MBs, the floating speed and shrinking speed decide the stability. Since it is possible to observe MBs with optical microscopies, the results of observing the behavior of a single MB have already been reported<sup>49,59</sup>. It was

experimentally confirmed that the floating speed can be estimated by the Hadamard-Rybczynski (H-R) equation or Stokes equation<sup>52,54</sup>. Shrinkage of MBs occurs by mass transfer of internal gas molecules induced by the partial pressure difference between the inside and outside of bubble. Iwakiri *et al.* reported that oxygen and air MBs shrink in water, and the gas transfer coefficient can be estimated by the Ranz-Marshall equation. They suggested that the surrounding gas concentration affected the shrinking speed of MBs<sup>60</sup>. In 2019, Jin *et al.* confirmed the shrinkage of MBs with poor solubility gas (SF<sub>6</sub>). Moreover, they suggested that the shrunken MBs became UFBs, and the hydrogen bonds at the gas-liquid interface formed during the shrinkage, which contributes to the stability of UFBs<sup>59</sup>. From the viewpoint of floating speed, MBs hardly disappear and remain in liquid for a long time. However, MBs disappear within 10 min by shrinking, although the gas type and surrounding gas concentration affect the shrinking speed. Oxygen MBs disappeared within 5 min in my study.

The stability of UFBs is a difficult and still ongoing issue. According to the Young-Laplace equation, the internal pressure of 100 nm UFBs reached 27 atm, which is too high to last for a few seconds. Therefore, some researchers doubted whether UFBs existed at all. However, Jadhav and Barigou proved the existence and stability of bulk UFBs in water and ethanol by 11 physical and chemical experiments in 2020<sup>61</sup>. They provided multiple pieces of evidence that the observed nanoparticles were UFBs, not contamination or solid nanoparticles. Moreover, some hypotheses about the mechanism of UFB stability have been explained in recent years as follow, 1) a repulsive force due to polarization at the gas-liquid interface: the dipole moments of adjacent dipoles provide the force to cancel the high internal pressure<sup>62</sup>; 2) a decrease in surface tension due to surface charge: the internal pressure is as small as atmospheric pressure because ionized hydroxy ions reduce the surface tension of UFBs<sup>63</sup>; 3) repulsive force due to Coulomb

force: inward radial force due to Coulomb interaction cancels the high internal pressure<sup>64</sup>;

4) an anomalous Young-Laplace equation considering polarized liquid molecules: the pressure difference between the inside and outside of UFBs is negligible following the anomalous Young-Laplace equation, which is corrected by considering the repulsive force due to polarization<sup>65</sup>;

5) dynamic equilibrium model: gas inflows and outflows occur through hydrophobic substances attached to a part of the surface of the UFB, and the UFB stabilizes when they are balanced<sup>66,67</sup>.

#### ***Effects of surfactant, salt, and pH on the stability of ultrafine bubbles***

Recently, the effects of some additives on stability of UFBs were reported. Nirmalakr *et al.* examined the effects of surfactants, salts, and pH adjustment<sup>64</sup>. They first prepared the UFB dispersion with pure water (pH 6.5) and then changed the conditions. Regarding of surfactants, non-ion surfactant (Tween 20) and anionic surfactant (SDS: sodium dodecyl sulfate) did not affect the concentration of UFBs. On the other hand, cationic surfactant (CTAB: cetyl trimethylammonium bromide) showed different effect from others. In the low concentration region of CTAB (0.092–0.64 mM), UFB concentration decreased with increasing CTAB concentration; however, there was no change in UFB concentration at high CTAB concentrations (0.64–4.6 mM). These changes were related to the absolute value of the  $\zeta$ -potential, and the UFB concentration decreased when the charge on the UFB surface near to be neutral. At high CTAB concentrations, the UFB surface has positive charge, which caused an electrostatic repulsive effect and maintained the stability of UFBs. The similar phenomenon that the charge on the UFB surface affect the UFB concertation was confirmed in the experiment of salt concentration (NaCl, CaCl<sub>2</sub>, and AlCl<sub>3</sub>), although the addition of salt decrease absolute UFB concentration<sup>64</sup>. Regarding the effect of pH, the UFB concentration could be kept high in the alkaline condition but decreased in the acidic condition. This

phenomenon is also related to the surface charge of UFBs. However, the effects of pH and surfactants are slightly different between pre-adjustment and post-adjustment of UFB dispersion medium. Comparing several studies, the effects of pH and salt concentration on UFB concentration is smaller when they are adjusted after UFB generation in pure water (pH 6.5)<sup>51,64,68</sup>. Moreover, it is known that the pH of pure water is slightly changed toward neutral condition by the generation of UFB<sup>69</sup>. This phenomenon has been confirmed in my experiment with pure water (pH:  $5.47 \pm 0.01$  [without FBs] to  $6.02 \pm 0.03$  [with FBs]) and with phosphate buffered saline (pH:  $7.84 \pm 0.03$  [without FBs] to  $7.78 \pm 0.02$  [with FBs]).

### **1.2.6. Applications of fine bubbles**

FBs are used in various fields due to their unique properties described in section 1.2.4. Although the major applications are water purification and washing agents, their applications are expanding. I describe the applications of FBs, except for FBs with perfluorochemicals as inner gas.

#### ***Water purification***

The purification method with FBs is called “floating separation” and is widely used for separating suspended solids in sewage. It is thanks to slow floating speed, liquid-gas interface, and negative surface charge. Debris and impurities: powders, surfactants, metal ions, oils, and organics, are absorbed into the FBs and removed at the water surface after floating to the surface with the FBs. Notably, positive-charged particles and hydrophobic particles readily attach to FBs. Although floating separation can be conducted with macro bubbles, FBs provide an excellent effect due to their slow floating speed and specific surface area<sup>70,71</sup>.

### ***Frictional resistance reducing***

There are two types of resistances when a ship is moving, frictional resistance and wave resistance. Large ships, like tankers, are greatly influenced by frictional resistance, which is mainly induced by the viscosity of water. FBs have been studied for this problem after McCormick and Bhattacharyya indicated that frictional resistance decreases with hydrogen bubbles generated by electrolysis<sup>72</sup>. Although the exact mechanism is still unknown, it is recognized that the number of bubbles, the distance between bubbles, and the surface of the ship are crucial<sup>71</sup>. Indeed, FBs reduced the resistance of a large ship and showed a 2% energy saving effect<sup>71</sup>.

### ***Gas hydrate (methane hydrate)***

A gas hydrate is a gas core and the surrounding water molecules. It is prepared by stirring water with the gas under low temperature and high-pressure. Researchers have noted FB's unique properties, such as high gas solubility and high internal pressure<sup>55</sup>. Yasuda reported that a higher yield of methane hydrate was obtained with a FB generator than conventional methods<sup>73</sup>.

### ***Cleaning and prevention of solid surfaces***

FBs have been applied to clean proteins and organic contaminants from various solid surfaces: pyrolytic graphite<sup>74</sup>, gold surface<sup>75</sup>, and stainless steel surface<sup>76</sup>. The effects of FBs are not only removal of the attached materials but also preventing the surface from fouling. Since this technique does not require chemicals and detergents, some companies have already introduced it to clean semiconductors. The conventional cleaning process of semiconductors (SPM cleaning) requires sulfuric acid, hydrogen peroxide, and heating (150°C); thus, there are issues on waste treatment and safety. Takahashi *et al.* showed that ozone FBs could remove photoresist from the substrate, and

the effect was similar to that of SPM cleaning; even ozone dissolved water (without FBs) could not remove as well<sup>77,78</sup>.

### ***Sterilization (ozone fine bubbles)***

Ozone FBs have been used for sterilization in various disciplines, such as water purification<sup>79</sup>, food preservation<sup>80</sup>, and in the medical field<sup>81-83</sup>. In general, ozone has antimicrobial activity against bacteria, fungi, and viruses by producing free radicals. Aqueous ozone is preferred to ozone gas for biomedical applications. It was reported that aqueous ozone showed high biocompatibility with fibroblasts, cementoblasts, and epithelial cells, whereas ozone gas has cytotoxicity<sup>84</sup>. Hayakumo *et al.* showed that ozone FBs had a bactericidal activity for oral bacteria and was not cytotoxic to human oral tissues<sup>83</sup>. Effects on normal cells were also evaluated with osteoblastic cells by Shimada *et al.*, and they reported that there was no cytotoxicity<sup>82</sup>. As a clinical application, ozone UFBs were used for irrigation therapy in patients with purulent arthritis. This showed that the sedation rate of inflammation improved 10% compared to conventional medicine (povidone-iodine or specific antimicrobial drugs). Moreover, irrigation therapy with ozone UFB water improved 34 of 35 cases in which inflammation did not ameliorate with convectional irrigation therapy<sup>82</sup>.

### ***Biological activity***

The first outcome of bioactivity in FBs was reported in the fisheries industry. Currently, bioactivity effects have been confirmed in some creatures: aquatic organisms<sup>85-87</sup>, plants<sup>88,89</sup>, and rodents<sup>90</sup>. These effects are considered due to oxygen supply. Oxygen supply affects not only the target creatures but also the coexisting microorganisms; thus, FBs also improve the surrounding environment. For instance, FBs showed a positive effect on removing viruses attached to shellfish<sup>71</sup>.

### ***Oxygenation for tissue hypoxia***

Gas transportation is one of the beneficial properties of FBs due to their large specific surface area. Swanson *et al.* developed phospholipid-stabilized oxygen microbubbles (LOM dispersion) for injectable oxygen delivery<sup>91</sup>. The LOM dispersion could be concentrated and controlled by its oxygen content within 50–90 vol%. However, the lipid concentration was 10 mg/mL; therefore, there was a limitation in the injectable volume to animals<sup>92</sup>. Feshitan *et al.* injected LOM dispersion peritoneally and reported the safety and effects of blood oxygenation on an ARDS model<sup>93</sup>. Matsuki *et al.* used normal saline containing oxygen FBs, and it improved the hypoxic conditions of blood under *in vitro* experiment<sup>94</sup>. Following this research, a research group used oxygen UFB dispersion for the treatment of tissue hypoxia<sup>95–97</sup>.

There are few reports on the safety of FB dispersion with intravascular administration. Stabilized FBs with a lipid or polymer shell were intravascularly injected and showed the capacity to be oxygen carriers<sup>98,99</sup>. In these studies, vascular embolism was prevented by controlling the particle size to be smaller than the capillary size of 5  $\mu\text{m}$ . Yoshida *et al.* examined the effects of intravascular administration of oxygen UFBs on an ARDS model in rats. Although there were no significant differences in blood oxygenation, mean arterial pressure, and inflammatory cytokines levels compared to the control group, no side effects due to intravascular administration were confirmed<sup>100</sup>. However, further safety evaluation on intravascular administration of FB dispersions is needed.

## References

1. Tawfic, Q. A. & Kausalya, R. Liquid ventilation. *Oman Med. J.* **26**, 4–9 (2011).
2. Shaffer, T. H., Wolfson, M. R. & Greenspan, J. S. Liquid Ventilation : Current Status. *Pediatr. Rev.* **20**, e134–e142 (1999).
3. Tamura, M. & Nakamura, T. Principle and Clinical Application of Liquid Ventilation. *Shinshu Med. J.* **49**, 239–248 (2001).
4. Kacmarek, R. M. *et al.* Partial Liquid Ventilation in Adult Patients with Acute Respiratory Distress Syndrome. *Am J Respir Crit Care Med* **173**, 882–889 (2006).
5. Clark, L. C. & Gollan, F. Survival of Mammals Breathing Organic Liquids Equilibrated with Oxygen at Atmospheric Pressure. *Science (80-. )*. **152**, 1755–1756 (1966).
6. Riess, J. G. Overview of progress in the fluorocarbon approach to in vivo oxygen delivery. *Biomater Artif Cells Immobil. Biotechnol.* **20**, 183–202 (1992).
7. Lowe, K. C. Perfluorinated blood substitutes and artificial oxygen carriers. *Blood Rev.* **13**, 171–184 (1999).
8. Shine, K. P. *et al.* Perfluorodecalin : global warming potential and first detection in the atmosphere. *Atmos. Environ.* **39**, 1759–1763 (2005).
9. Change, F. convention on C. *Report of the Conference of the Parties on its nineteenth session, held in Warsaw from 11 to 23 November 2013.* (2014).
10. Greenspan, J. S., Cleary, G. M. & Wolfson, M. R. is liquid ventilation a reasonable alternative? *Clin Perinatol.* **25**, 137–157 (1998).
11. Hirschl, R. B. *et al.* Liquid ventilation improves pulmonary function, gas exchange, and lung injury in a model of respiratory failure. *Ann Surg* **221**, 79–88 (1995).

12. Jiang, L. *et al.* Total Liquid Ventilation Reduces Lung Injury in Piglets After Cardiopulmonary Bypass. *Ann. Thorac. Surg.* **82**, 124–130 (2006).
13. Pohlmann, J. R. *et al.* Total liquid ventilation provides superior respiratory support to conventional mechanical ventilation in a large animal model of severe respiratory failure. *ASAIO J.* **57**, 1–8 (2011).
14. Kakiuchi, K. *et al.* Establishment of a total liquid ventilation system using saline-based oxygen micro/nano-bubble dispersions in rats. *J. Artif. Organs* **18**, 220–227 (2015).
15. Campo, I. *et al.* Whole lung lavage therapy for pulmonary alveolar proteinosis : a global survey of current practices and procedures. *Orphanet J. Rare Dis.* **11**, 115–125 (2016).
16. Winternitz, M. C. & Smith, G. H. Intratracheal pulmonary irrigation. in *Contributions to Medical and Biological Research* (ed. William, O.) 1255–1266 (P.B. Hoeber, 1919).
17. Winternitz, M. C. & Smith, G. H. PRELIMINARY STUDIES IN INTRATRACHEAL THERAPY. in *COLLECTED STUDIES ON THE PATHOLOGY OF WAR GAS POISONING* (ed. WINTERNITZ, M. C.) 143–160 (Yale University Press, 1920).
18. Rogers, R. M., Braunstein, M. S. & Shurman, J. F. Role of bronchopulmonary lavage in the treatment of respiratory failure: a review. *Chest* **62**, 95S-106S (1972).
19. Ramirez-R, J. Pulmonary Alveolar Proteinosis: treatment by massive bronchopulmonary lavage. *Arch. Intern. Med.* **119**, 147 (1967).
20. Kylstra, J. A., Rausch, D. C., Hall, K. D. & Spock, A. Volume-Controlled Lung Lavage in the Treatment of Asthma, Bronchiectasis, and Mucoviscidosis. *Am.*

- Rev. Respir. Dis.* **103**, 651–665 (1971).
21. Ramirez, J., Kieffer, R. F. & Ball, W. C. Bronchopulmonary lavage in man. *Ann. Intern. Med.* **63**, 819–828 (1965).
  22. Ramirez-R, J. Bronchopulmonary Lavage. *Dis. Chest* **50**, 581–588 (1966).
  23. Kylstra, J. A., Tissing, M. O. & Van der Maen, A. of mice as fish.pdf. *Trans Am Soc Artif Intern Organs* **8**, 378–383 (1962).
  24. Kylstra, J. A., Paganelli, C. V. & Lanphier, E. H. Pulmonary gas exchange in dogs ventilated with hyperbarically oxygenated liquid. *J Appl Physiol.* **21**, 177–184 (1966).
  25. Shaffer, T. H. & Moskowitz, G. D. Demand-controlled liquid ventilation of the lungs. *J Appl Physiol.* **36**, 208–213 (1974).
  26. Schwieler, G. H. & Robertson, B. Liquid ventilation in immature newborn rabbits. *Biol Neonate.* **29**, 343–353 (1976).
  27. Greenspan, J. S., Wolfson, M. R., Rubenstein, S. D. & Shaffer, T. H. LIQUID VENTILATION OF PRETERM BABY. *Lancet* **Nov. 4**, 1095 (1989).
  28. Greenspan, J. S., Wolfson, M. R., Rubenstein, S. D. & Shaffer, T. H. Liquid ventilation of human preterm neonates. *J Pediatr.* **117**, 106–111 (1990).
  29. Fuhrman, B. P., Paczan, P. R. & Francis, M. Perfluorocarbon-associated gas exchange. *Crit. Care Med.* **19**, 712–722 (1991).
  30. Leach, C. lowe, Fuhrman, B. P., Morin, F. C. & Rath, M. G. Perfluorocarbon-associated gas exchange (partial liquid ventilation) in respiratory distress syndrome a prospective, randomized, controlled study. *Crit. Care Med.* **21**, 1270–1278 (1993).
  31. Houmes, R. J. M., Verbrugge, S. J. C., Hendrik, E. R. & Lachmann, B. Hemodynamic effects of partial liquid ventilation with perfluorocarbon in acute

- lung injury. *Intensive Care Med.* **21**, 966–972 (1995).
32. Tütüncü, A. S., Faithfull, N. S. & Lachmann, B. Intratracheal perfluorocarbon administration combined with mechanical ventilation in experimental respiratory distress syndrome: dose-dependent improvement of gas exchange. *Crit Care Med.* **21**, 962–969 (1993).
  33. Fuhrman, B. P. *et al.* Perfluorocarbon associated gas exchange (PAGE): gas ventilation of the perfluorocarbon filled lung. *Artif Cells Blood Substit Immobil. Biotechnol.* **22**, 1133–1139 (1994).
  34. Leach, C. L. *et al.* Partial Liquid Ventilation With Perflubron in Premature Infants With Severe Respiratory Distress Syndrome. *N. Engl. J. Med.* **335**, 761–767 (1996).
  35. Greenspan, J. S. *et al.* Partial Liquid Ventilation in Critically Ill Infants Receiving Extracorporeal Life Support. *Pediatrics.* **99**, E2 (1997).
  36. Hirschl, R. B. *et al.* Prospective , Randomized , Controlled Pilot Study of Partial Liquid Ventilation in Adult Acute Respiratory Distress Syndrome. *Am J Respir Crit Care Med* **165**, 781–787 (2002).
  37. Jonson, B. & Svantesson, C. Elastic pressure-volume curves: What information do they convey? *Thorax* **54**, 82–87 (1999).
  38. RAMIREZ-R., J., SCHULTZ, R. B. & DUTTON, R. E. Pulmonary Alveolar Proteinosis A New Technique and Rationale for Treatment. *Arch Intern Med.* **112**, 419–431 (1963).
  39. Calderwood, H. W. *et al.* Residual levels and biochemical changes after ventilation with perfluorinated liquid. *J Appl Physiol* **39**, 603–607 (1975).
  40. Gupta, J., Olsthoorn, X. & Rotenberg, E. The role of scientific uncertainty in compliance with the Kyoto Protocol to the Climate Change Convention. *Environ.*

- Sci. Policy* **6**, 475–486 (2003).
41. Tissier, R. *et al.* Total Liquid Ventilation Provides Ultra-Fast Cardioprotective Cooling. *J. Am. Coll. Cardiol.* **49**, 601–605 (2007).
  42. Tissier, R. *et al.* Rapid cooling preserves the ischaemic myocardium against mitochondrial damage and left ventricular dysfunction. *Cardiovasc. Res.* **83**, 345–353 (2009).
  43. Wolfson, M. R. & Shaffer, T. H. Liquid-assisted ventilation : from concept to clinical application. *Semin. Neonatol.* **2**, 115–127 (1997).
  44. Wolfson, M. R., Greenspan, J. S., Deoras, K. S., Rubenstein, S. D. & Shaffer, T. H. Comparison of gas and liquid ventilation: Clinical, physiological, and histological correlates. *J. Appl. Physiol.* **72**, 1024–1031 (1992).
  45. Foust, R. *et al.* Liquid assisted ventilation: An alternative ventilatory strategy for acute meconium aspiration injury. *Pediatr. Pulmonol.* **21**, 316–322 (1996).
  46. Richman, P. S., Wolfson, M. R. & Shaffer, T. H. Lung lavage with oxygenated perfluorochemical liquid in acute lung injury. *Crit. care Med.* **21**, 768–774 (1993).
  47. Zhu, Y. Bin *et al.* Partial liquid ventilation decreases tissue and serum tumor necrosis factor- $\alpha$  concentrations in acute lung injury model of immature piglet induced by oleic acid. *Chin. Med. J. (Engl.)*. **125**, 123–128 (2012).
  48. Zhu, Y.-B. *et al.* Total liquid ventilation reduces oleic acid-induced lung injury in piglets. *Chin. Med. J. (Engl.)*. **126**, 4282–4288 (2013).
  49. Terasaka, K., Himuro, S., Ando, K. & HATA, T. *Introduction to Fine Bubble Science and Technology*. (NIKKAN KOGYO SHIMBUN,LTD., 2016).
  50. Ohmori, M., Haruta, K., Kamimura, S., Uchida, T. & Takeyama, H. A Simple Method for Nanobubble Generation and Stability of the Bubbles. *J. Environ.*

- Biotechnol.* **15**, 41–44 (2015).
51. Nirmalkar, N., Pacek, A. W. & Barigou, M. On the Existence and Stability of Bulk Nanobubbles. *Langmuir* **34**, 10964–10973 (2018).
  52. Takahashi, M. Zeta Potential of Microbubbles in Aqueous Solutions : Electrical Properties of the Gas-Water Interface. *J. Phys. Chem. B* **109**, 21858–21864 (2005).
  53. Tsuge, H. Fundamentals of Microbubbles and Nanobubbles (Japanese). *Bull. Soc. Sea Water Sci. Japan* **64**, 4–10 (2010).
  54. Parkinson, L., Sedev, R., Fornasiero, D. & Ralston, J. The terminal rise velocity of 10 – 100  $\mu\text{m}$  diameter bubbles in water. *J. Colloid Interface Sci.* **322**, 168–172 (2008).
  55. Takahashi, M. *et al.* Effect of shrinking microbubble on gas hydrate formation. *J. Phys. Chem. B* **107**, 2171–2173 (2003).
  56. Chaplin, M. Theory vs Experiment : What is the Surface Charge of Water ? *water* **1**, 1–28 (2009).
  57. Ohgaki, K., Quoc, N., Joden, Y., Tsuji, A. & Nakagawa, T. Physicochemical approach to nanobubble solutions. *Chem. Eng. Sci.* **65**, 1296–1300 (2010).
  58. Pérez-garibay, R., Bueno-tokunaga, A., Estrada-ruiz, R. H. & Camacho-ortegón, L. F. Effect of surface electrical charge on microbubbles' terminal velocity and gas holdup. *Miner. Eng.* **119**, 166–172 (2018).
  59. Jin, J., Feng, Z., Yang, F. & Gu, N. Bulk Nanobubbles Fabricated by Repeated Compression of Microbubbles. *Langmuir* **35**, 4238–4245 (2019).
  60. Iwakiri, M. *et al.* Mass Transfer from a Shrinking Single Microbubble Rising in Water (Japanese). *JAPANESE J. Multiph. FLOW* **30**, 529–535 (2017).
  61. Jadhav, A. J. & Barigou, M. Bulk Nanobubbles or Not Nanobubbles : That is the

- Question. *Langmuir* **36**, 1699–1708 (2020).
62. Ghaani, M. R., Kusalik, P. G. & English, N. J. Massive generation of metastable bulk nanobubbles in water by external electric fields. *Sci. Adv.* **6**, 1–6 (2020).
  63. Ulatowski, K., Sobieszuk, P., Mróz, A. & Ciach, T. Stability of nanobubbles generated in water using porous membrane system. *Chem. Eng. Process. Process Intensificatio* **136**, 62–71 (2019).
  64. Nirmalkar, N., Pacek, A. W. & Barigou, M. Interpreting the interfacial and colloidal stability of bulk nanobubbles. *Soft Matter* **14**, 9643–9656 (2018).
  65. Araki, T., Kondo, W., Nakamura, K., Tejima, S. & Ono, Y. *Large-scale simulation of nanobubble formation and behavior (Japanese)*. (2015).
  66. Yasui, K., Tuziuti, T., Kanematsu, W. & Kato, K. Dynamic Equilibrium Model for a Bulk Nanobubble and a Microbubble Partly Covered with Hydrophobic Material. *Langmuir* **32**, 11101–11110 (2016).
  67. Yasui, K., Tuziuti, T. & Kanematsu, W. Mysteries of bulk nanobubbles (ultrafine bubbles); stability and radical formation. *Ultrason. - Sonochemistry* **48**, 259–266 (2018).
  68. Ferraro, G., Jadhav, A. J. & Barigou, M. A Henry's law method for generating bulk nanobubbles. *Nanoscale* **12**, 15869–15879 (2020).
  69. Ushikubo, F. Y. *et al.* Evidence of the existence and the stability of nano-bubbles in water. *Colloids Surfaces A Physicochem. Eng. Asp.* **361**, 31–37 (2010).
  70. Temesgen, T., Thuy, T., Han, M., Kim, T. & Park, H. Micro and nanobubble technologies as a new horizon for water-treatment techniques : A review. *Adv. Colloid Interface Sci.* **246**, 40–51 (2017).
  71. Tsuge, H. *The latest technology on microbubbles and nanobubbles/popular edition (Japanese)*. (CMC Publishing Co.,Ltd., 2015).

72. McCormick, M. E. & Bhattacharyya, R. DRAG REDUCTION OF A SUBMERSED HULL BY ELECTROLYSIS. *Nav. Eng. J.* **85**, 11–16 (1973).
73. Yasuda, K. Application of Finebubbles to Resources and Environmental Area (Japanese). *Japanese J. Multiph. Flow* **30**, 37–44 (2016).
74. Wu, Z. H. *et al.* Cleaning using nanobubbles: Defouling by electrochemical generation of bubbles. *J. Colloid Interface Sci.* **328**, 10–14 (2008).
75. Liu, G., Wu, Z. & Craig, V. S. J. Cleaning of protein-coated surfaces using nanobubbles: An investigation using a Quartz Crystal Microbalance. *J. Phys. Chem. C* **112**, 16748–16753 (2008).
76. Broekman, S., Pohlmann, O., Beardwood, E. S. & de Meulenaer, E. C. Ultrasonic treatment for microbiological control of water systems. *Ultrason. Sonochem.* **17**, 1041–1048 (2010).
77. Takahashi, M., Ishikawa, H., Asano, T. & Horibe, H. Effect of microbubbles on ozonized water for photoresist removal. *J. Phys. Chem. C* **116**, 12578–12583 (2012).
78. TAKAHASHI, M. Microbubble : Fundamental Properties and Application for Semiconductor Cleaning (Japanese). *J. Japan Soc. Precis. Eng.* **83**, 636–640 (2017).
79. Batagoda, J., Hewage, S. A. & Meegoda, J. N. Nano-Ozone Bubbles for Drinking Water Treatment. *J. Environ. Eng. Sci.* **14**, 57–66 (2019).
80. Ikeura, H., Kobayashi, F. & Tamaki, M. Ozone Microbubble Treatment at Various Water Temperatures for the Removal of Residual Pesticides with Negligible Effects on the Physical Properties of Lettuce and Cherry Tomatoes. *J. Food Sci.* **78**, 350–355 (2013).
81. Hayashi, K., Onda, T., Honda, H., Ozawa, N. & Ohata, H. Effects of ozone nano-

- bubble water on mucositis induced by cancer chemotherapy. *Biochem. Biophys. Reports* **20**, 100697 (2019).
82. Kawashima, M., Tamura, H. & Kawashima, M. hyperbaric oxygen therapy and irrigation therapy with ozone nano-bubble water for arthrempyesis (Japanese). *Mon. B. Orthop.* **31**, 140–148 (2018).
83. Hayakumo, S. *et al.* Effects of ozone nano-bubble water on periodontopathic bacteria and oral cells - in vitro studies. *Sci. Technol. Adv. Mater.* **15**, 055003 (2014).
84. Huth, K. C. *et al.* Effect of ozone on oral cells compared with established antimicrobials. *Eur J Oral Sci* **114**, 435–440 (2006).
85. Ohnari, H. *All about microbubble (Japanese)*. (NIPPON JITSUGYO PUBLISHING, 2006).
86. Marui, T. An Introduction to Thyristors and Their Applications. *J. Syst. Cybern. Informatics* **11**, 68–73 (2013).
87. Srithongouthai, S. *et al.* Control of dissolved oxygen levels of water in net pens for fish farming by a microscopic bubble generating system. *Fish. Sci.* **72**, 485–493 (2006).
88. Ahmed, A. K. A. *et al.* Influences of Air, Oxygen, Nitrogen, and Carbon Dioxide Nanobubbles on Seed Germination and Plant Growth. *J. Agric. Food Chem.* **66**, 5117–5124 (2018).
89. Park, J.-S. & Kurata, K. Application of Microbubbles to Hydroponics Solution Promotes Lettuce Growth. *Am. J. Hortic. Sci.* **19**, 212–215 (2009).
90. Ebina, K. *et al.* Oxygen and Air Nanobubble Water Solution Promote the Growth of Plants, Fishes, and Mice. *PLoS One* **8**, e65339 (2013).
91. Swanson, E. J., Mohan, V., Kheir, J. & Borden, M. A. Phospholipid-stabilized

- microbubble foam for injectable oxygen delivery. *Langmuir* **26**, 15726–15729 (2010).
92. Kheir, J. N. *et al.* Oxygen gas-filled microparticles provide intravenous oxygen delivery. *Sci. Transl. Med.* **4**, 140ra88 (2012).
  93. Feshitan, J. A., Legband, N. D., Borden, M. A. & Terry, B. S. Systemic oxygen delivery by peritoneal perfusion of oxygen microbubbles. *Biomaterials* **35**, 2600–2606 (2014).
  94. Matsuki, N. *et al.* Blood oxygenation using microbubble suspensions. *Eur Biophys J* **41**, 571–578 (2012).
  95. Noguchi, T. *et al.* Oxygen ultra-fine bubbles water administration prevents bone loss of glucocorticoid-induced osteoporosis in mice by suppressing osteoclast differentiation. *Osteoporos. Int.* **28**, 1063–1075 (2017).
  96. Matsuoka, H. *et al.* Administration of oxygen ultra-fine bubbles improves nerve dysfunction in a rat sciatic nerve crush injury model. *Int. J. Mol. Sci.* **19**, (2018).
  97. Sayadi, L. R. *et al.* Micro/nanobubbles: Improving Pancreatic Islet Cell Survival for Transplantation. *Ann. Plast. Surg.* **83**, 583–588 (2019).
  98. Kheir, J. N. *et al.* Oxygen gas-filled microparticles provide intravenous oxygen delivery (supplemental data). *Sci. Transl. Med.* **4**, 1–5 (2012).
  99. Polizzotti, B. D. *et al.* Oxygen delivery using engineered microparticles. *Proc. Natl. Acad. Sci.* **113**, 12380–12385 (2016).
  100. Yoshida, K., Ikegami, Y., Obara, S., Sato, K. & Murakawa, M. Investigation of anti-inflammatory effects of oxygen nanobubbles in a rat hydrochloric acid lung injury model. *nanomedicine* **15**, 2647–2654 (2020).

## **Chapter 2: Studies on fine bubble dispersion as oxygen carrier using a novel oxygen measurement method**

### **2.1. Background of this chapter**

2.1.1. Measurement method for oxygen content in water

2.1.2. Measurement method for oxygen content in fine bubble dispersion

2.1.3. Fine bubble dispersion as an oxygen carrier

### **2.2. Development of novel oxygen measurement method for oxygen fine bubble dispersion**

2.2.1. Purpose

2.2.2. Materials and experimental procedures

2.2.3. Results and discussion

### **2.3. Evaluation of properties of oxygen fine bubbles as an oxygen carrier**

2.3.1. Purpose

2.3.2. Materials and experimental procedures

2.3.3. Results and discussion

### **2.4. Conclusions of this chapter**

### **References**

## **2.1. Background of this chapter**

### **2.1.1. Measurement method for oxygen content in water**

Oxygen content in water refers to dissolved oxygen (DO) and is crucial for biological and chemical reactions in water. The methods for measuring DO can be divided into four categories: 1) gasometric determination, 2) volumetric (titration) determination, 3) colorimetric determination, 4) electrochemical determination, and 5) fluorometric determination.

In gasometric determination, the oxygen content is measured by converting all the DO to the gas state. The DO is removed from water (liquid) either by boiling or by bubbling CO<sub>2</sub>, and the volume of oxygen is measured with a gas burette or a manometer<sup>1,2</sup>. This is the oldest method, which was also used by William Henry<sup>3</sup>. The measurement is not affected by the presence of impurities (e.g., ions, metals, and suspended matters). However, it is difficult to extract only oxygen gas from the sample liquid.

Volumetric (titration) determination, especially Winkler's method (see p. 38), has been widely used for many decades. According to the Japanese Industrial Standards (JIS), this is a reliable method for the measurement of DO. The original Winkler's method involved several factors and phenomena that could introduce errors in the measurement. These included the oxidation of iodide ions, volatilization of iodine, contamination of oxygen and iodic acid in analytical reagents, consumption or production of iodine by impurities in reagents, and difficulty in determination of the titration endpoint. However, some improved techniques were developed to mitigate these effects<sup>1,4-7</sup>.

Colorimetric determination utilizes the chemical reactions with oxygen, similar to those in volumetric determination. However, the accuracy of this method is lower than that of volumetric determination, and these methods are affected by the presence of iodide, oxalate, and other reducing and oxidizing agents<sup>1,2</sup>.

Electrochemical determination includes two methods: galvanometric method and polarographic method. For the two methods, the electrolytic cell structure is similar and consists of an electrolyte solution, a working electrode, a counter electrode, and a diaphragm with high oxygen permeability. In the galvanometric method, current is generated when the working electrode (Pt, Au, or Ag) and the counter electrode (Pb, or Al) are electrically connected; the current is detected by an external ammeter. DO is calculated from the magnitude of the current, which is proportional to the oxygen content in the liquid sample. This method does not require aging. However, the electrodes in this method have a shorter lifetime compared to those in the other two methods because the electrodes always react with DO<sup>8</sup>. In the polarographic method, DO is calculated based on the current that is applied to reduce the DO. Although this method requires aging prior to use, the electrodes in this system last longer compared to those in the galvanometric method, because the reaction occurs only when current is applied from an external device<sup>8</sup>.

In the fluorometric determination, the oxygen quenching is utilized to calculate DO. The system is composed of a blue light-emitting diode (LED), two light-receiving diodes with blue and red filters, a carrier layer, a light-emitting material, and an oxygen-permeable layer. Blue light emitted from the LED excites the light-emitting material, and the light-receiving diodes detect the light emitted from the material. Since the intensity of the emitted light depends on the amount of DO in the liquid sample, the DO content can be calculated. Since this device detects oxygen that has permeated the oxygen-permeable membrane, bubbles do not exist in the detection unit. This method is currently disseminated in several fields because it does not require frequent maintenance and fluid flow during the measurement. Moreover, the measurement range of this method is relatively broad compared to those of the other two methods<sup>9</sup>.

### 2.1.2. Measurement method for oxygen content in fine bubble dispersion

It is well known that the oxygen content in fine bubble (FB) dispersion is higher than that in oxygen-saturated water under atmospheric conditions<sup>10,11</sup>. The fluorescence method can be used to measure the oxygen content in FB dispersion<sup>12</sup>. However, there are concerns regarding the low measurement limit (< 50 mg/L) and the adhesion of bubbles to the probe surface. Therefore, there is no standardized method approved by the Union of Fine Bubble Science and Engineers for measuring the oxygen content in FB dispersions. Researchers use different methods/equipment such as Winkler's method<sup>13</sup>, blood gas analyzer<sup>10</sup>, and DO meter<sup>14</sup> in their studies. Some researchers have calculated the oxygen content in FB dispersions after diluting the sample with solvents<sup>15-17</sup>. For example, Swanson *et al.* constructed a new system with micro cathodes to measure the oxygen content in a lipid-coated oxygen micro bubble (LOM) dispersion that contained 50–90 vol% of oxygen. The system measured the amount of oxygen released from the LOM dispersion to deoxidized water. They examined the LOM dispersion by comparing the rate of increase of the amount of oxygen<sup>16</sup>. However, this method required a complex system and expensive electrodes. Although there were other dilution methods, they required large volumes of the deoxygenated water and sample. Furthermore, it was difficult for these methods to eliminate the effects of ambient air; therefore, there is no report of effective dilution method which quantify oxygen content.

I previously proposed a new method for the measurement of oxygen content in FB dispersions using a hemoglobin (Hb) solution<sup>18</sup>. This method utilizes the oxygen-binding capacity of Hb. The oxygen content is calculated from the percentage of oxygenated Hb, which is generated from deoxygenated Hb upon sample (FB dispersion) injection (Fig. 2.1). This method shows good reproducibility, and the oxygen content in the FB

dispersion can be measured using less than 1 mL of sample. However, this method has some drawbacks. First, Hb tends to be oxidized in one week after purification even in a refrigerator. Second, it is necessary to evaluate the oxygen-binding curve of the Hb solution each time when an Hb solution is newly prepared, that is time consuming<sup>18</sup>.

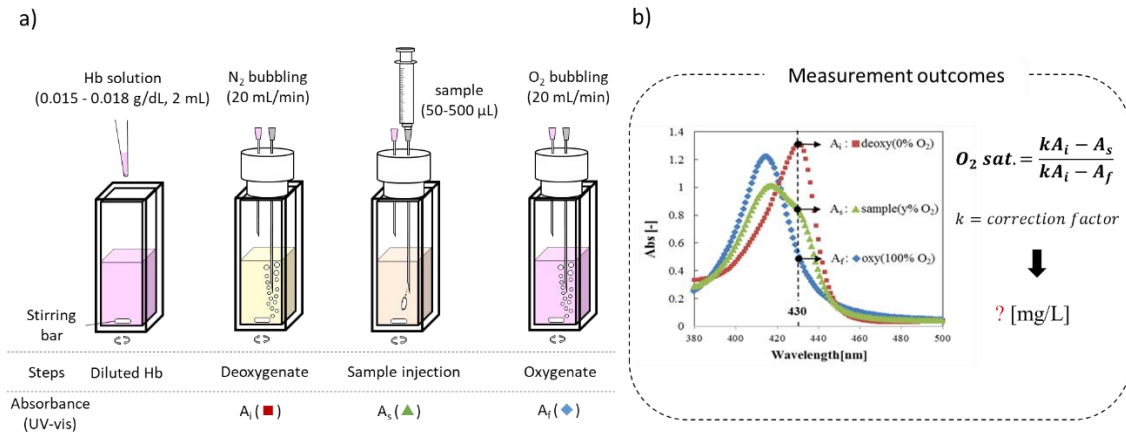


**Fig. 2.1. Oxygen measurement method with Hb solution.** a) Experimental procedure. b) Spectrum of the solution at each step, showing the state of the Hb solution. Oxygen content can be calculated from an oxygen-binding curve of the Hb solution and oxygen saturation level of the Hb solution.

### 2.1.3. Fine bubble dispersion as an oxygen carrier

In 1999, a problem arose from *Heterocapsa* red tide at oyster farming areas in Hiroshima, Japan, could be solved using air microbubbles (MB)<sup>19</sup>. The red tide covered the surface of sea, caused a low-oxygen environment, and did a serious damage to oysters. MB could quickly increase the DO level, while a mechanical agitation system had failed to do so. Ohnari, who is a pioneer in FB research, concluded that MB was a useful tool for the efficient supply of oxygen (air) into liquid<sup>19</sup>. In 2003, Takahashi *et al.* reported that a supersaturated state formed the surrounding region of FBs due to their high internal pressure<sup>20</sup>. Following this, air or oxygen MBs were used for water treatments<sup>21</sup>, chemical

reactions<sup>22</sup>, and blood oxygenation<sup>23</sup> to increase the oxygen level. From 2010, oxygen ultra FB (UFB,  $< 1 \mu\text{m}$ ) began to be used as an oxygen carrier, and Ebina's group demonstrated its utility in *in vivo* experiments<sup>13,24,25</sup>. They suggested that UFB is theoretically superior to MBs due to the high internal pressure of the former<sup>25</sup>. However, they could not obtain any evidence that oxygen UFB improved the hypoxic condition at a cellular level, although oxygen UFB accelerated nerve regeneration and functional recovery in a rat nerve crush injury model<sup>25</sup>. Other researches also reported the superiority of UFB as an oxygen carrier<sup>23,26</sup>; however, they suggested this on the basis of the internal pressure calculated by the Young-Laplace equation, and did not confirm it experimentally. One of the reasons that this has not been examined so far is that there are no methods for accurately measuring the oxygen content in FB dispersions.

## **2.2. Development of novel oxygen measurement method for oxygen fine bubble dispersion**

### **2.2.1. Purpose**

There is no standard method to quantitatively measure the oxygen content in FB dispersions. I previously developed a method for measuring oxygen in FB dispersions using Hb solution. However, the preparation and evaluation of the Hb solution before measurement are time consuming. Although Winkler's method is used to measure the oxygen content in FB dispersions over a wide range of oxygen content, this is also time consuming and requires complex procedures. Therefore, the purpose of this experiment is to develop a novel method that can be used to determine the oxygen content in FB dispersions and the high oxygen contents in liquids ( $> 50$  mg/L) more quickly and easily.

### **2.2.2. Materials and experimental procedures**

#### ***Development of a novel method for quantitative oxygen content measurement***

I studied a novel method to measure the oxygen content in FB dispersion using a commercial oxygen electrode (Fig. 2.2). This method is not only a simple (4 steps) and rapid ( $< 8$  min) method but also a method which requires only small volume of sample ( $< 500$   $\mu$ L). Pure water (2 mL) was introduced into a sample chamber of a Clark-type oxygen electrode device (OXYG1-PLUS; Hansatech Instruments Ltd, Norfolk, UK) and deoxygenated by bubbling nitrogen ( $N_2$ ) via a 70-mm needle (22G Cathelin needle; TERUMO CORPORATION, Tokyo, Japan), with stirring (80 rpm) at room temperature (Fig. 2.2a). A microsyringe with a 70-mm needle was used to inject the sample after confirming that the oxygen concentration in the pure water was less than 1.0 nmol/mL. Immediately after sample injection, a screw lid was lowered into the water surface of the pure water to minimize the contact area with ambient air.  $N_2$  gas was flowed over

the water surface to completely eliminate the effects of oxygen from ambient air (Fig. 2.2a). Since the lid has a 1 mm hole through it, the gas reflux is possible while minimizing the contact area with the gas phase. The oxygen level in the pure water increased due to the oxygen from the injected sample. This was monitored using a software (Fig. 2.2b), and the measurement decided to be completed when the oxygen level became stable. The oxygen content in the sample was calculated using Equation (2.1):

$$\text{Oxygen content [nmol/mL]} = \frac{I_{O_2} \times (2+V_S)}{V_S} \quad (2.1)$$

where,  $I_{O_2}$  is the extent of increase in oxygen (nmol/mL) and  $V_S$  is the volume of the injected sample (mL). Finally, the values were converted from mmol/mL to mg/L.

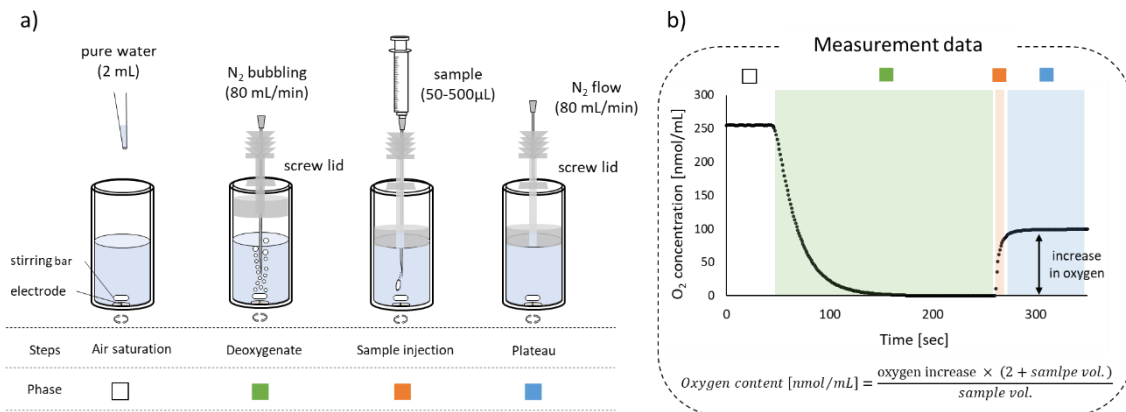


**Fig. 2.2. Novel oxygen content measurement method.** a) A Clark-type oxygen electrode was used to measure the oxygen content in a FB dispersion. Measurement procedure consists of four steps: first step, air saturation (white); second step, deoxygenation (green); third step, sample injection (orange); fourth step, saturation (blue). b) Change in the oxygen content during measurement. A two-way arrow indicates that the oxygen level increases with sample injection.

### ***Evaluation of accuracy of the method***

The errors in the measurement were examined at several temperatures (10, 20, 30, and 40 °C) and for several sample volumes (50, 100, 300, 450, and 500  $\mu\text{L}$ ) using pure water as a sample. As a control experiment, oxygen content of the sample was simultaneously measured with a DO meter (DO meter 1; OM-71, HORIBA, Ltd., Kyoto, Japan). Air-saturated pure water (3 L) was prepared by bubbling air, with stirring for > 30 min. The temperature was controlled by a thermostat (ZS-211; ZENSUI Co., Ltd., Osaka, Japan), that was connected with a heater (NISSO protect PRO heater; Marukan Co., Ltd., Osaka, Japan) and a magnetic pump (MD-6K-N; IWAKI Co., Ltd., Tokyo, Japan) for circulating cold water through a cooling coil.

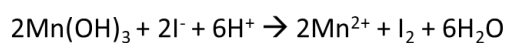
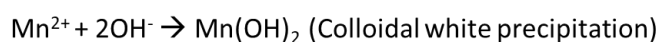
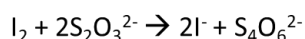
The accuracy of the measurement at several temperatures was evaluated by comparing the results obtained by measuring with three different DO meters (DO meter 1; DO meter 2: HI9146, HANNA instruments, Inc., Rhode Island, USA; DO meter 3: Seven2Go Pro S9, METTLER TOLEDO, Ohio, USA).

### ***Evaluation of oxygen content in oxygen fine bubble dispersions***

The oxygen contents in the same FB dispersions at several temperatures (15, 20, 30, and 40 °C) were tested using the novel method and the three DO meters. FBs were generated in 5 L pure water using a FB generator (GALF; Ultrafine GALF FZ1N-02, IDEC Corporation, Osaka, Japan) under the following conditions: oxygen supply, 0.5 L/min; dissolution pressure, 270–320 kPa; pump pressure, 1390–1420 kPa. GALF adopts a pressurized dissolution method in which FBs are generated by quick decompression of oxygen that is dissolved under pressure. The temperature was controlled with the same system as that in the previous experiment. The oxygen content in the FB dispersions was measured with Winkler's method to examine the accuracy of the novel measurement method.

**Winkler's method**<sup>1,7</sup>

Chemical reactions of Winkler's method are shown in Scheme 2.1. A manganese sulfate solution (fixative 1; 2.15 mol/L MnSO<sub>4</sub> (aq)), an alkali-iodine-azide solution (fixative 2; 6 mol/L NaI in 10 mol/L NaOH (aq)), a sulfuric acid solution (6.8 mol/L H<sub>2</sub>SO<sub>4</sub>), a 1% starch solution, a sodium thiosulfate solution (0.02 mol/L Na<sub>2</sub>S<sub>2</sub>O<sub>3</sub>), and a potassium iodide solution (0.001667 mol/L KIO<sub>3</sub>) were prepared a few days before performing the titration. The exact concentration of the sodium thiosulfate solution was determined just before the titration by standardization with potassium iodide solution. The chemical reactions in Winkler's method are represented in Scheme 1.

**<Oxygen fixation>****<Iodine titration>****Scheme 2.1. Chemical reactions of Winkler's method**

The liquid sample (FB dispersion or air-saturated water) was poured into a 100 mL stoppered biological oxygen demand bottle (BOD bottle) by siphoning. During this, 200–300 mL of the sample was overflowed to eliminate the influence of air inside the bottle. Subsequently, 1 mL of fixatives 1 and 2 were added sequentially into the BOD bottle. The fixatives were injected to the bottom of the BOD bottle carefully. The BOD bottle was sealed with a specific lid and inverted up and down 30 times. Brown precipitates were generated depending on the oxygen content. In case of bubble contamination, I restarted the procedure from the sample collection step. Ten minutes later, 2 mL of sulfuric acid was added from the surface of the liquid sample to stop the reaction. The BOD bottle was

sealed again with the lid and inverted up and down 30 times to dissolve the precipitate under the acidic condition. The liquid sample was transferred to a 200- or 500-mL beaker, and the titration was performed with the sodium thiosulfate solution using a 10 mL titrator with continuous stirring. When the color became lighter, a starch solution was added for easier identification. The endpoint of the titration was determined using an UV-vis (V-660; Jasco Corporation, Tokyo, Japan) spectrophotometer. The titration was ended when the peak at 350 nm disappeared. The oxygen content in the liquid sample was calculated using Equation (2.2):

$$\text{oxygen content [mg/L]} = \frac{800nv}{V-2r} - 0.04 \quad (2.2)$$

where,  $n$  is the concentration of the sodium thiosulfate solution (mol/L),  $v$  is the titration volume (L),  $V$  is the volume of the BOD bottle (L) ( $\approx 100$  mL), and  $r$  is the injection volume of fixatives (L) ( $2r \approx 2$  mL); 0.04 mg/L is the correction value due to oxygen contamination during the process<sup>7</sup>.

### 2.2.3. Results and discussion

#### *Evaluation of accuracy of the oxygen content measurement method*

Fig. 2.3a shows the relationship between DO and sample volume at four temperatures. The values tended to be low for larger sample volumes (300–500  $\mu\text{L}$ ). Fig. 2.3b shows the error percentage for each sample volume. It was indicated that the error percentage was relatively large with small sample volumes (50 and 100  $\mu\text{L}$ ). Since the oxygen content is corrected by the sample volume (Eq. 2.1), a small sample volume induces a large deviation. On the other hand, when the sample volume ranged from 300 to 500  $\mu\text{L}$ , the accuracy was almost the same as that of DO meter 1. The amount of sample is important not only for the correction factor but also for sufficiently increasing the oxygen level in the 2 mL deoxidized pure water. Therefore, when testing a sample with

a high oxygen content, such as a FB dispersion, a volume of 100–200  $\mu\text{L}$  is enough to obtain a good reproducibility (shown in the next section). Fig. 2.3c shows the error percentage at different temperatures. It indicated that the influence of temperature on the error percentage was smaller than that of sample volume. If the results obtained with 50  $\mu\text{L}$  sample volume excluded, the average error improves to 2.8% from 3.2%. However, a measurement error of 5% or less is acceptable; hence, quantitative measurement was validated under the conditions examined in this study.

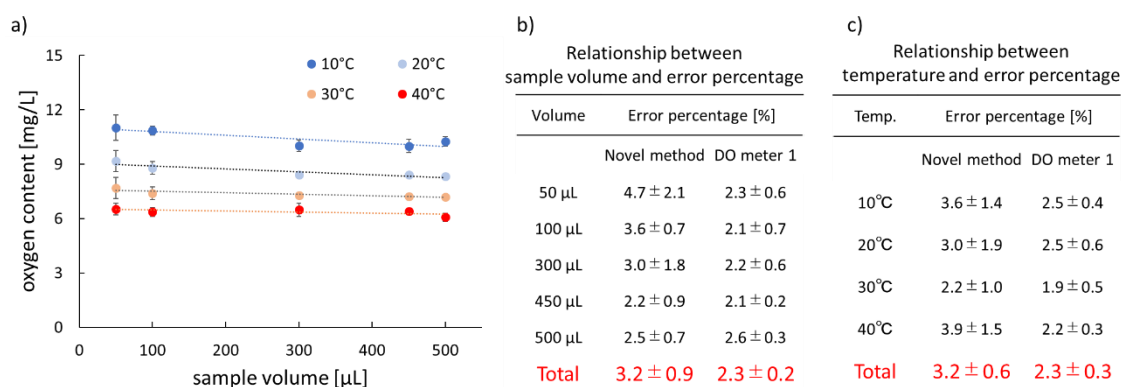


**Fig. 2.3. Error in the novel oxygen measurement method.** a) Relationship between DO and sample volume at different temperatures ( $n = 5$ ). Measurement error for different b) sample volumes ( $n = 20$ ) and c) sample temperatures ( $n = 25$ ). Data are presented as the mean  $\pm$  standard deviation (SD).

Next, I evaluated the accuracy of the novel method by comparing the values obtained from the conventional DO meters. Oxygen contents in the air-saturated pure water measured using different methods are shown in Fig. 2.4. The values obtained using this method are only  $\sim 0.5$  mg/L more or less than the values obtained using the other DO meters and the theoretical values, except for the value obtained at 40°C using DO meter 2. These results prove that this method has comparable accuracy to the present standard devices in the range of 6–12 mg/L.

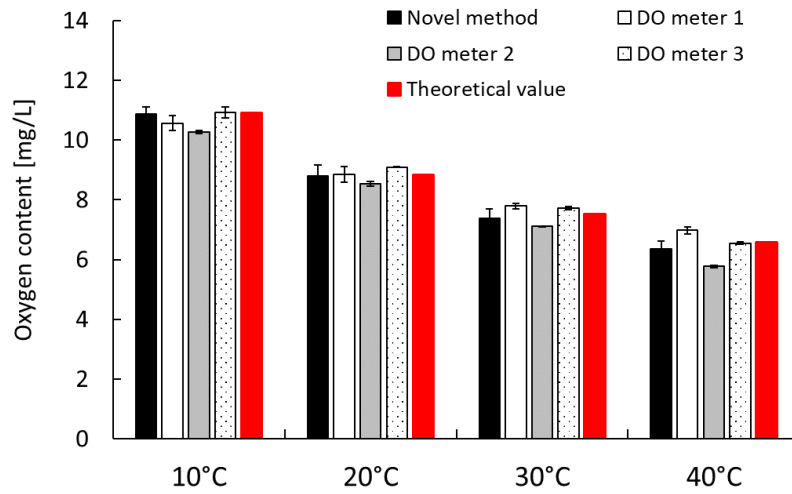


**Fig. 2.4. Accuracy of novel oxygen measurement method.** DO in air-saturated water measured using the novel method (black bars,  $n = 5$ ), DO meter 1 (white bars,  $n = 5$ ), DO meter 2 (gray bars,  $n = 5$ ), DO meter 3 (dot bars,  $n = 5$ ). Red bars represent the theoretical values. Data are presented as the mean  $\pm$  SD.

### ***Oxygen content in oxygen fine bubble dispersions***

Fig. 2.5a shows the oxygen content in oxygen FB dispersions under different temperatures. Black bars show the results obtained using the novel method, and only this method could be used to measure all the samples. Oxygen content in the FB dispersions decreased with raising temperature, and this can be correlated to the temperature dependence of DO—with temperature increase, more oxygen molecules are released from the water surface due to increased molecular dynamics. Dot bars represent the results obtained using DO meter 3, which adopts the fluorescence method, and the values are almost the same as those obtained from this method. However, DO meter 3 could not measure the oxygen contents at 20 and 15°C as the oxygen content was beyond the measurement range. Gray bars represent the results obtained using DO meter 2, which employs the galvanic electrode. It represents the oxygen contents at all the temperatures, except 15°C; I did not make the measurement at 15°C. However, the values at 20, 30, and

40°C were obviously different from those obtained using other methods. Since the measurement range of the device is 0–45 mg/L, the results at 20 and 30°C are unreliable. The white bars represent the results obtained using DO meter 1, of which measurement range is 0–20 mg/L. It could not show an accurate value at 40°C, and no result was obtained at 15–30°C. The values given by the DO meters were not stable during the measurement; thus, the instantaneous results were read visually. Furthermore, in the case of DO meter 3, it was confirmed that the value decreased when bubbles were adhered to the sensor surface. Fig 2.5a shows that DO meter 3 could measure the oxygen content in FB dispersions; however, it is necessary to pay attention to the position and orientation of the sensor. Therefore, the novel method is preferable compared to conventional DO meters for quantitative measuring the oxygen contents in FB dispersions.

Next, the oxygen content in the FB dispersion was measured using Winkler's method to confirm the accuracy of the novel method. Fig. 2.5b shows that there is no difference in the values obtained from the two methods. Although it takes more than 30 min for Winkler's method to measure the oxygen content, it is a reliable method in terms of accuracy. Therefore, this method could be used to accurately measure the total oxygen content in FB dispersions. Since Winkler's method uses chemical fixation, it is considered that the entire oxygen content in the FB dispersions can be measured. On the other hand, this method measures the oxygen content by diluting the sample. Since the sample volume is remarkably less than 2 mL deoxygenated water (approximately 1/4–1/10), most oxygen in the sample is dissolved into the deoxygenated water.

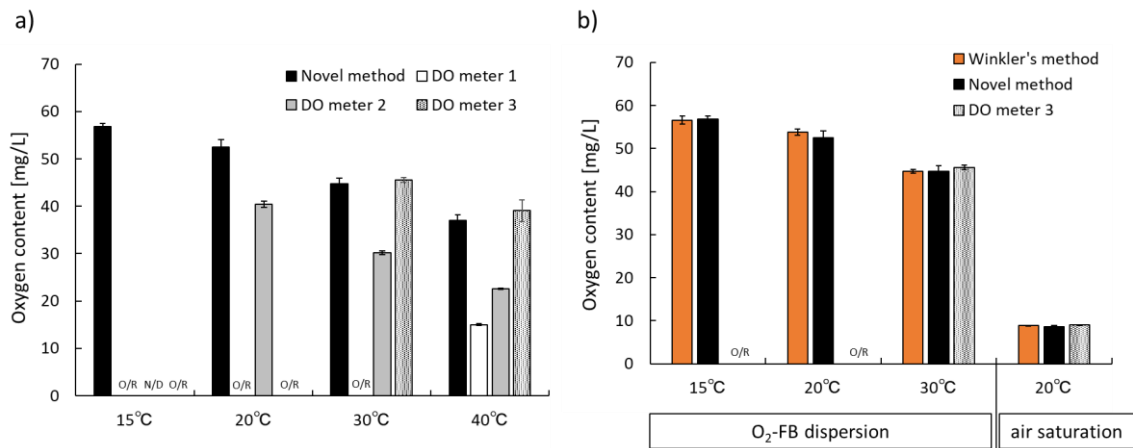


**Fig. 2.5. Oxygen content in oxygen fine bubble dispersion.** a) Oxygen content in fine bubble dispersion under different temperatures ( $n = 5$ ). b) Oxygen content in fine bubble dispersion measured using Winkler's method ( $n = 5$ ). Data are presented as the mean  $\pm$  SD. O/R and N/D mean "over the range" and "no data", respectively.

### **2.3. Evaluation of properties of oxygen fine bubbles as an oxygen carrier**

#### **2.3.1. Purpose**

Oxygen FBs are used as an oxygen carrier in various fields. However, no studies have examined the relationship between the oxygen content of the FB dispersion and the concentration of FBs in the dispersion in detail. The purpose of this study is to reveal the fundamental properties of oxygen FBs as an oxygen carrier by measuring the UFB concentration and oxygen content simultaneously. Some experiments were performed to clarify the following four aspects: 1) effects of UFB concentration on the oxygen content, 2) effects of ambient oxygen level on the oxygen content and stability of UFB, 3) effects of ambient temperature on the oxygen content and stability of UFB, 4) effects of air-water equilibrium on the oxygen content and stability of UFB. Here, “ambient” means the underwater environment around the FBs

#### **2.3.2. Materials and experimental procedures**

##### ***Oxygen content measurement***

Oxygen content in the FB dispersion was measured using the novel method, which is described in section 2.2. The sample volume was set in the range of 150–250  $\mu\text{L}$ .

##### ***Nanoparticle tracking analysis (NTA)***

The concentration and size distribution of UFB were measured by an NTA instrument (NanoSight LM10, Malvern Panalytical, Malvern, U.K.). A sample dispersion was injected into the measurement unit, and the images of the nanoparticles were recorded as a movie. A software was used to analyze the Brownian motion of each nanoparticle from the movie, and the size was calculated using the Stokes–Einstein equation. The concentration of nanoparticles was calculated from the number of nanoparticles in the captured images (movie). In this experiment, the FB dispersion was introduced into the

sample chamber through a Teflon tube (ID: 0.5 mm) by siphoning, to avoid acute pressure changes. A syringe pump (780100J, KD scientific Inc., MA, USA), which was connected to the Teflon tube, continuously pushed (5 mL/h) the sample dispersion during recording to shoot a wide field of the sample area. The following parameters were used for recording and analysis: recording time, 60 sec; camera level, 12; threshold, 6.

### ***Microparticle analysis***

The size distribution (5–1500  $\mu\text{m}$ ) of MB was determined using a particle size analyzer (PartAn SI, Microtrac-bel Corp., Osaka, Japan). The device captures images of the flowing sample, and the size distribution is calculated by image analysis. The FB dispersion was circulated at 100 rpm (90 mL/min) by a tubing pump (07528-30, Masterflex, Gelsenkirchen, Germany) between the analyzer and the container in which the FB dispersion was continuously generated.

### ***Dilution test***

The effect of ambient oxygen level on the oxygen content and stability of UFB was examined by diluting the FB dispersion with four different diluents: oxygen-saturated water, air-saturated water, nitrogen-saturated water, and degassed water (Fig. 2.6). The FB dispersions were prepared in 5 L distilled water (conductivity:  $< 5 \mu\text{S/cm}$ ) using a FB generator (GALF; Ultrafine GALF FZ1N-02; IDEC Corporation, Osaka, Japan) at 30°C. The temperature was controlled with the thermostat system, which is connected with the heater and a cooling chiller (CCA-1111, EYELA, TOKYO RIKAKIKAI CO, LTD, Tokyo, Japan). The FB dispersion was collected in a 10 mL glass vial (total volume: 14 mL) by siphoning. In order to eliminate the influence of air in the vial, the FB dispersion was overflowed at twice the volume. Then, the collected FB dispersion was left for 5 min with the rubber lid to remove the MBs. During this period, a diluent was introduced into another 10 mL vial, and the gas phase in the vial was replaced with the gas that was filled

in the diluent. After 5 min, the FB dispersion was gently injected into the diluent, and the vial was inverted up and down five times with the rubber lid. During this, the vial was completely filled with the liquid (FB dispersion and diluent), and there was no air contamination. Oxygen measurement and NTA were performed after mixing. Gas-saturated diluents were prepared by stirring and bubbling a specific gas ( $O_2$ , air, or  $N_2$ ) at room temperature (23–25 °C). Degassed water was prepared by boiling water without stirring. Samples were diluted to 2-, 5-, and 10-folds. Measurement values were compared with the value calculated from Equation 2.3.

$$\text{calculated value [mg/L]} = O_2(\text{no dilution}) \times \frac{1}{x} + DO_2(\text{diluent}) \times \frac{(x-1)}{x} \quad (2.3)$$

Here,  $O_2$  is oxygen content in an oxygen FB dispersion (mg/L),  $DO_2$  is dissolved oxygen in each diluent (mg/L),  $x$  is a dilution rate ( $x$ -fold dilution).

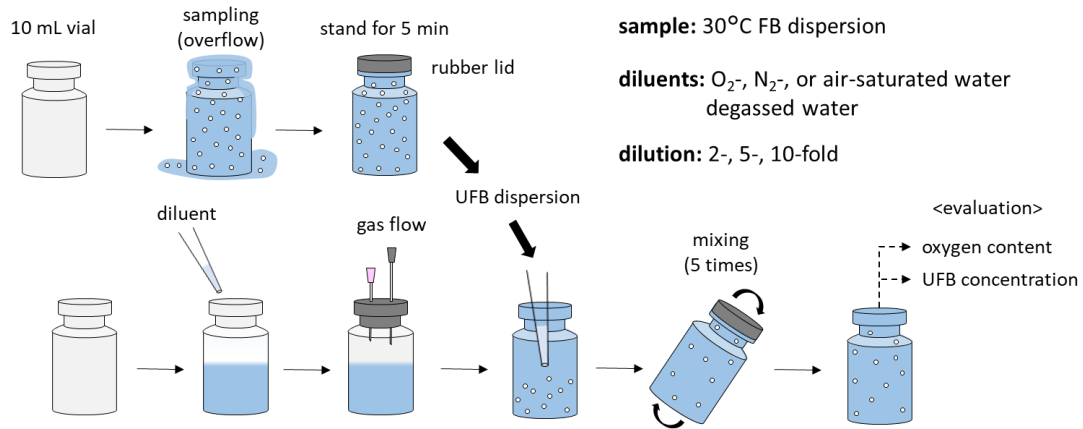


**Fig. 2.6. Schematic representation of the dilution test**

### ***Stability test of UFB dispersion***

The effects of the ambient temperature and air-liquid equilibrium on the oxygen content and stability of UFB were examined by changing the storage temperature and by removing or inserting the lid (Fig. 2.7). The UFB dispersions were generated in 5 L distilled (conductivity:  $<5 \mu\text{S/cm}$ ) water with GALF at 20, 30, and 40°C. The temperature was controlled by the same system as that mentioned in section 2.2. The UFB dispersions

were collected in 10 mL glass vials, and the body of the vials was immersed in water that was maintained at the same temperature as that during UFB generation. The UFB dispersions were stood for 15, 30, and 60 min. A new vial was prepared for each condition to eliminate the effects of the measurement procedures on the UFBs and oxygen content. These experiments were conducted both in the presence and absence of a rubber lid during storage. Under the open condition (without lid), a plastic wrap covered the storage field to ensure free mass transfer and to avoid contamination from ambient air. The oxygen content measurement and NTA were performed after each storage duration. Only under the open condition, measurements were conducted after one day.

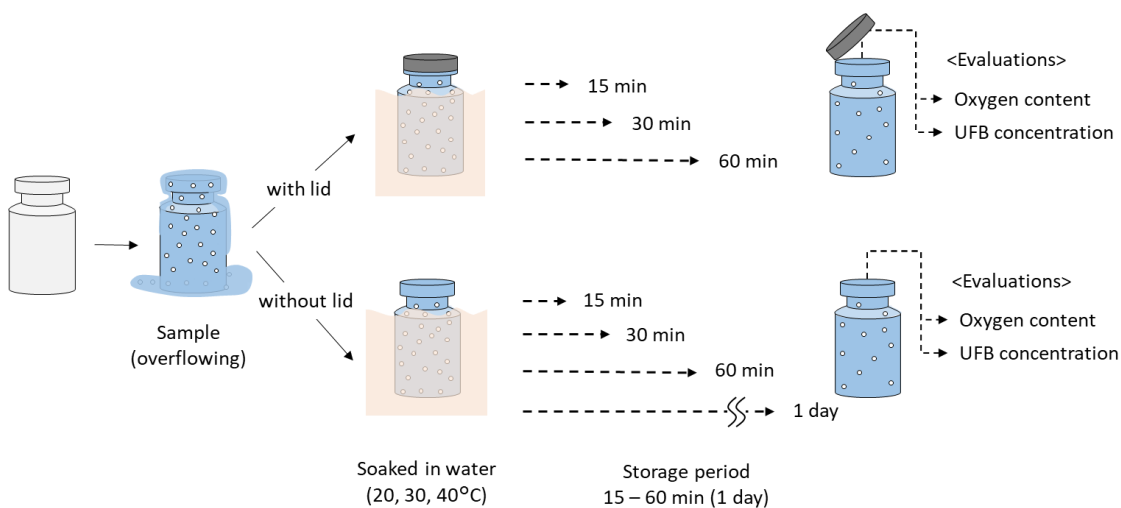


**Fig. 2.7. Schematic representation of the stability test**

### ***Stability test of oxygen-saturated water***

The change in the DO in oxygen-saturated water was evaluated over time to investigate the effect of air–water equilibrium. Oxygen-saturated water (3 L) was prepared with O<sub>2</sub> bubbling ( $0.15 \pm 0.05$  L/min) and stirring (500 rpm) for > 60 min. The storage procedure and oxygen measurement were performed under the same conditions as those used to determine the stability of the UFB dispersion.

### ***Evaluation of the change in oxygen content and fine bubble concentration***

The relationship between the oxygen content and FB concentration was evaluated by simultaneous comparison of the changes in the number of MB, UFB concentration, and oxygen contents. FB dispersions were prepared in 50 mL distilled (conductivity: < 5  $\mu\text{S}/\text{cm}$ ) water by another FB generator (FBG; FBG-OS Type 1, PMT Inc., Kanagawa, Japan) at 30°C, because the generating conditions can be changed in this device. In addition, FBG adopts a pressurized dissolution method. In this experiment, the dissolution pressure was changed to 0.3, 1.0, and 3.0 MPa. The changes in the number of MBs, UFB concentration, and oxygen contents were measured 0, 5, 15, 25, 35, 45, 55, and 65 min after starting the experiment. The operating condition of FBG were as follows: liquid flow, 50 mL/min; oxygen flow, 25 mL/min (void fraction: 50%); dissolution pressure, 0.3, 1.0, or 3.0 MPa.

### **2.3.3. Results and discussion**

#### ***Dilution test***

Fig. 2.8 shows the oxygen content and UFB concentration in the diluents. The oxygen content in gas-saturated water was reasonable whereas that in degassed water was slightly higher than the predicted value. This is because degassed water easily absorbs oxygen from ambient air during the experiments (Fig. 2.6). Although sonication and vacuuming are generally used in combination for degassing, it was not possible to adopt this approach in this experiment due to the excess generation of UFB ( $> 1.0 \times 10^8$  particles/mL) in this method. Therefore, the degassed water was prepared by boiling to reduce the generation of UFB, although a trace amount of UFB may generate during boiling. Fig. 2.8b shows the nanoparticle concentration in diluents, and there are  $7.0 \times 10^6$  to  $3.5 \times 10^7$  nanoparticles/mL. Since only  $2.5 \times 10^6$  nanoparticles/mL were detected in the

untreated distilled water, it is considered that some UFBs were generated or the diluents were contaminated with nanoparticles while preparing the diluents. These values were used as the background values and subtracted from the experimentally determined UFB concentration. Although the background values seem high, they are reasonable. This is because the presence of one nanoparticle in a picture significantly would affect the value of the total concentration obtained using the NTA instrument.

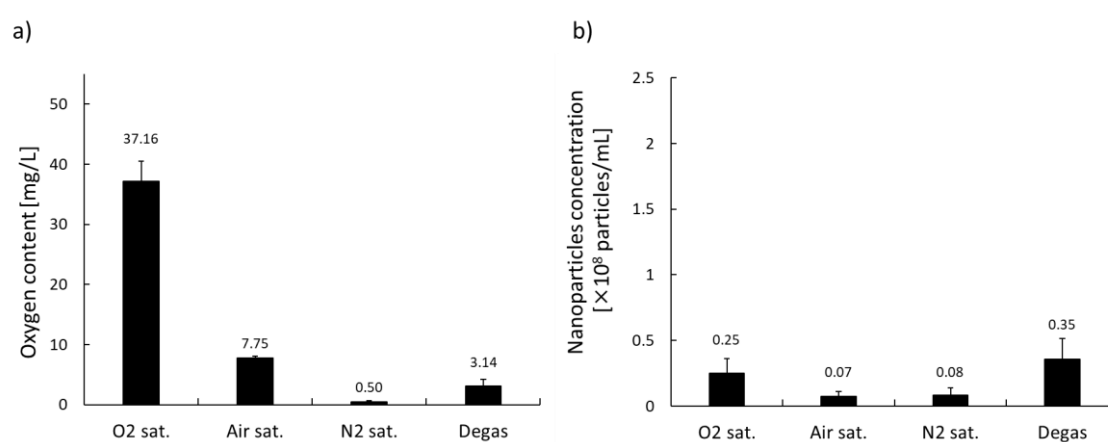


**Fig. 2.8. Physical properties of diluents.** a) oxygen content in diluents ( $n = 3$ ). b) Concentration of nanoparticles in diluents ( $n = 3$ ). Data are presented as the mean  $\pm$  SD.

Fig. 2.9a shows the oxygen content in the FB dispersion diluted with four different diluents. No dilution means the oxygen content in original FB dispersion, and four bars denote the same sample measured on different day. Discontinuous red bars are the calculated values. Since there is no difference between the measured values and calculated values, it was concluded that the dilution was performed accurately, and no oxygen was released from the liquid. However, the oxygen content in the UFB dispersion diluted with oxygen saturated water maintained the high oxygen content ( $>80\%$  of that without dilution), even the UFB concentration decreased lower than 20%. It means that influence of UFB itself was smaller than that of the dissolved oxygen in the diluents.

Fig. 2.9b shows the UFB concentration in the diluted UFB dispersion. Although

the UFB concentration decreased with the dilution rate in all the experiments. The measured values tended to be higher than the calculated values in the experiment with gas-saturated diluents ( $O_2$ , Air, or  $N_2$  saturated water). Although the differences were marginal, a similar phenomenon was reported in a conference proceeding<sup>26</sup>. This was probably due to the generation of a small amount of UFBs while mixing the FB dispersion with the diluent. Previous studies have shown that UFB can be generated by mixing two solutions with different gas solubilities such as ethanol and water<sup>27,28</sup>. Since this phenomenon also occurs in the combination of water and salt water<sup>29</sup>, UFBs may be generated while mixing FB dispersion and gas-saturated diluents.

On the other hand, in the experiment with degassed water, the UFB concentration was lower than the calculated value. In other words, some of the UFBs disappeared upon diluting with degassed water. Tuziuti *et al.* reported a similar result—the volumetric concentration of air-UFBs decreased in degassed water<sup>30</sup>. This is an interesting phenomenon and suggests that gas diffuses inside and outside the UFBs. Thus, it is possible that a portion of the internal gas in the UFBs is replaced with ambient gas. The effect of ambient gas content on the stability of MBs, not UFBs, have been reported by Iwakiri *et al.*<sup>31</sup>. However, this is the first experiment to simultaneously evaluate the effect of ambient gas content on the oxygen content and stability of UFBs.

Fig. 2.9c shows the change in size upon dilution. The size of UFBs tends to decrease upon dilution, except for the case of oxygen-saturated water. It is suggested that oxygen diffuses from the interior of the UFB to the dispersion medium. However, the average size and variation were large at 10-fold dilution and 5-fold dilution with degassed water. It is considered that the UFB concentration dropped to the background concentration, and the influence of contaminant particles (80–300 nm) on the average particle size increased. When NanoSight is used to examine the UFB size, it is necessary to secure at least  $5.0 \times$

$10^7$  particles/mL. Since the size of the UFB has a significant influence on the volume of the UFBs, it is difficult to discuss the volume change in this experiment.

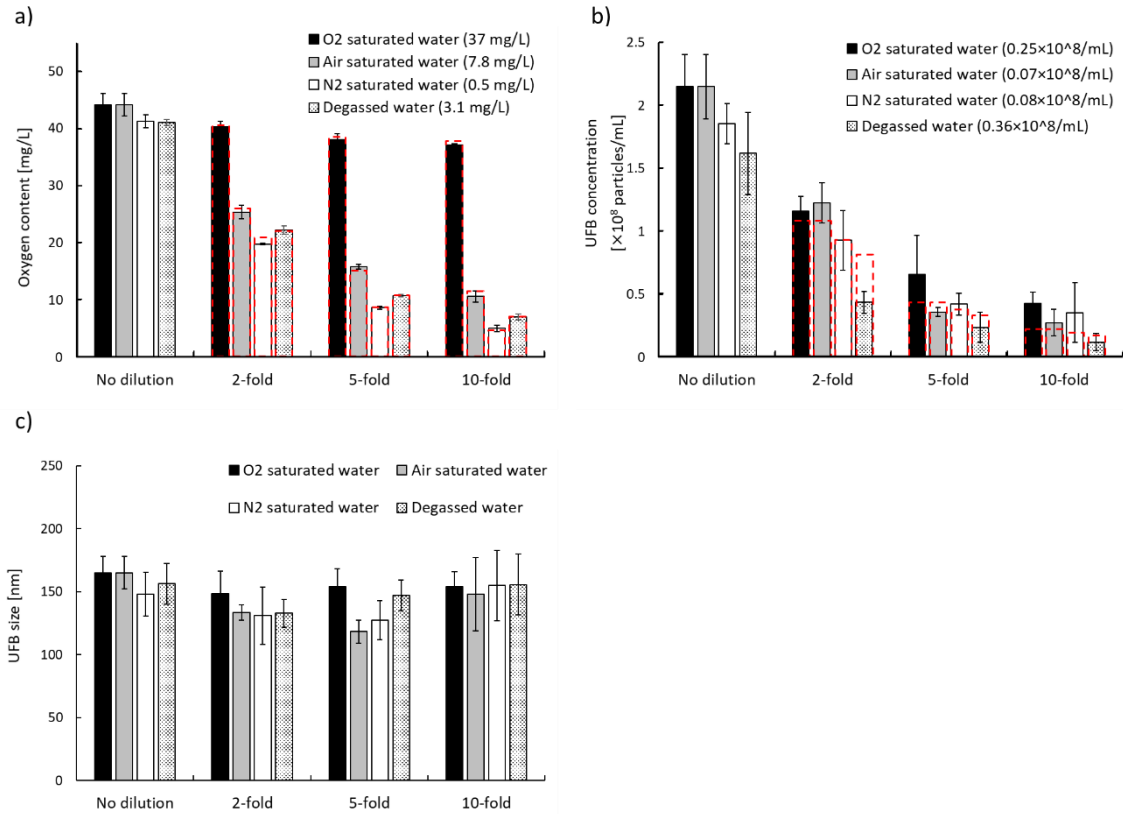
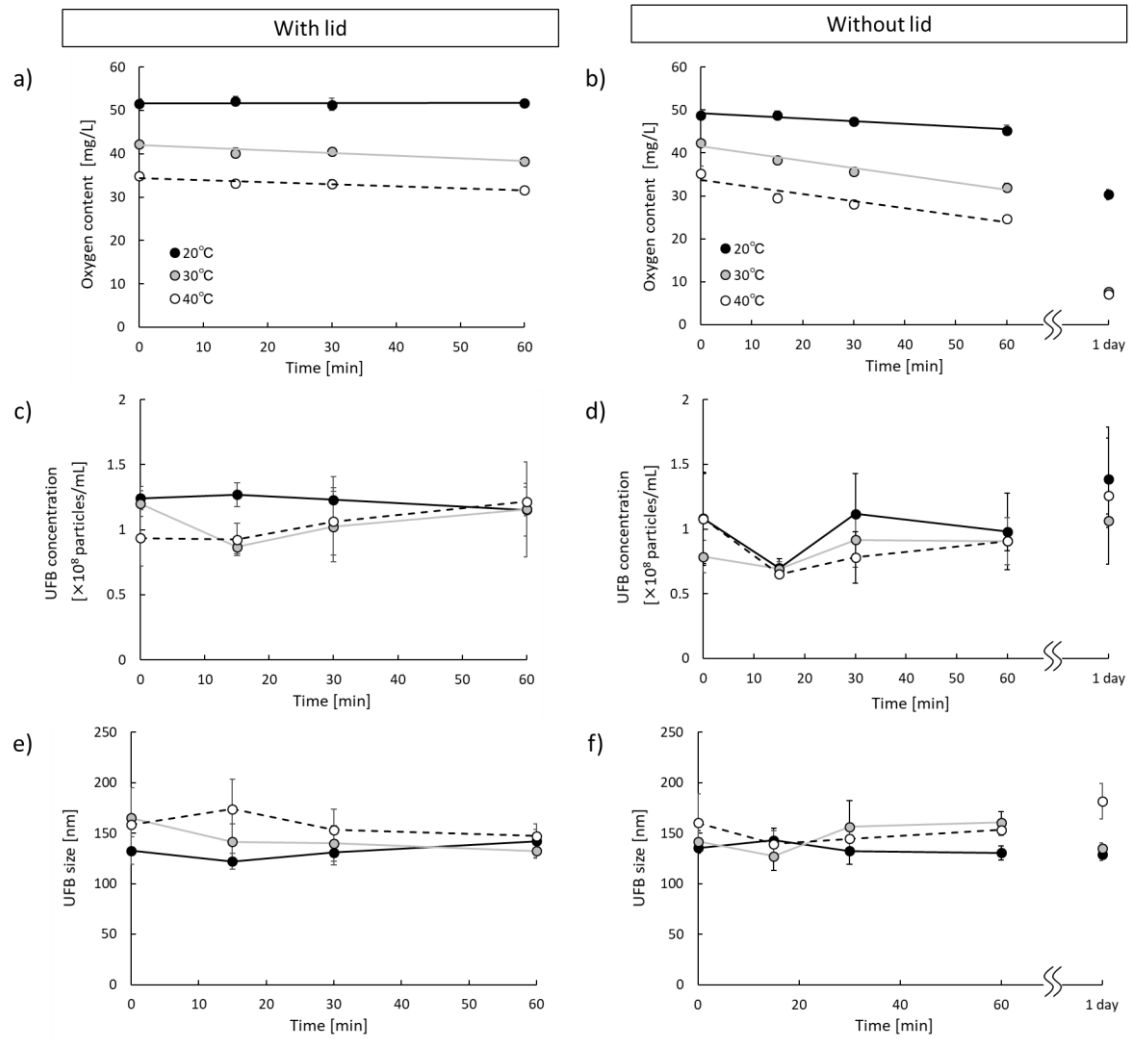


**Fig. 2.9. Stability of UFB dispersion after dilution.** Change in a) oxygen content, b) UFB concentration, and c) average size of UFB ( $n = 3$ ). Discontinuous red bars are calculated values. Data are presented as the mean  $\pm$  SD.

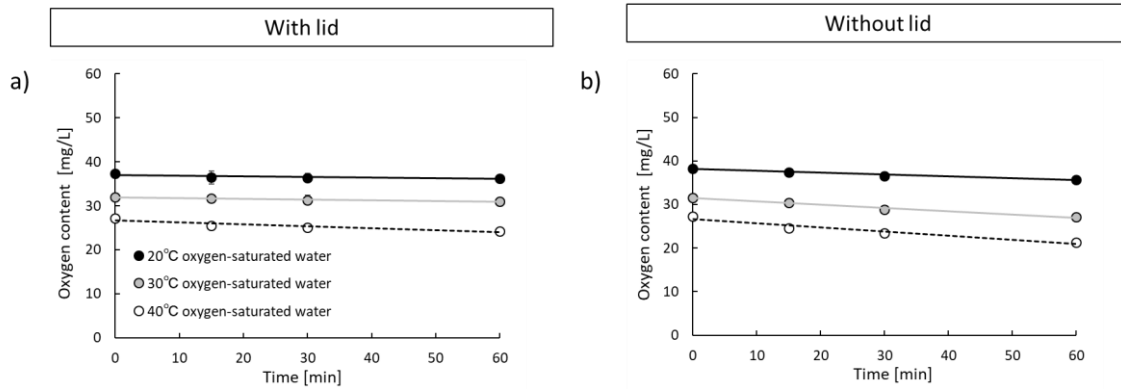
### *Stability test for FB dispersion*

Fig. 2.10a and b show the time change of the oxygen contents in the FB dispersions that were stored with or without a lid. The lid prevented the decrease in the oxygen content; particularly, there was no change at 20°C (Fig. 2.10a). On the other hand, the oxygen content decreased over time without the lid and dropped to a value lower than that of the oxygen-saturated state after one day (Fig. 2.10b). This behavior was the same as that for oxygen-saturated water (Fig. 2.11). Comparing the decreasing rate in oxygen content of the UFB dispersions and oxygen-saturated water, the former decreased their

oxygen 1.5 to 2 times faster than the latter without the lid; whereas, there was no difference between them with the lid. It is thought to be because the difference between the oxygen partial pressure in the liquid and that in the atmospheric air is greater in the case of the UFB dispersions. In other words, it was suggested that oxygen in the UFB dispersion behaves similarly to dissolved oxygen, and UFB has a small effect on the decrement of oxygen due to air-liquid equilibrium. However, the FB dispersion remained in a supersaturated state for 30 min even without the lid. Fig. 2.10c and d show the change in UFB concentration; there was almost no change for 60 min under both the conditions. Interestingly, the UFB concentration without the lid tended to increase after one day, in contrast to the change in the oxygen content. The reason for the increase in the number of UFBs was not clarified. However, raw data showed that one out of the three data of UFB concentrations significantly increased at 20 and 40°C, and it affected the average values. Since the size of the UFBs did not change after one day (Fig. 2.10f), it is unlikely that the bubbles went under fission and increased in number. Ulatowski *et al.* showed that the nitrogen- and oxygen-UFBs were stable for over 10 days, and it did not depend on the presence or absence of a lid. However, they discussed the stability of the UFBs with respect to the size and zeta potential and did not measure the UFB concentration directly<sup>32</sup>. Since I measured the UFB concentration in this experiment, I could provide a strong evidence to support their argument and some additional information on the oxygen content. These results indicated that there was no relationship between the change in the UFB concentration and the oxygen content.



**Fig. 2.10. Stability of UFB dispersion with or without lid.** Change over time in the a) oxygen content, c) UFB concentration, and e) UFB size in the UFB dispersion stored with lid (n = 3). Change over time in the b) oxygen content, d) UFB concentration, and f) UFB size in the UFB dispersion stored without lid (n = 3). Data are presented as the mean  $\pm$  SD.



**Fig. 2.11. Change in the DO in oxygen-saturated water stored with or without lid.**

Change over time in the DO in oxygen-saturated water stored a) with lid and b) without lid ( $n = 3$ ). Data are presented as the mean  $\pm$  SD.

***Evaluation of the change in oxygen content and fine bubble concentration***

The relationship between MB, UFB, and oxygen content was evaluated using an FB generator that could be used to change the preparation conditions. Fig. 2.12a and b show the change in the oxygen content and the number of MB up to 65 min after starting the operation. The oxygen content and the number of MBs reached saturation after 5 min. Both the parameters increased with increasing dissolution pressure (from 0.3 to 3.0 MPa). Although it seemed that there is a good correlation between the two parameters, these results were not enough to prove the relationship. On the other hand, the UFB concentration gradually increased and did not reach saturation till 65 min. Furthermore, the values varied for each measurement, although the increasing trend was confirmed for all the cases (Fig. 2.12c).

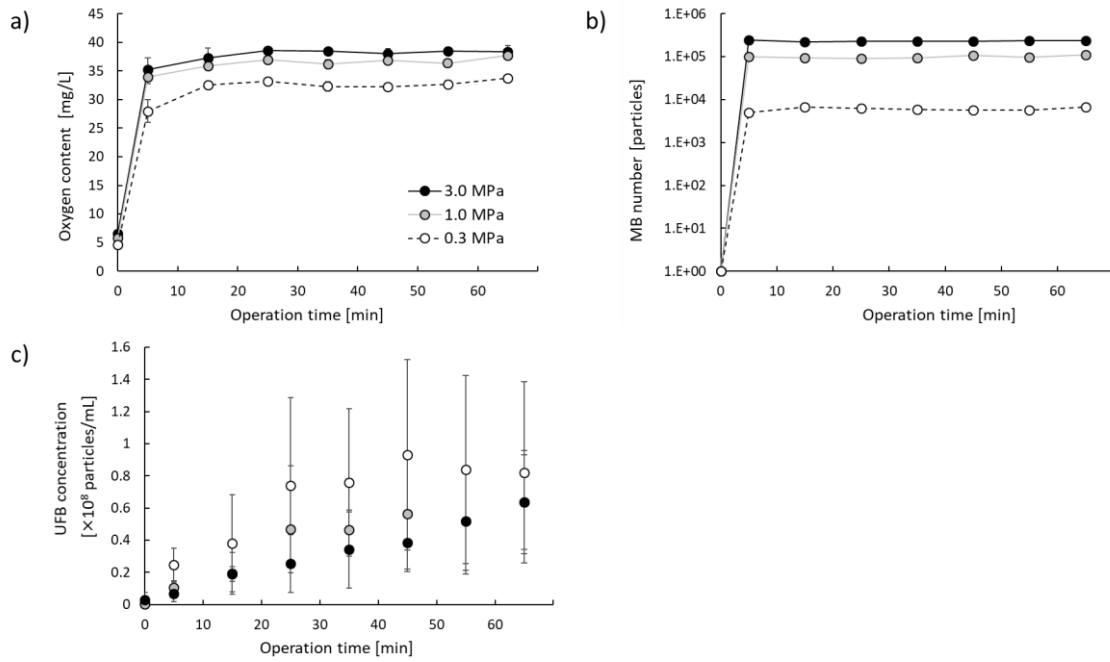


**Fig. 2.12. Changes in the oxygen content and FBs during device operation.** Changes in the a) oxygen content, b) number of MBs, and c) UFB concentration over time during FB generation ( $n = 3$ ). Data are presented as the mean  $\pm$  SD.

During the evaluation of relationship between FB and oxygen content, some macro bubbles which were not detected via particle measurement devices, were visually observed in the FB dispersion. It is believed that oxygen content in FB dispersion could be increased by reducing the generation of macro bubbles that float up rapidly. For macro bubbles are generated from supersaturated water, known as champagne phenomenon, pressure difference is important for controlling the density and size of the bubbles<sup>32</sup>. Therefore, in order to alleviate sudden pressure release and reduce the generation of macro bubbles, decompression method after a back-pressure regulator (BPR) was changed (Fig. 2.13a). It was speculated that the sudden pressure release could be alleviated by reducing the diameter of the discharge tube to increase the flow resistance. Thus, the inner diameter of the discharge tube was changed from 1 mm to 0.5 mm, and the MB, UFB, and oxygen contents were evaluated once again (Fig. 2.13).

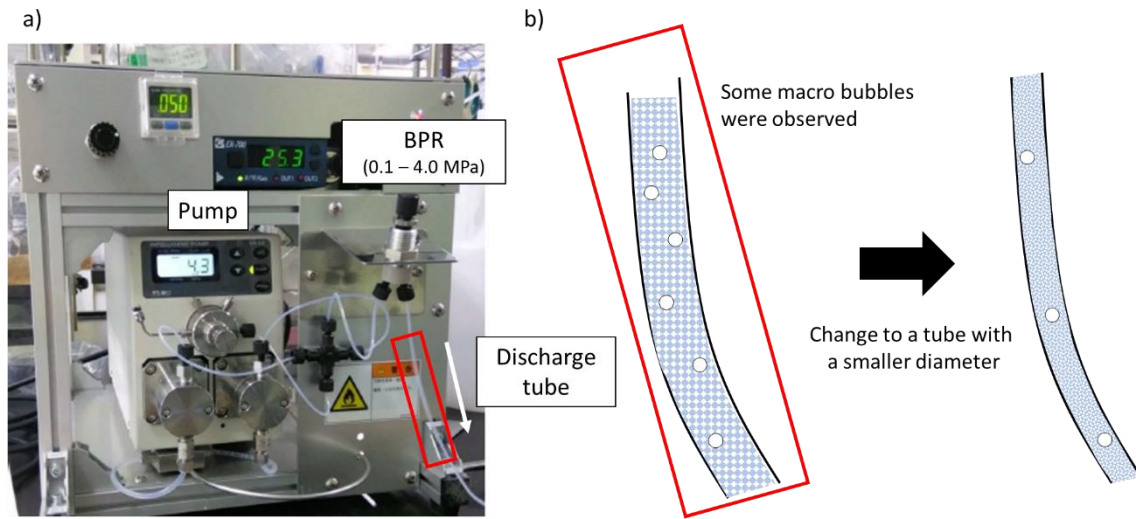


**Fig. 2.13. Issue in FB generator.** a) A picture of a FB generator (FBG; FBG-OS Type 1, PMT Inc., Kanagawa, Japan) that can be used to change some parameters of the generating conditions. b) Issue in FBG: Some macro bubbles are generated with FBs, and they may lead to the wastage of oxygen for FB formation and decrease the oxygen content.

Fig. 2.14 shows the oxygen content, number of MB, and UFB concentration before and after changing the discharge tube. The oxygen content increased by 29%, while the number of MB decreased by 22%. The oxygen content was the highest of those which had observed ever; however, the results were contrary to the hypothesis in previous experiment that there is a positive correlation between the number of MBs and oxygen content (Fig. 2.12).

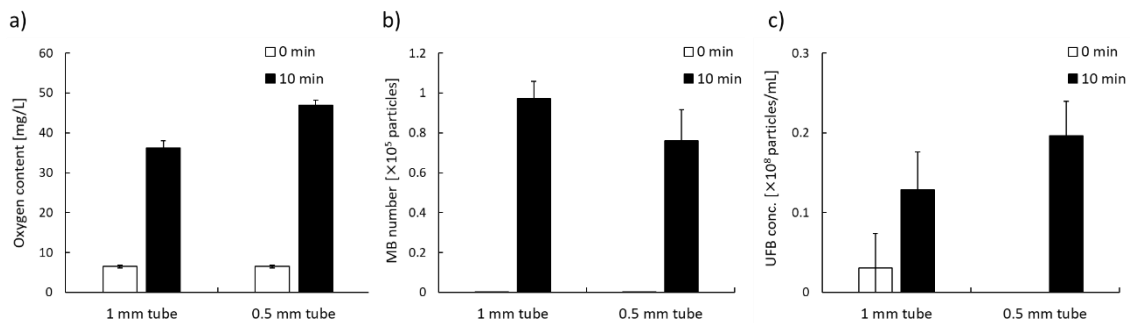


**Fig. 2.14. Effect of the diameter of discharge tube on FBs and oxygen content.** a) Oxygen content, b) number of MBs, and c) UFB concentration before and after changing

to a discharge tube with a smaller diameter ( $n = 3$ ). White bars show the results before operation and black bars show the results 10 min after generation. Data are presented as the mean  $\pm$  SD.

The results in Fig. 2.14 suggested that the oxygen content in the FB dispersion increased by suppressing the generation of MBs. Considering the principle of the pressure dissolution method for FBG, the DO is the highest immediately before decompression. MBs and UFBs were generated from a portion of the supersaturated oxygen. Therefore, unless the MBs remain stable for a long time in the dispersion, it is better to suppress the amount of MBs generated in order to increase the oxygen content. Previous studies have shown that MBs shrink because the enclosed gas dissolve in the surrounding liquid<sup>30,33</sup>. However, in the experiments, the dispersion media were air-saturated water and degassed water, and not oxygen-saturated water. Therefore, the MBs actively behave as an oxygen carrier when the dispersion medium has not reached oxygen saturation. Moreover, since

the internal pressure of MBs is slightly higher than atmospheric pressure (Table 2.1), the dispersion becomes slightly supersaturated. In this experiment, the dispersion medium was already beyond supersaturation when the MBs were generated. Furthermore, since the average size of the MBs was  $62 \pm 4 \mu\text{m}$ , and it was confirmed that MBs disappeared within 5 min, the contribution of MBs to the oxygen content was considered minor in this experiment.

Table 2.1 Internal pressure of micro bubble

Size [ $\mu\text{m}$ ]	Internal pressure <sup>1</sup> [atm]	Floating speed <sup>2</sup> [cm/min]
100	1.03	40.6
50	1.06	10.1
30	1.10	3.65
20	1.14	1.62
10	1.29	0.41
5	1.57	0.10
1	3.87	0.004

100

50

30

20

10

5

1

1: calculated by Young-Laplace equation (at 30°C)

2: calculated by Stoke's law (at 30°C)

Although it is said that UFBs are excellent oxygen carriers due to their high internal pressure<sup>25</sup>, there was no correlation between the UFB concentration and oxygen content

in this experiment. The high oxygen content in the FB dispersion is considered to be supersaturated dissolved oxygen formed during the FB generation process. It is because the volume of the UFBs was too small to increase the oxygen content in the dispersion medium. For instance, even if there are  $2 \times 10^8$  particles/mL of 150 nm UFB in a liquid, their total volume is only 0.00004% of the volume of dispersion, with 0.0005 mg/L of oxygen content. This is a trace amount of oxygen, even when considering that the internal pressure is 20 atm in 150 nm UFB. However, since UFBs do not float up and remain stable in liquid for several days, oxygen content in the liquid is dependent on the concentration of the UFBs.

## **2.4. Conclusions of this chapter**

This chapter covers two topics: (a) development of a novel method to measure the oxygen content and (b) fundamental properties of FBs as an oxygen carrier. The important findings in these two topics are summarized below.

### ***1) Development of a novel oxygen content measurement method***

The novel method could be used to quantitatively measure the oxygen content in the FB dispersion. This method is easy (4 steps) and rapid (< 8 min). The measurement range is wide (0–320 mg/L), and very low sample volumes (50–500  $\mu$ L) are required. Therefore, this is superior to any conventional methods for measuring the oxygen content in FB dispersions.

### ***2) Fundamental properties of FB dispersion as oxygen carrier***

I revealed four aspects of oxygen UFBs: 1) there was no relationship between the UFB concentration and oxygen content in FB dispersion within the range of  $10^8$ - $10^9$  particles/mL; 2) the apparent UFB concentration was not influenced by the ambient oxygen level, but UFBs disappeared when diluted with degassed water; 3) the UFB concentration did not change in the temperature range of 20–40°C, but the oxygen content in the FB dispersion was dependent on temperature as well as general dissolved oxygen; 4) gas equilibrium at the air-water interface did not affect the stability of the UFBs but affected the oxygen content in FB dispersion. Furthermore, it was found that there is no positive correlation between the oxygen content and the amount of MBs. FB generators are excellent devices for preparing a large amount of supersaturated water in a short time. However, the oxygen originated from the FBs did not contribute to the oxygen content in the dispersion

## References

1. Kitano, Y. Dissolved oxygen measurement method for freshwater and seawater (Japanese). *BUNSEKI KAGAKU* **13**, 573–577 (1964).
2. Wetze, R. G. & Likens, G. E. Dissolved Oxygen. in *Limnological Analyses* (eds. Wetze, R. G. & Likens, G. E.) 73–84 (Springer, 2000).
3. William, H. Experiments on the Quantity of Gases Absorbed by Water , at Different Temperatures , and under Different Pressures. *Philos. Trans. R. Soc. London* **93**, 29–42 (1803).
4. Miyao, T., Shinichiro, U., Yusuke, T. & Naoki, N. Accuracy improvement of dissolved oxygen measurement (Japanese). *Weather Serv. Bull.* **80**, 149–157 (2013).
5. Miller, J. A field method for determining dissolved oxygen in water. *J. Soc. Chem. Ind.* **33**, 185–186 (1914).
6. Carpenter, J. H. New measurements of oxygen solubility in pure and natural water. *Limnology Oceanogr.* **11**, 264–277 (1966).
7. Saito, H., Uchoyama, H. & Tanaka, Y. A Measurement of Oxygen Solubility in Pure Water (Japanese). *Japan J. water Pollut. Res.* **6**, 237–244 (1983).
8. HORIBA. Diaphragm Electrode Method. *HORIBA Ltd.* 1–2 (2020).
9. HORIBA. Fluorescence method. *HORIBA Ltd.* 1 (2020).
10. Matsuki, N. *et al.* Oxygen supersaturated fluid using fine micro/nanobubbles. *Int. J. Nanomedicine* **9**, 4495–4505 (2014).
11. Ushikubo, F. Y. *et al.* Evidence of the existence and the stability of nano-bubbles in water. *Colloids Surfaces A Physicochem. Eng. Asp.* **361**, 31–37 (2010).
12. Terasaka, K., Himuro, S., Ando, K. & HATA, T. *Introduction to Fine Bubble Science and Technology*. (NIKKAN KOGYO SHIMBUN,LTD., 2016).

13. Ebina, K. *et al.* Oxygen and Air Nanobubble Water Solution Promote the Growth of Plants, Fishes, and Mice. *PLoS One* **8**, e65339 (2013).
14. Ushikubo, F. Y. *et al.* Evidence of the existence and the stability of nano-bubbles in water. *Colloids Surfaces A Physicochem. Eng. Asp.* **361**, 31–37 (2010).
15. Cavalli, R. *et al.* Preparation and characterization of dextran nanobubbles for oxygen delivery. *Int. J. Pharm.* **381**, 160–165 (2009).
16. Swanson, E. J., Mohan, V., Kheir, J. & Borden, M. A. Phospholipid-stabilized microbubble foam for injectable oxygen delivery. *Langmuir* **26**, 15726–15729 (2010).
17. Zhao, W. *et al.* Oxygen release from nanobubbles adsorbed on hydrophobic particles. *Chem. Phys. Lett.* **608**, 224–228 (2014).
18. Kakiuchi, K. *et al.* Establishment of a total liquid ventilation system using saline-based oxygen micro/nano-bubble dispersions in rats. *J. Artif. Organs* **18**, 220–227 (2015).
19. Ohnari, H. *All about microbubble (Japanese)*. (NIPPON JITSUGYO PUBLISHING, 2006).
20. Takahashi, M. *et al.* Effect of shrinking microbubble on gas hydrate formation. *J. Phys. Chem. B* **107**, 2171–2173 (2003).
21. Khuntia, S. & Majumder, S. K. Microbubble-aided water and wastewater purification: a review. *Rev. Chem. Eng.* **28**, 191–221 (2012).
22. Mase, N., Mizumori, T. & Tatemoto, Y. Aerobic copper / TEMPO-catalyzed oxidation of primary alcohols to aldehydes using a microbubble strategy to increase gas concentration in liquid phase reactions. *Chem Comm* **47**, 2086–2088 (2011).
23. Matsuki, N. *et al.* Blood oxygenation using microbubble suspensions. *Eur*

- Biophys J* **41**, 571–578 (2012).
24. Noguchi, T. *et al.* Oxygen ultra-fine bubbles water administration prevents bone loss of glucocorticoid-induced osteoporosis in mice by suppressing osteoclast differentiation. *Osteoporos. Int.* **28**, 1063–1075 (2017).
  25. Matsuoka, H. *et al.* Administration of oxygen ultra-fine bubbles improves nerve dysfunction in a rat sciatic nerve crush injury model. *Int. J. Mol. Sci.* **19**, (2018).
  26. Alheshibri, M., Qian, J., Jehannin, M. & Craig, V. S. J. A History of Nanobubbles. *Langmuir* **32**, 11086–11100 (2016).
  27. Jadhav, A. J. & Barigou, M. Bulk Nanobubbles or Not Nanobubbles : That is the Question. *Langmuir* **36**, 1699–1708 (2020).
  28. Millare, J. C. & Basilia, B. A. Nanobubbles from Ethanol-Water Mixtures : Generation and Solute Effects via Solvent Replacement Method. *Chem. Sel.* **3**, 9268–9275 (2018).
  29. Guo, W. *et al.* Investigation on nanobubbles on graphite substrate produced by the water-NaCl solution replacement. *Surf. Sci.* **606**, 1462–1466 (2012).
  30. Tuziuti, T., Yasui, K. & Kanematsu, W. Influence of addition of degassed water on bulk nanobubbles. *Ultrason. - Sonochemistry* **43**, 272–274 (2018).
  31. Iwakiri, M. *et al.* Mass Transfer from a Shrinking Single Microbubble Rising in Water (Japanese). *JAPANESE J. Multiph. FLOW* **30**, 529–535 (2017).
  32. Ulatowski, K., Sobieszuk, P., Mróz, A. & Ciach, T. Stability of nanobubbles generated in water using porous membrane system. *Chem. Eng. Process. Process Intensificatio* **136**, 62–71 (2019).
  33. Jin, J., Feng, Z., Yang, F. & Gu, N. Bulk Nanobubbles Fabricated by Repeated Compression of Microbubbles. *Langmuir* **35**, 4238–4245 (2019).

## **Chapter 3: Evaluation and improvement of total liquid ventilation system with oxygen fine bubble dispersion**

### **3.1. Background of this chapter**

3.1.1. Total liquid ventilation system with perfluorocarbons

3.1.2. Total liquid ventilation system with oxygen fine bubble dispersion

### **3.2. Short-time total liquid ventilation test with oxygen fine bubble dispersion and gas liposome dispersion**

3.2.1. Purpose

3.2.2. Materials and experimental procedures

3.2.3. Results and discussion

### **3.3. Improvement of the total liquid ventilation system with oxygen fine bubble dispersion**

3.3.1. Purpose

3.3.2. Materials and experimental procedures

3.3.3. Results and discussion

### **3.4. Conclusions of this chapter**

### **References**

### 3.1. Background of this chapter

#### 3.1.1. Total liquid ventilation system with perfluorocarbons

In the initial period of liquid ventilation (LV) research (1962–1973), there were two techniques: “total body immersion” and “gravity-assisted liquid ventilation.” In the former technique, an animal was submerged and made to spontaneously breathe inside a solution in a hyperbaric container<sup>1</sup>. A total LV (TLV) system using water-head pressure was designed. A TLV experiment was conducted in a hyperbaric chamber, wherein a few people and an animal could be accommodated<sup>2,3</sup>. Even after the development of perfluorocarbons (PFCs), the same techniques were used for several years<sup>4-6</sup>. In 1974, Shaffer *et al.* developed a demand-regulated TLV system with PFCs (time-cycled and pressure-limited TLV system) to perform sufficient gas exchange. The system consists of 1) an electrically operated pump, 2) a liquid regenerator with a heater, 3) a pressure and temperature transducer, 4) solenoid valves, 5) flow control valves, and 6) a respiration controller<sup>7</sup>. They reported that the delivery of oxygen and removal of carbon dioxide (CO<sub>2</sub>) were improved when the TLV system was used, although the tendency toward progressive hypercarbia still existed<sup>7-9</sup>. Thereafter, methods that were based on Shaffer’s system were widely used for various animal experiments<sup>10-14</sup>. Moreover, the system was refined with the computer-controlled system to select time-cycled, pressure-limited and volume-limited regulation, as well as mechanical gas ventilation (MGV) system<sup>15-17</sup>. In 2003, Matsuda *et al.* developed a TLV system for rodents (Fig. 3.1a) and evaluated the influence of respiratory conditions on hemodynamics, gas exchange, and airway pressure. This experiment provided valuable information for deciding the optimal respiratory conditions for other experiments<sup>13</sup>. Micheau *et al.*, who are mechanical engineers, have developed a TLV system for large animals, including humans (Fig. 3.1b). Their current system (Inolivent-6, <http://www.inolivent.ca/>) has reached a readiness level for clinical

applications. It can be manipulated with a touch-panel display, like a conventional MGTV device<sup>18</sup>. Their device allowed ventilation control with several parameters: tidal volume, respiratory pressure, oxygen concentration in PFCs, and positive end expiratory pressure<sup>18,19</sup>. They collaborated with medical doctors for many years and reported some papers on animal experiments<sup>9</sup>; thus, they are one of the most advanced researchers in TLV research with PFCs.

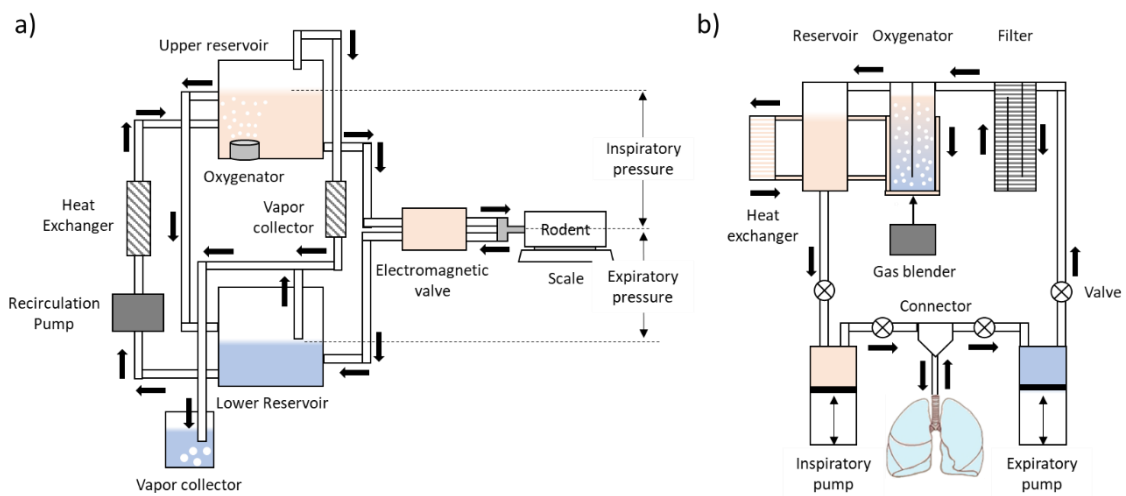


**Fig. 3.1. Schematic illustration of total liquid ventilation systems with perfluorocarbons.** The structure of a) the time-cycled, pressure-limited TLV system designed by Matsuda *et al.*<sup>13</sup> and b) the newest TLV system developed by Micheau *et al.*<sup>9</sup>

### 3.1.2. Total liquid ventilation system with oxygen fine bubble dispersion<sup>20</sup>

Few papers about TLV systems using other liquids, except PFCs, have been reported since 1966. I constructed a pressure-limited, time-cycled TLV system with fine bubble (FB) dispersions, derived from the Matsuda's device in 2015 (Fig. 3.2a). The system was concise and composed of 1) two liquid containers, 2) two electromagnetic valves with digital timers, 3) a bubble generator, and 4) a tracheal tube. By changing medium from PFCs to saline, we no longer needed a re-circulation system, filters, and

tight connections of the parts. Thus, a new system was developed. As saline is an inexpensive material, fresh liquid can be used with each breath; moreover, as saline has high surface tension (72 dyne/cm), leakage from the connection part is not a concern. However, the 1<sup>st</sup> generation TLV system with FB dispersion had disadvantages in the contamination of macro bubbles and a temperature regulation system. Oue in Takeoka laboratory improved the TLV system to overcome these issues by introducing an electronic cooling chiller and overflow system in the inspiratory line (Fig. 3.2b). Furthermore, she evaluated the effect of buffer solutions by using phosphate-buffered saline (PBS) or dialysate instead of saline, which solved the issue of the increment of PaCO<sub>2</sub> during TLV. However, metabolic acidosis owing to severe hypoxia remained a major issue<sup>21</sup>.

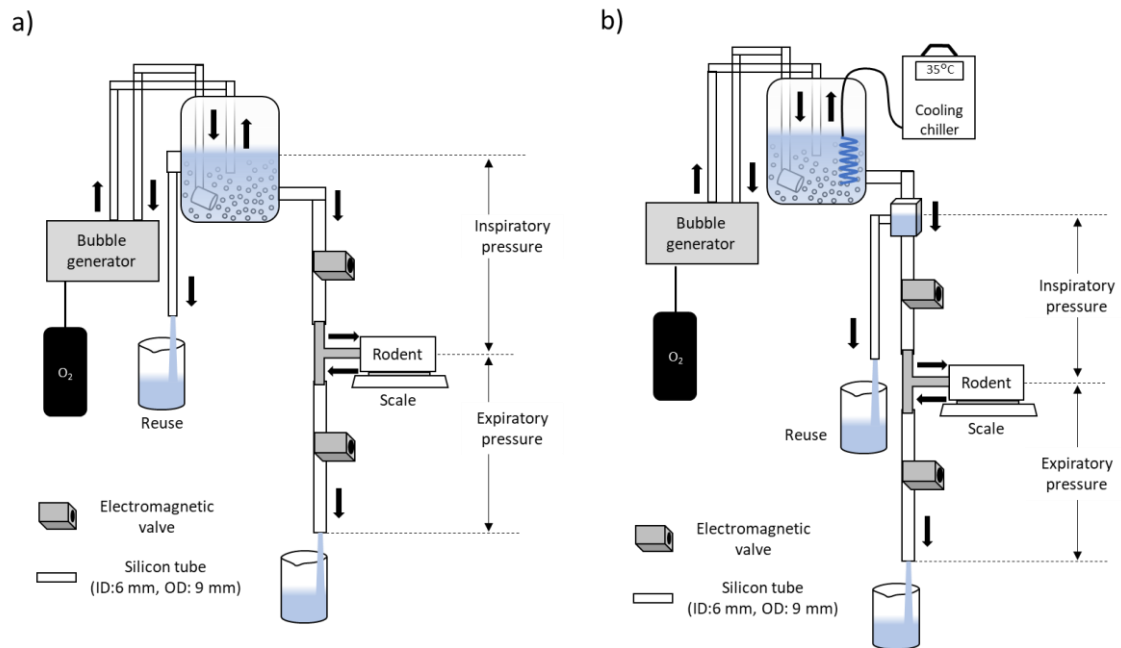


**Fig. 3.2. Schematic illustration of the TLV systems designed in our laboratory.** The structure of a) the 1<sup>st</sup> generation TLV system with fine bubbles (FB) dispersion, and b) the 2<sup>nd</sup> generation TLV system with FB dispersion

## **3.2. Short-time total liquid ventilation test with oxygen fine bubble dispersion and gas liposome dispersion**

### **3.2.1. Purpose**

#### ***Experiment 1 (Exp. 1)***

The TLV system with FB dispersion has been evaluated from the viewpoint of the lifetime of rats during TLV. However, assuming an application for lung lavage, the therapeutic effect is expected to be obtained in a short time with the TLV system. Thus, the purpose of this experiment is to evaluate the conditions of the rats after 5- or 15-min TLV and decide the treatment time for lung lavage.

#### ***Experiment 2 (Exp. 2)***

It is a crucial issue to increase the oxygen supply during TLV to avoid hypoxemia condition. Gas liposomes (GLs) are stabilized MB with a lipid layer and have a high potential for delivering a copious amount of oxygen (50–90 vol%)<sup>22</sup>. However, GLs are highly viscous materials, and their large-scale production is difficult owing to the high cost of lipids. Thus, in this experiment, the GLs were combined with FB dispersion. The purpose of this experiment is to verify the feasibility of the combination of FB and GL dispersions in the TLV system.

### **3.2.2. Materials and experimental procedures**

The protocols for the *in vivo* experiment were approved by the Committee of Laboratory Animals at the University of Yamanashi, and the *in vivo* experiments were conducted in accordance with institutional guidelines.

#### ***Evaluation of fine bubble dispersion (Exp. 1)***

The properties of the FB dispersion, oxygen content, zeta potential, and size distribution were evaluated. The FB were generated in 5 L of PBS, saline (150 mM NaCl,

prepared in-house), and deionized water (water) using a FB generator (GALF; Ultrafine GALF FZ1N-02, IDEC Corporation, Osaka, Japan) under the following conditions:  $F_{I}O_2$ : 1.0;  $O_2$  flow, 0.5 L/min; liquid temperature,  $34 \pm 1^\circ C$ ; and dissolution pressure, 270-320 kPa. The oxygen content was measured using the novel method described in Chapter 2. The zeta potential and size distribution were measured using a particle analyzer (Zetasizer Nano ZS90; Malvern Panalytical Ltd, Malvern, UK).

#### ***Animal preparation (Exp. 1 and Exp. 2)***

Sprague-Dawley male rats were subcutaneously anesthetized with a 37.5 mg/kg ketamine hydrochloride (Ketalar; Daiichi Sankyo Company, Tokyo, Japan). After 10 min, 6.9 mg/kg propofol (1% Propofol; Maruishi Pharmaceutical, Osaka, Japan) was administered and maintained at 10 mg/h for continuous anesthesia. Tracheotomy was performed and cannulated with a trachea tube that was 15 mm long (Surflo IV. 14 G Catheter; TERUMO Corporation, Tokyo, Japan). A 24G angiocatheter (Surflo IV. 24 G Catheter; TERUMO Corporation, Tokyo, Japan) was inserted into the carotid artery and anchored with a medical thread. MGV was performed with an animal ventilator (SAR-830/P; CWE Inc., Pennsylvania, USA) with the following settings: respiratory rate (RR), 60 breaths/min; inspiratory/expiratory time, 0.5/0.5 sec; tidal volume ( $V_T$ ),  $9.2 \pm 0.4$  ml/kg;  $FIO_2$ : 1.0.

#### ***Short-time total liquid ventilation test with fine bubble dispersion (Exp. 1)***

Eight Sprague-Dawley male rats, weighing between 400 g and 465 g ( $437 \pm 18.4$  g), were randomly divided into two groups of four rats each: 5 min TLV group and 15 min TLV group. The 2<sup>nd</sup> generation TLV system (Fig. 3.2b) was used and operated with the following conditions: inspiratory/expiratory pressures, 30/-30 cmH<sub>2</sub>O; inspiratory/expiratory time, 3/5 s (a rat received 3 and 4 s); and  $V_T$ ,  $65.7 \pm 4.02$  (in 5 min

TLV) and  $67.5 \pm 5.14$  (in 15 min TLV), which exhibited no significant difference. PBS was used as FB dispersion medium due to its buffer effect<sup>21</sup>.

Before starting TLV, 1.25-2.83 mg/kg rocuronium bromide (Eslax, MSD K.K., Tokyo, Japan) was administered intravenously for myorelaxation. Thereafter, TLV was performed for 5- or 15-min. Blood sampling (0.1 mL) from the carotid artery line was conducted before and after the TLV test. Blood gas analyses were performed with a blood gas analyzer (i-STAT; Abbott, Illinois, USA) for potential of hydrogen (pH), arterial oxygen partial pressure (PaO<sub>2</sub>, mmHg), arterial carbon dioxide partial pressure (PaCO<sub>2</sub>, mmHg), and base excess (B.E., mmol/L). The mean arterial pressure (MAP) and heart rate were measured and recorded using a bio-signal acquisition system (Power Lab system; ADINSTRUMENTS, Aichi, Japan). After the TLV experiment, the rats were killed using propofol anesthesia.

### ***Preparation of gas liposome dispersion (Exp. 2)***

The lipid dispersion consisted of dipalmitoyl phosphatidylcholine (DPPC; NOF, Tokyo, Japan) and polyoxyethylene-40 stearate (PEG40S; Sigma Aldrich, St. Louis, USA) at a molar ratio of 9:1 (weight ratio of 3:1). This composition was referenced from Swanson's papers, which demonstrated how to prepare the gas liposomes<sup>22</sup>.

The compounds were dispersed in PBS (DPBS; FUJIFILM Wako Pure Chemical Corp., Osaka, Japan) to obtain a final concentration of 5 mg/mL with sonication at 55°C until the dispersion became translucent. Fig. 3.3 presents an illustration of a reactor that was designed for preparing the GL dispersion. The 40 mL lipid dispersion was poured into a 50 mL three-necked round-bottom flask,

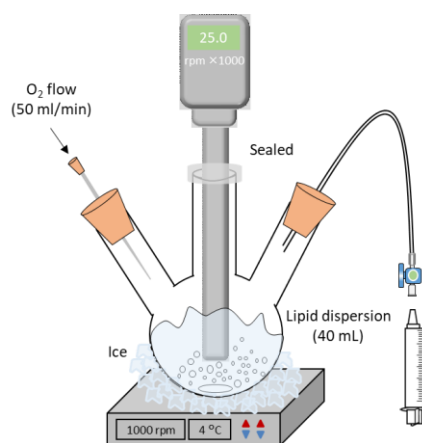


**Fig. 3.3. Illustration of a reactor for gas liposome dispersion**

and the tip of a homogenizer (Silent Crusher M; Heidolph Instruments GmbH & Co., Schwabach, Germany) was set in the middle neck. Oxygen gas (50 mL/min) was infused into the flask via a rubber cap fitted in the left neck. A Teflon tube (fluorine tube; inner diameter [ID]: 2 mm, and outer diameter [OD]: 4 mm) penetrated a rubber cap fitted in the right neck, and another side of the tube was connected to a 10 mL plastic syringe.

GLs were generated by agitating at 25,000 rpm for 15 min along with simultaneously stirring (1000 rpm) the lipid dispersion. The temperature of the flask was maintained at approximately 4°C with ice. During the preparation step, the Teflon tube was not immersed in the lipid dispersion. After 15 min, the tube was put into the GL dispersion; thus, the GL dispersion was collected in the syringe by pushing out with the internal pressure. GL dispersion of 20 mL (2 × 10 mL syringe) could be obtained from the 40 mL lipid dispersion. Thereafter, the GL dispersion was concentrated by centrifuging at 300 × G for 10 min at 4°C and removing the separated medium (PBS phase). Finally, the entire body of the syringe was sealed with a parafilm and then stored at 4°C until *in vitro* evaluations or animal experiments were conducted.

#### ***Evaluation of gas liposome dispersion (Exp. 2)***

The concentrated GL dispersion was too viscous to be sampled with a microsyringe. Therefore, 2-fold diluted sample was used to measure the oxygen content, and 5-fold diluted sample was used for the observation with a digital microscope (IX71; OLYMPUS Corporation, Tokyo, Japan). A GL dispersion in which Rhodamine B (Tokyo chemical industry CO., LTD., Tokyo, Japan) was dissolved in the PBS phase was prepared to visualize the gas and liquid phases clearly.

A hemolysis test (*in vitro* experiment) was conducted with rats' blood to assess the hemolytic potential of the GL dispersion. Blood was collected from rats and diluted with heparinized saline (heparin: 100U/mL). The GL dispersion was mixed with the blood in

equal volume and stood for 30 min. Hemolysis was assessed after sedimentation of cellular components by centrifugation ( $2000 \times g$ , 10 min,  $4^{\circ}\text{C}$ ). Ultrapure (MilliQ) water and DPBS were examined as positive and negative control, respectively.

#### ***Total liquid ventilation test with fine bubble and gas liposome dispersions (Exp. 2)***

Six Sprague-Dawley male rats, weighing between 390 g and 440 g ( $406 \pm 13.7$  g), were randomly divided into two groups of three rats each: FB group and FB+GL group. The 2<sup>nd</sup> generation TLV system (Fig. 3.2b) was used and operated with the following conditions: inspiratory/expiratory pressures, 30/−30 cmH<sub>2</sub>O; inspiratory/expiratory time, 3/5 s (in FB group) and 4/5 s (in FB+GL group); and  $V_T$ ,  $66.9 \pm 2.89$  mL/min (in FB group) and  $52.1 \pm 0.64$  mL/min (in FB+GL group). Differences in the respiratory conditions between the two groups will be mentioned in the discussion section. The GL dispersion was integrated into a 50 mL syringe prior to the TLV. It was directly introduced into the inspiratory line with a syringe pump (TE-331S; TERUMO Corporation, Tokyo, Japan) during TLV with the FB dispersion.

Before starting the TLV test, 1.25 mg/kg rocuronium bromide (Eslax, MSD K.K., Tokyo, Japan) was administered intravenously for myorelaxation. Thereafter, TLV was performed for 15 min. The blood gas analyses and hemodynamic measurements were performed in the same way as that in Exp. 1. After the TLV experiment, the rats were sacrificed using propofol anesthesia.

#### ***Statistical analysis***

All results are expressed as the mean  $\pm$  SD. Comparison between the two groups was performed using the student t-test, whereas those between multiple groups were performed using the Tukey–Kramer test following the one-way analysis of variance (ANOVA). The statistical analyses were performed using Statcel version 3 (OMS

Publishing Ltd., Tokyo, Japan), and  $p$  values  $< 0.05$  were considered to be statistically significant.

### 3.2.3. Results and discussion

#### *Characteristics of fine bubble dispersions (Exp. 1)*

Black bars in Fig. 3.4a show the oxygen content in the FB dispersions of water, saline, and PBS, which were 40.9 mg/L, 41.7 mg/L, and 41.4 mg/L, respectively. There was no significant difference for the different types of liquid. The white bars in Fig. 3.4a denote the oxygen content in each liquid without FBs, and there was no difference among the three groups. From the results in Chapter 2, the oxygen content in the FB dispersion might be dissolved in liquid; hence, it was not influenced by the oxygen from FBs. Since salt concentration in saline and PBS was low, the effect of dispersion medium on the oxygen content should be negligible. Considering the relationship between the oxygen content and lifetime of rats during TLV, as reported in a previous paper<sup>20</sup>, these values indicate that rats can survive for 38 min. Fig. 3.4b presents the surface potentials of each FB dispersion. All FB dispersions exhibited negative charges; however, the zeta potential in the water-FB dispersion was significantly lower ( $< -30$  mV) than those in the other two samples ( $p < 0.01$ ). These differences were induced by salt concentration. Zeta potential contributes to the stability of FB in liquid. Electrostatic repulsion is induced from  $\pm 10$  mV, and the repulsive force increases as the absolute value increases. Therefore, it is believed that electrostatic repulsion by the surface potential is weak in the saline-FB dispersion ( $-5.13$  mV); this sample was not used in this study. The size distributions are shown in Fig. 3.4c–e. All the results showed broad peaks and polydisperse. The results in a saline-FB dispersion revealed a bigger and broader distribution than those in the other FB dispersions. This is because its electrostatic repulsion was weaker than those of the

others. However, the quality of the results in size distribution was slightly poor owing to the low density and intensity of FBs.

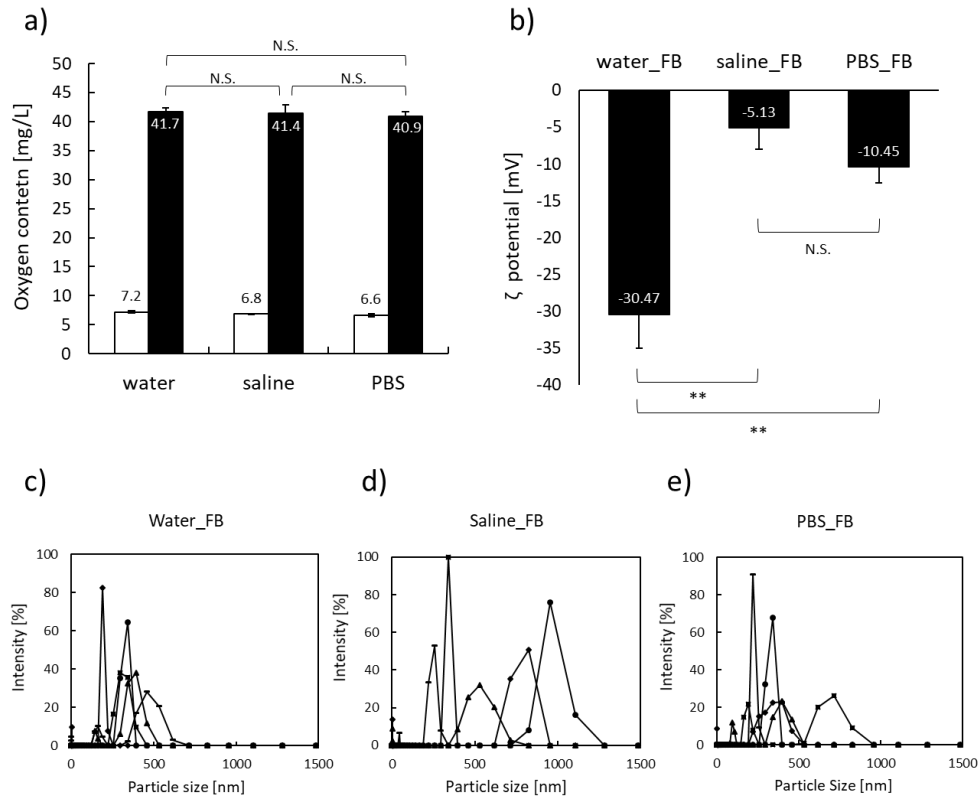


**Fig. 3.4. Fundamental properties of the FB dispersion.** a) Oxygen content in water-FB dispersion, saline-FB dispersion, and PBS-FB dispersion (n = 5). b) Zeta potential of water-FB, saline-FB, and PBS-FB (n = 4). The size distribution of c) Water-MNB, d) Saline-MNB, and e) PBS-MNB (circle, 1st measurement; triangle, 2nd measurement; bar, 3rd measurement; diamond, 4th measurement; square, 5th measurement; and n = 5). \*\*p < 0.01, N.S. means not significant.

#### **Short-term total liquid ventilation test with a fine bubble dispersion (Exp. 1)**

Fig. 3.5 presents the results for blood gas analyses and hemodynamics analyses. The PaO<sub>2</sub> in both groups were significantly decreased after the TLV (p < 0.01); there was no difference between the groups. Thus, the rats exhibited severe hypoxia within 5 min (Fig. 3.5a). There was no significant difference among the results in PaCO<sub>2</sub> (Fig. 3.5b);

CO<sub>2</sub> removal during TLV was successfully performed. The pH and B.E. in both groups were significantly decreased and bellowed their normal ranges after the TLV (pH:  $p < 0.01$ , B.E.:  $p < 0.05$ ). It means that metabolic acidosis was induced. The MAP and heart rate dropped during the first 1 min. Then, they were maintained at 80–90 mmHg and 250–300 bpm until 5 min, respectively. Thereafter, these parameters gradually decreased over time (Fig. 3.5e and f). After 15 min, MAP and heart rate exhibited 30 mmHg and 150 bpm, respectively; the cardiac function faced a severe issue.

These results indicate that metabolic acidosis owing to hypoxemia was induced in both groups. The parameters of blood gas analyses in the 5 min TLV group were more severe than those in the 15 min TLV group. The phenomenon of the recovery of pO<sub>2</sub> over time after once it drops was also confirmed in a previous study<sup>23</sup>. However, it was considered that these recoveries in the 15 min TLV group were associated with a reduction in systemic oxygen consumption. The oxygen consumption in the body might be decreased as a result of reduced cell activity and the necrosis due to hypoxia. Hence, the cardiac functions continued to decline and did not recover after 5 min (Fig. 3.5e and f). Therefore, the recovery was not a positive event. At first, it was expected the rats maintained good conditions in terms of blood oxygen level and cardiac function for a short TLV, the result showed severe hypoxia was induced within 5 min. However, the rats maintained their blood pressure of 80 mmHg or higher and heart rate of 200 bpm or higher at 5 min. It is experimentally expected the rats could recover if they will receive the sufficient oxygen by changing from TLV to MGV within 5 min.

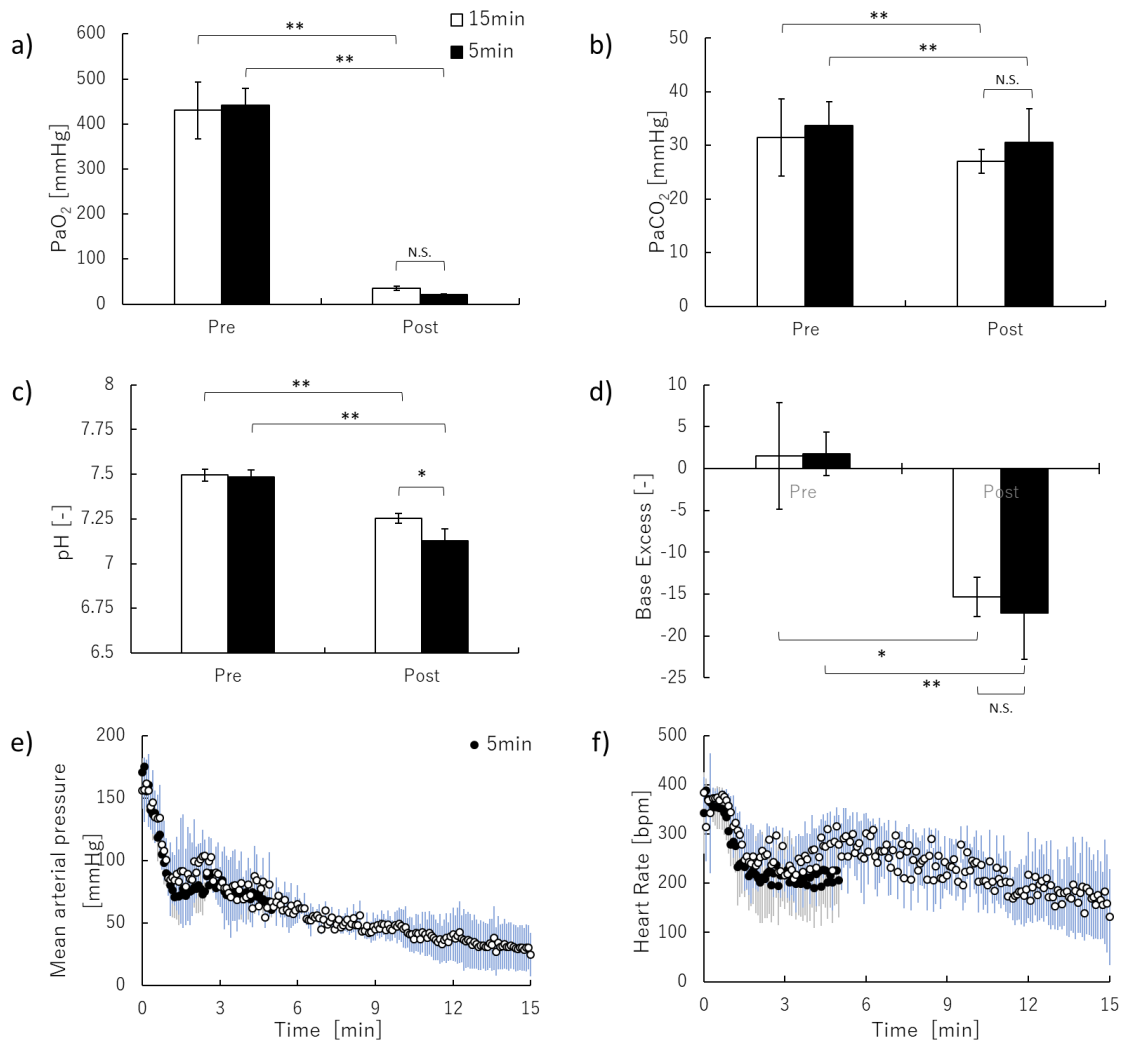


**Fig. 3.5. Physiological conditions of the rats after short-time total liquid ventilation with FB dispersion.** The changes before and after the total liquid ventilation test in the a) partial oxygen pressure, b) partial carbon dioxide pressure, c) acidity, and d) base excess ( $n = 4$ ). The time-course change in e) mean arterial blood pressure, and f) heart rate. The opened circle represents the 15 min TLV group; the closed circle denotes the 5 min TLV group ( $n = 4$ ). The light-blue and gray bars indicate the standard deviation of the 15 min TLV and 5 min TLV groups, respectively. \* $p < 0.05$ , \*\* $p < 0.01$ , N.S. means not significant.

Oxygen delivery of the FB dispersion during TLV has been confirmed in a previous study by measuring the partial pressure of oxygen ( $pO_2$ ) in the FB dispersion at the inspiratory and expiratory tubes<sup>24</sup> (Fig. 3.6). Since oxygen supply is dependent on oxygen diffusion, increasing the  $pO_2$  in the FB dispersion and increasing tidal volume per minute ( $V_T$ ) improves oxygen supply to blood. Under the current TLV setting ( $V_T$ : 65 mL/min), the required oxygen content in rat is 100–141 mg/L, which is calculated from the oxygen consumption of anesthetized rats ( $1.2\text{--}1.5$  [ml/min/100 g])<sup>25</sup> and the  $V_T$ . Because the oxygen content in the FB dispersion is 40–45 mg/L, oxygen content must be increased by at least 2.5 times more than the current state.

It has been reported that FBs are attached to a cell surface and can be absorbed to the cell<sup>26,27</sup>. However, the liquids should be replaced at intervals of 5–9 s during TLV; therefore, it is believed that the biological interaction between FBs and pneumocytes during TLV hardly occurs.

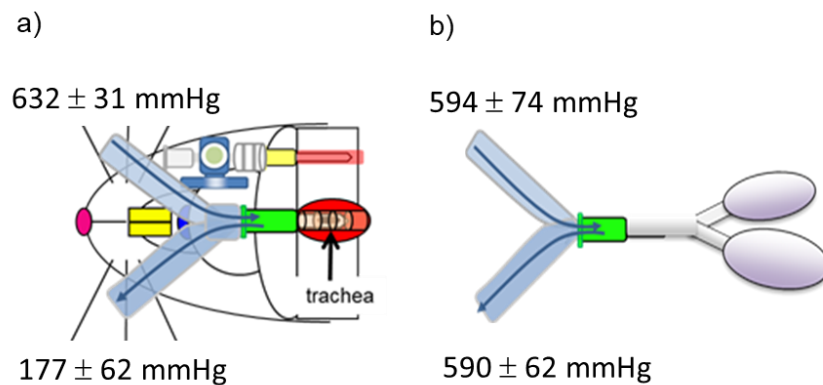


**Fig. 3.6. Oxygen consumption during the total liquid ventilation test.** The  $pO_2$  in FB dispersion before inflow and after drainage using (a) TLV model rats or (b) model lungs ( $n = 3$ ,  $35\text{--}37$  °C)<sup>24</sup>

### ***Characteristics of gas liposome dispersion (Exp. 2)***

The GL dispersion immediately after preparation was white liquid with fluidity (Fig. 3.7a). After centrifugation, the dispersion was separated into three phases: gas, concentrated GL, and PBS (Fig. 3.7b). The PBS phase was removed, and the concentrated GL phase with a mousse form was obtained (Fig. 3.7c). Although the GL dispersion could be stored for several days at 4°C, the GLs gradually coalesced each other.

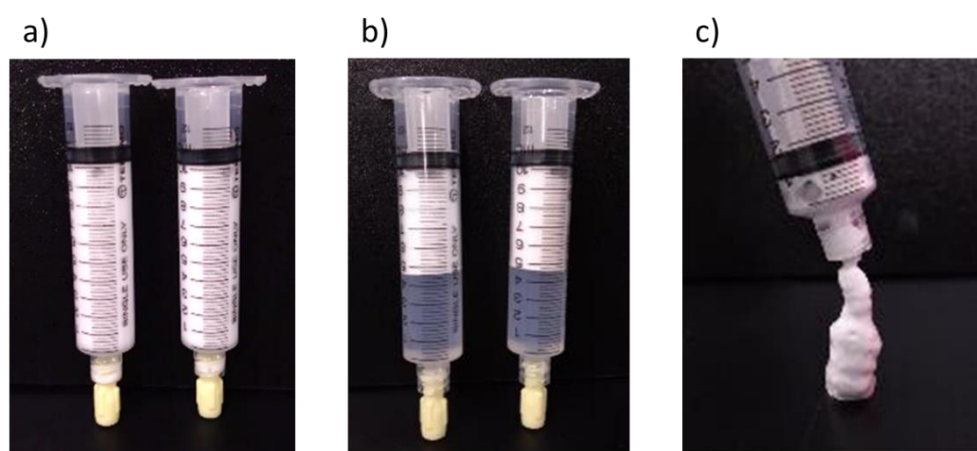


**Fig. 3.7. Images of gas liposome (GL) dispersion.** a) GL dispersion before and b) after centrifugation, and c) concentrated GL dispersion, which was in a mousse form.

Fig. 3.8a presents a microscopic image of the 5-fold diluted GL dispersion, which had a polydisperse distribution of 2–50  $\mu\text{m}$ . Fig. 3.8b shows an image of the GL dispersion with a colored medium, and no fluorescence is inside the particle. This suggests that no liquid exists inside the particle, but gas (oxygen) does; thus, GLs were successfully prepared. The oxygen content in the 2-fold diluted GL dispersion was measured to be 341 mg/L, which is eight times larger than that in the FB dispersion and 43 times larger than that in normal saline (Fig. 3.8c). This value was larger than the target value (100–150 mg/L), which was calculated from the oxygen consumption of rats. Thus, it was expected that the GL dispersion would be useful for TLV if it releases the oxygen inside the lungs.

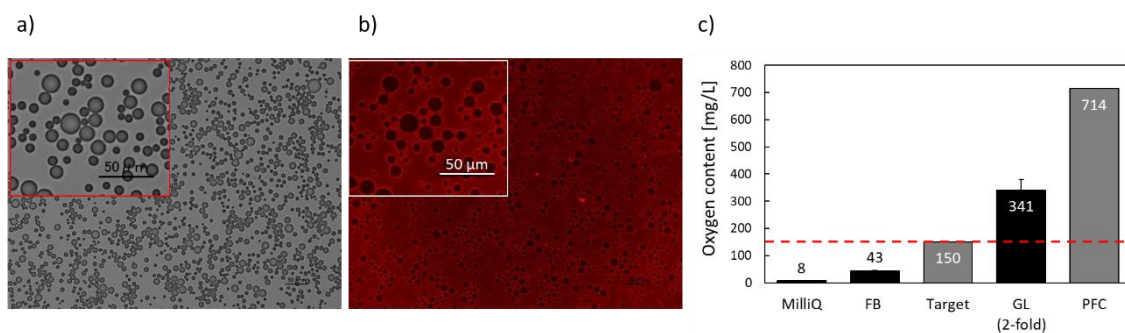


**Fig. 3.8. Characteristics of GL dispersion.** a) Microscopic images of the 5-fold GL dispersion without and b) with rhodamine B for visualizing the water phase. The left top windows show magnified pictures of the original image. Scale bar, 50  $\mu\text{m}$ . c) Oxygen content in the 2-fold GL dispersion. The black bars represent the measurement values ( $n = 6$ ), and the gray bars denote the calculated values.

#### ***Total liquid ventilation test with fine bubble and gas liposome dispersion (Exp. 2)***

The TLV experiment with FB and GL dispersion was conducted to examine the feasibility of GLs. However, problems occurred in terms of 1) method for introduction of the GL dispersion, 2) the tidal volume, and 3) the toxicity. First, the GL dispersion was difficult to treat with the syringe pump. GL dispersion was clogged at the tip of the syringe; thus, the pump was stopped owing to a pressure error. Manual restarting was repeated during 15 min TLV; thus, the exact dose and speed of the injection were unknown. Approximately 1/40 to 1/20 dose against the FB dispersion was delivered to the lungs of the rats. A slight increase in the oxygen content in the FB dispersion was expected.

Second, the ventilation efficiency was inferior to that with only FB dispersion.  $V_T$  in the FB+GL group was smaller than that in the FB group even though the ventilatory condition in the FB+GL group was better in terms of  $V_T$  according to previous research (Fig. 3.9a, b). In this experiment, only a small dose of the GL dispersion was administered into the FB dispersion. However, the liquid became cloudy, and macro bubbles were confirmed in the expiratory line. It is believed that GLs coalesced through intensive

collision inside the lungs and became the macro bubbles. These macro bubbles might blockade respiratory bronchioles; thus, the ventilation volume was reduced. After TLV in the FB+GL group, the lungs had areas where no liquid seemed to be introduced (Fig. 3.10a, black arrows).

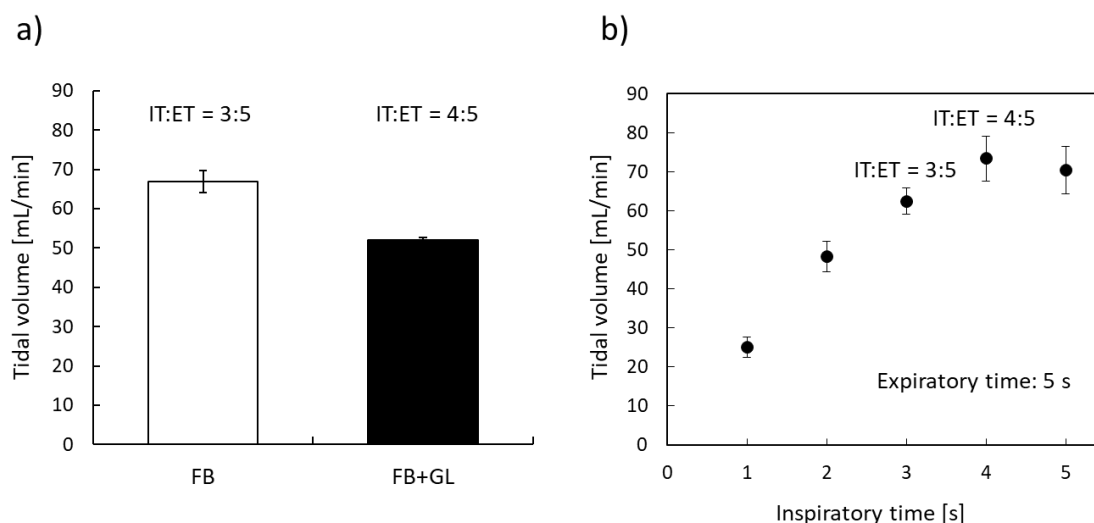


**Fig. 3.9. Tidal volume during total liquid ventilation test with FB and GL dispersions.**

a) Tidal volume during the TLV test ( $n = 4$ ). b) Relationship between tidal volume and inspiratory time ( $n = 3$ )<sup>20</sup>.

Third, the toxicity of the GL dispersion was suggested by the isolated lungs after the TLV experiment. Fig. 3.10a-c present the representative isolated lungs from rats in the FB and FB+GL groups. The surface colors were different, and the feature of the lung in Fig 3.10c implied hemolysis. To confirm this suggestion, a hemolysis test was conducted with the blood of the rats. The results revealed the toxicity of free PEG40S, whereas the toxicity of DPPC+PEG40S was not revealed (Fig. 3.10d and e, respectively). It was suggested that if the GLs structure collapsed and PEG40S was released from the shell, it would be toxic.

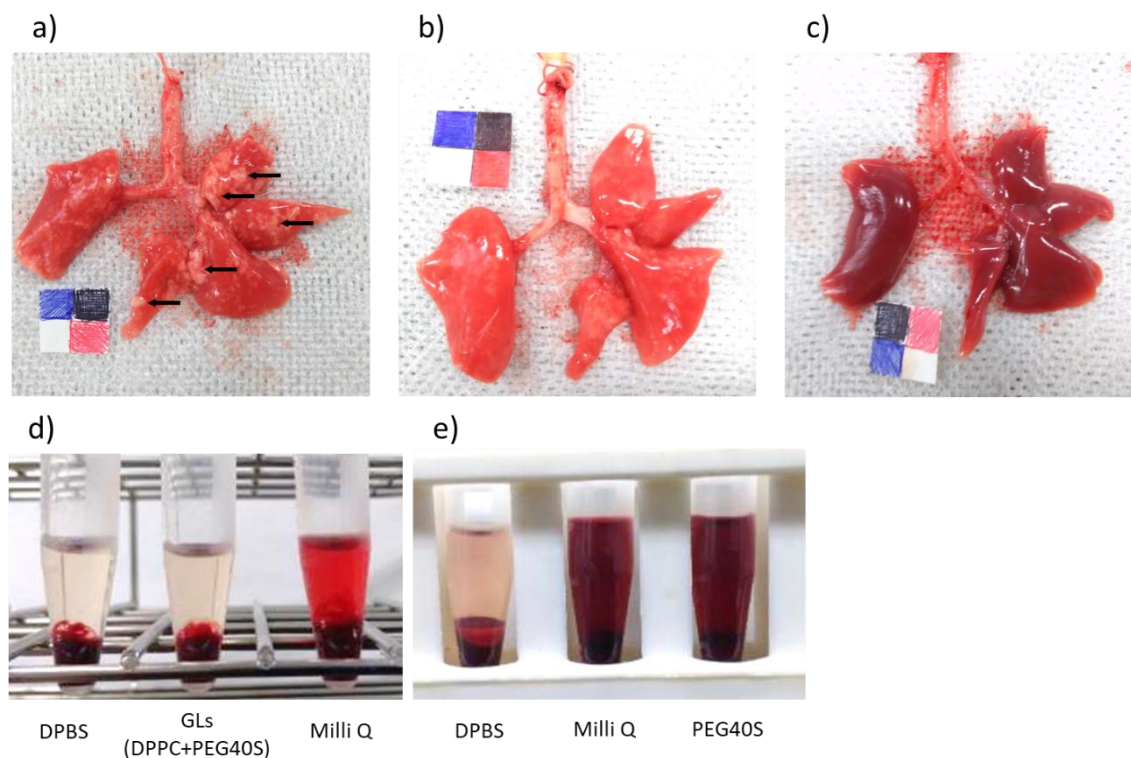


**Fig. 3.10. Effects of the GL dispersion on the lungs.** a) The isolated lungs from a rat in the FB+GL group. The black arrows indicate the area where liquid was not introduced. b) The isolated lungs from a rat in the FB group. c) The isolated lung from a rat in the FB+GL group. The square sheets show the color and length scale with a 10 mm square (5 mm square in four colors). Hemolysis test for d) GL dispersion and e) PEG40S dispersion. DPBS and MilliQ were used as the negative and positive controls, respectively.

Fig. 3.11 presents the results for blood gas analyses and hemodynamics. The  $\text{PaO}_2$  in both groups were significantly decreased after TLV ( $p < 0.01$ ); there was no difference between the groups. Therefore, both FB and FB+GL dispersion could not supply sufficient oxygen, resulting in severe hypoxia (Fig. 3.11a). There was no significant difference in  $\text{PaCO}_2$  among any elements (Fig. 3.11b). The  $\text{CO}_2$  removal was sufficiently performed in both groups. The pH after TLV in the FB+GL group tended to be lower than that in the FB group (Fig. 3.11c,  $p = 0.09$ ). Because there was no accumulation of  $\text{PaCO}_2$

in the FB+GL group, the decrement in pH was induced by metabolic acidosis. Therefore, it was believed that multiple organ failure owing to severe hypoxemia was progressing in the FB+GL group. The B.E. in both groups were significantly dropped after the TLV (Fig. 3.11d). These results also revealed that metabolic acidosis occurred, and it was more severe in the FB+GL group. Fig. 3.11e and f depict the change over time in the hemodynamics parameters. They gradually decreased over time in both groups; there was no difference between the groups.

The expected effect was not obtained in the FB+GL group because GLs exhibited problems in its fluidity and toxicity. Liquids with high formability such as the GL dispersion induce foam clogging inside the lungs and impaired fluid ventilation. Regarding the toxicity, there was no toxicity immediately after GL preparation (Fig. 3.10d). However, when PEG40S, which is anchored to the lipid membrane, is released from the membrane, it begins to exhibit toxicity. Black *et al.* reported that the administration of concentrated GL dispersion induced a decrease in hemodynamic parameters, and they considered that lipid debris caused impairment<sup>28</sup>. In this experiment, although GLs were used to increase the oxygen content in the FB dispersion, they could not be applied to TLV due to its fluidity and toxicity problems, not regarding to the oxygen supply. The results also showed that the fluidity of liquid inside the lungs should be consider when adding additives to FB dispersion.

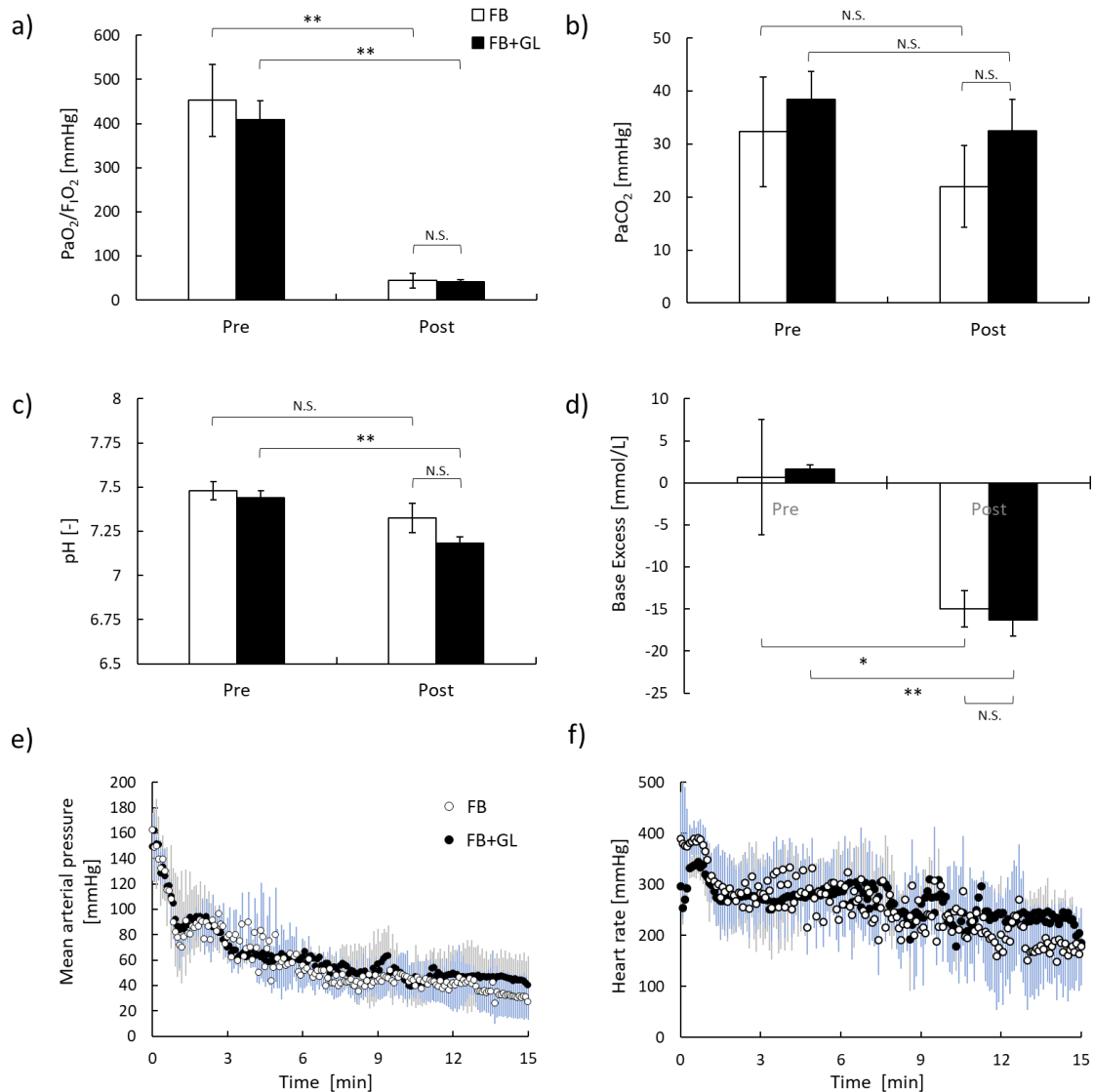


**Fig. 3.11. Physiological conditions of the rats after total liquid ventilation test with FB and GL dispersion.** The changes before and after total liquid ventilation test in the a) partial oxygen pressure, b) partial carbon dioxide pressure, c) potential of hydrogen, and d) base excess. The time-course change during 15 min TLV in the e) blood pressure and f) heart rate. The opened circle and white bar represent the FB group; the closed circle and black bar represent the FB+GL group (n = 3). The light-blue and gray bars indicate the standard deviations of the opened and closed circles, respectively. \*p < 0.05, \*\*p < 0.01, N.S. means not significant.

### **3.3. Improvement of the total liquid ventilation system with oxygen fine bubble dispersion**

#### **3.3.1. Purpose**

The oxygen supplied during TLV can be elevated by increasing the oxygen content in the liquid and tidal volume per minute. Although the optimization of temperature and pressure of the TLV system was conducted, efficient delivery of the FB dispersion has not been optimized. Thus, the purpose of this experiment is to tune the TLV system for increment of tidal volume.

#### **3.3.2. Materials and experimental procedures**

A pressure-limited time-cycled TLV system was constructed (Fig. 3.12a). The FB dispersion was prepared in the upper reservoir and constantly flowed to a middle reservoir, which had an overflow system to maintain the water-head pressure. At the beginning of the inspiratory phase, the electromagnetic valve in the inspiratory line was opened, and the valve in the expiratory line was closed. The FB dispersion was introduced into the lungs through a tracheal tube by the gravity force. Conversely, at the end of the inspiratory phase, the electromagnetic valve in the inspiratory line was closed, and the valve in the expiratory line was opened. The FB dispersion was drained from the lungs owing to the siphoning principle. TLV was performed by repeating these procedures.

The tidal volume during TLV was calculated from the weight difference of a model lung (prepared in-house) (*in vitro* experiment) and rats (*in vivo* experiment). A free-license software (Tera Term, Tera Term project, Japan) was introduced to transfer the weight data from the electronic balance to a PC and save them automatically. Because the density of the FB dispersion was nearly the same as that of normal saline (1 mg/mL), correction by density was not required. The tidal volume per minute was used as the

primary outcome to evaluate the performance of the TLV system in this study, and it was calculated as follows:

$$\text{Tidal volume (mL/min)} = \text{ave. tidal volume (mL/breath)} \times \text{respiratory rate (breath/min)} \quad (3.1)$$

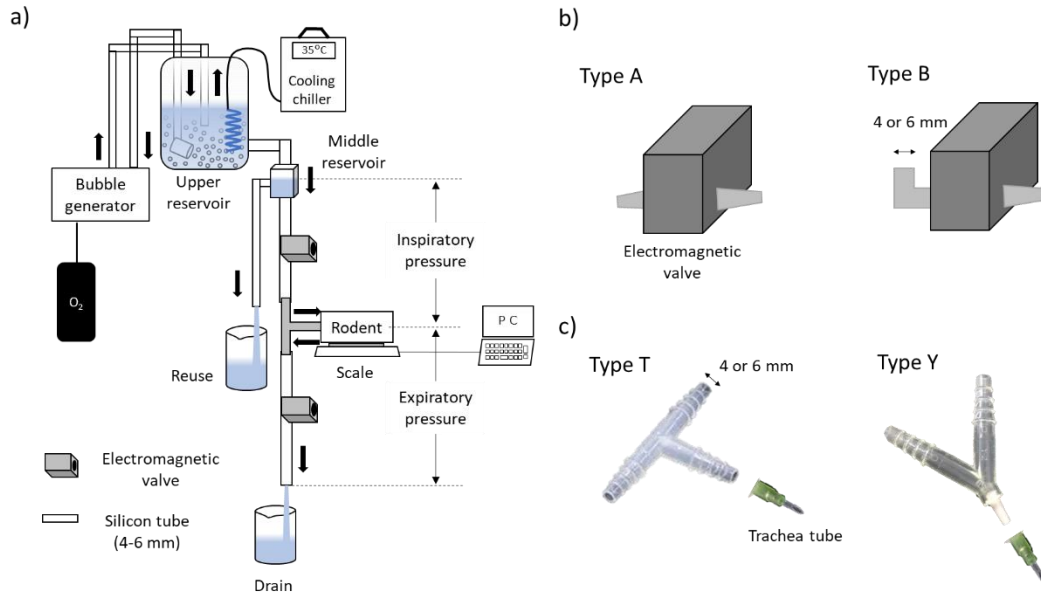


**Fig. 3.12. Improved total liquid ventilation system with FB dispersion and its components.** a) Schematic illustration of a pressure-limited time-cycled total liquid ventilation with FB dispersion. b) Types of connector to electromagnetic valves, type A: straight type and type B: half elbow type. c) Types of the connector to the trachea tube, type T: T-shaped connector and type Y: Y-shaped connector.

#### ***Examination of components in the total liquid ventilation system (Exp. 1)***

First, tubes for the fluid route and the connectors of the electromagnetic valves were examined (Fig. 3.12). The evaluation factors are summarized in Table 3.1. The effect of the factors on the tidal volume was examined using model lungs as an *in vitro* experiment. In this experiment, a type T connector of 4 mm was used as a connector of the trachea tube (Fig. 3.12c).

**Table 3.1. Evaluation factors in experiment 1**

Tube		Connector of electromagnetic valves	
Size [mm]	Material	Size [mm]	Shape
4, 5, or 6	Silicon or Fluorine	4 or 6	Straight type or Half elbow type

Second, the connector of the tracheal tube was examined. The size (4 or 6 mm) and the shape (type T vs. type Y [Fig. 3.12c])) of the connector were changed, and then, the effect on the tidal volume with the model lung as an *in vitro* experiment was evaluated. In this experiment, a type A connector of 6 mm was used for the electromagnetic valve (Fig. 3.12b).

#### ***Examination of the expiratory conditions (Exp. 2)***

Finally, the expiratory conditions were optimized by changing the expiratory time and pressure on the postmortem rats as an *in vivo* experiment. The TLV system was constructed with the selected components in *examination 1*. The effect of expiratory conditions on the tidal volume was evaluated. The inspiratory conditions were determined by referring to a previous study (inspiratory pressure: 35 cmH<sub>2</sub>O and inspiratory time: 3 s)<sup>21</sup>.

**Table 3.2 Summary of examination factors in experiments 1 and 2**

	Tube [size, type]	Connector 1 [size, type]	Connector 2 [size, type]	IP [cmH <sub>2</sub> O]	IT [s]	EP [cmH <sub>2</sub> O]	ET [s]
Exp. 1	target	target	target	30	2–5	30	5
Exp. 2	6 mm, silicon	6 mm, type A	6 mm, type Y	35	3	target	target

Exp.: experiment; Connector 1: connectors of the electromagnetic valves; Connector 2: a connector of a trachea tube; IP: inspiratory pressure; IT: inspiratory time; EP: expiratory pressure; ET: expiratory time; target: target for examination.

### 3.3.3. Results and discussion

#### *Examination of components in the total liquid ventilation system (Exp. 1)*

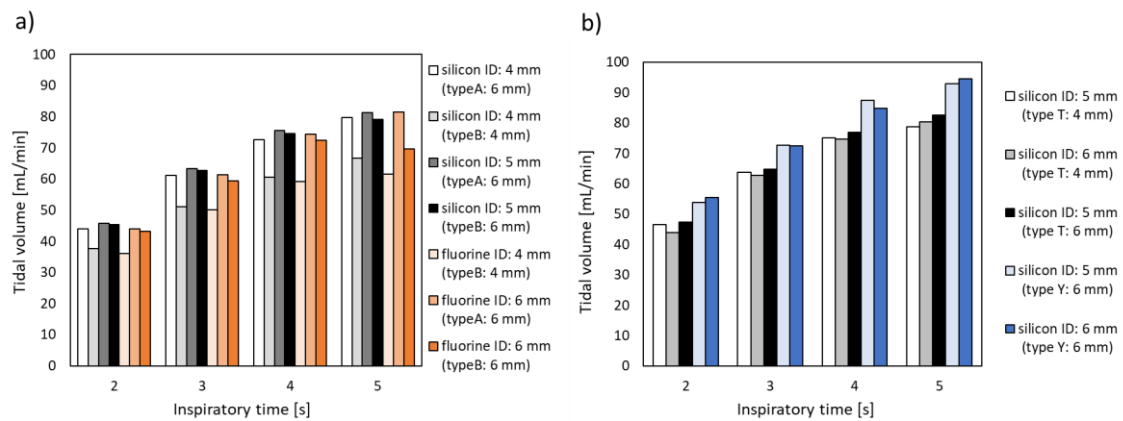
Fig. 3.13a presents the effects of the tubes and the connectors of electromagnetic valves on the tidal volume. Four bars from the left side show the result with silicon tubes, whereas the remaining three bars show the result with fluorine tubes. The effects of the conditions on tidal volume were evaluated under different inspiratory times. The light-gray bars show the lowest values among the silicon tube conditions in each inspiratory condition. Therefore, the size of the connector is an important factor on the tidal volume. Comparing the results depicted by the white bars and the dark-gray bars, it is believed that a 5 mm silicon tube was slightly superior to a 4 mm silicon tube. This is because the effect of pressure loss owing to friction is small in the large tube diameter. Considering the results of the dark-gray and black bars, the type A connector was slightly superior to type B. This is because the larger angle of bend affected the pressure loss at the corner part (bending loss). The same tendency was confirmed in the case with the fluorine tube, which is represented by the orange bars.

Fig. 3.13b presents the effects of the connector of trachea tube on the tidal volume. The left three bars show the results with the type T connector, and the right two bars show the results with the type Y connector. The results with the type Y connector show a larger tidal volume than those with the type T connector under every inspiratory condition. Although the diameter of the tube and the connector slightly affected the tidal volume, those differences were negligible. The effect on the shape of the connector can be also explained with the bending loss.

The difference between the silicon and fluorine tube can be discussed by comparing the light-orange bar from Fig. 3.13a (6 mm type A with a 6 mm fluorine tube) and the gray bar from Fig. 3.13b (6 mm type A with 6 mm silicon tube). The results are 81.6

mL/min and 80.4 mL/min, respectively. Therefore, there was no difference between the silicon and fluorine tube in terms of the tidal volume.

Accordingly, the size of the connector of electromagnetic valves and the shape of the connector of trachea tube are crucial factors for the tidal volume in the TLV system. Therefore, it is important to design the pipe resistance to be small because of the pressure loss. The 6 mm type A connector, 6 mm type Y connector, and 5 mm silicon tube were selected in the following experiments.



**Fig. 3.13. Examination of the effect of the components on tidal volume during total liquid ventilation.** a) Effect of tube and connector of electromagnetic valves on tidal volume ( $n = 1$ , average for 5 min). b) Effect of connector of tracheal tube on tidal volume ( $n = 1$ , average for 5 min).

### *Examination of the expiratory conditions (Exp. 2)*

Fig. 3.14a shows the relationship between tidal volume and expiratory time under four expiratory pressure conditions. When the expiratory time is 3 s, the expiratory pressure considerably affected the tidal volume. However, at 4.5 s, there was no difference between  $-20$  cmH<sub>2</sub>O and  $-30$  cmH<sub>2</sub>O. Longer than 6 s, the tidal volume did not increase despite the expiratory time was being extended; it reached a stable condition. Therefore, the FB dispersion in the lungs was completely drained at 6 s. At the beginning of the

expiratory phase, the liquid inside the lungs was drained by negative pressure, and the trachea was filled with the liquid (Fig. 3.14b). However, after a few seconds, the trachea collapsed owing to the negative pressure (choking phenomenon) caused by insufficient liquid flow, which could not maintain the shape of the airway under the negative pressure (Fig. 3.14c). At the condition with  $-30$  cmH<sub>2</sub>O, the choking phenomenon occurred even in an early phase. Therefore,  $20$  cmH<sub>2</sub>O and  $6$  s was chosen for the optimized expiratory conditions in this experiment.

In this study, some components of the TLV system and respiratory conditions were improved. It is difficult to compare the current data and previous data because there are no previous data under the same conditions. However, comparing the current data with the data under similar conditions reported by Sato of Takeoka laboratory<sup>23</sup>, it is believed that the tidal volume improved with about 19% through optimization of the components.

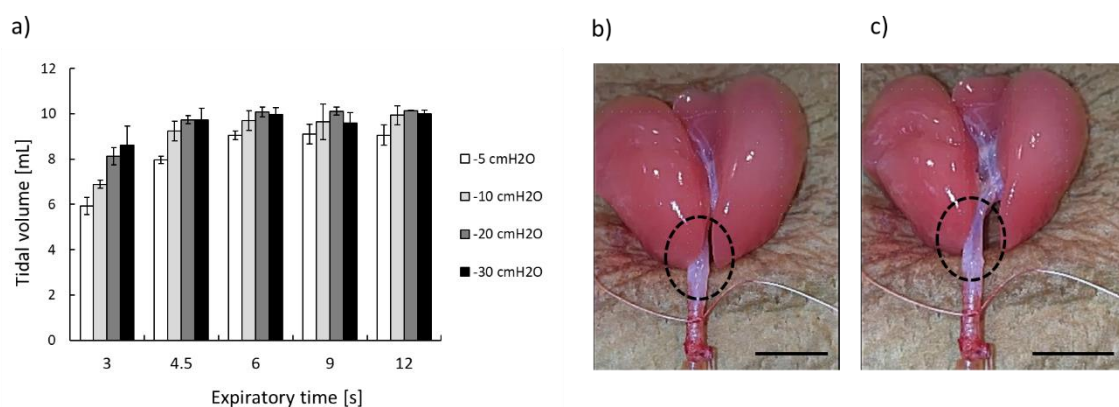


**Fig. 3.14. Examination of the effect of expiratory conditions on the tidal volume during total liquid ventilation.** a) Relationship between tidal volume and expiratory time under four expiratory pressure conditions (*in vivo*). b) A picture of the lung 1 s after starting to suck with  $-30$  cmH<sub>2</sub>O pressure. c) A picture of the lung 5 s after starting to suck with  $-30$  cmH<sub>2</sub>O pressure (*ex vivo*). A part of the trachea was collapsed (*ex vivo*). Scale bar, 1 cm.

### **3.4. Conclusions of this chapter**

This chapter includes three experiments: a short-time TLV test with the FB dispersion, a TLV test with the combination of the GL and FB dispersions, and the improvement of the TLV system. The important findings for each experiment are summarized below:

#### ***1) Short-time TLV test with FB dispersion***

It was found that a severe hypoxemia was already induced within 5 min with the TLV system using the FB dispersion. Cardiac function worsened further after 5 min; thus, the treatment time for lung lavage was determined as 5 min. It is important to increase the oxygen supply during TLV for a safe TLV treatment.

#### ***2) TLV test with the combination of GLs and FB dispersions***

The combination of the GL and FB dispersions did not increase the oxygen supply during TLV as expected. It is because that coalesced GL blocked the respiratory tract and disturbed the flowing of the dispersion. However, it is an important finding when considering additives in the FB dispersion.

#### ***3) Improvement of the TLV system***

The tidal volume was improved by about 19% compared to the previous TLV system by optimization of the components and expiratory condition. In order to achieve the target oxygen supply, further improvements of TLV system and an increase of the oxygen content in the liquid are required.

## References

1. Kylstra, J. A., Tissing, M. O. & Van der Maen, A. of mice as fish.pdf. *Trans Am Soc Artif Intern Organs* **8**, 378–383 (1962).
2. Douglas, G., Hayes, J. A. & Carolina, N. Bilateral lung lavage with hyperbarically oxygenated saline in dogs. *J Appl Physiol.* **29**, 786–793 (1970).
3. Kylstra, J. A., Paganelli, C. V. & Lanphier, E. H. Pulmonary gas exchange in dogs ventilated with hyperbarically oxygenated liquid. *J Appl Physiol.* **21**, 177–184 (1966).
4. Clark, L. C. & Gollan, F. Survival of Mammals Breathing Organic Liquids Equilibrated with Oxygen at Atmospheric Pressure. *Science (80-. ).* **152**, 1755–1756 (1966).
5. Modell, jerome H., Hood, C. Ian, Kuck, earlene J. & Ruiz, B. C. oxygenation by ventilation with fluorocarbon liquid (FX-80). *Anesthesiology* **34**, 312–320 (1971).
6. Tuazon, jaime G., Modell, jerome H., Hood, C. & Swenson, E. W. pulmonary function after ventilation with fluorocarbon liquid (Caroxin-D). *Anesthesiology* **38**, 134–140 (1973).
7. Shaffer, T. H. & Moskowitz, G. D. Demand-controlled liquid ventilation of the lungs. *J Appl Physiol.* **36**, 208–213 (1974).
8. Shaffer, T. H. & Moskowitz, G. D. An Electromechanical Demand Regulated Liquid Breathing System. *IEEE Trans. Biomed. Eng.* **22**, 412–417 (1975).
9. Kohlhauser, M. *et al.* A new paradigm for lung-conservative total liquid ventilation. *EBioMedicine* **52**, 102365 (2020).
10. Shaffer, T. H., Rubenstein, D., Moskowitz, G. D. & Delivoria-Papadopoulos, M. Gaseous exchange and acid-base balance in premature lambs during liquid

- ventilation since birth. *Pediatr Res.* **10**, 227–231 (1976).
11. Jackson, J. C., Standaert, T. A., Truog, W. E. & Hodson, W. A. FULL-TIDAL LIQUID VENTILATION WITH PERFLUOROCARBON FOR PREVENTION OF LUNG INJURY IN NEWBORN NON-HUMAN PRIMATES. *ART. CELLS, BLOOD SUBS., IMMOB. BIOTECH.* **22**, 1121–1132 (1994).
  12. Hirschl, R. B. *et al.* Liquid ventilation improves pulmonary function, gas exchange, and lung injury in a model of respiratory failure. *Ann Surg* **221**, 79–88 (1995).
  13. Matsuda, K., Sawada, S., Bartlett, R. H. & Hirschl, R. B. Effect of ventilatory variables on gas exchange and hemodynamics during total liquid ventilation in a rat model. *Crit. Care Med.* **31**, 2034–2040 (2003).
  14. Jiang, L. *et al.* Total Liquid Ventilation Reduces Lung Injury in Piglets After Cardiopulmonary Bypass. *Ann. Thorac. Surg.* **82**, 124–130 (2006).
  15. Baba, Y. *et al.* A Volume-Controlled Liquid Ventilator with Pressure-Limit Mode : Imperative Expiratory Control. *Artif. Organs* **20**, 1052–1056 (1996).
  16. Meinhardt, J. P., Quintel, M. & Hirschl, R. B. Development and application of a double-piston configured , total liquid ventilatory support device. *Crit. Care Med.* **28**, 1483–1488 (2000).
  17. Larrabe, J. L. *et al.* Development of a Time-Cycled Volume-Controlled Pressure-Limited Respirator and Lung Mechanics System for Total Liquid Ventilation. *IEEE Trans. Biomed. Eng.* **48**, 1134–1144 (2001).
  18. Nadeau, M. *et al.* Core Body Temperature Control by Total Liquid Ventilation Using a Virtual Lung Temperature Sensor. *IEEE Trans. Biomed. Eng.* **61**, 2859–2868 (2014).
  19. Micheau, P. *et al.* A Liquid Ventilator Prototype for Total Liquid Ventilation

- Preclinical Studies. in *Progress in Molecular and Environmental Bioengineering* (ed. Carpi, A.) 323–343 (2011). doi:10.5772/21490
20. Kakiuchi, K. *et al.* Establishment of a total liquid ventilation system using saline-based oxygen micro/nano-bubble dispersions in rats. *J. Artif. Organs* **18**, 220–227 (2015).
  21. Oue, A. Improvement of total liquid ventilation with oxygen micro/nano bubble dispersion. Master thesis, Waseda University (Japanese). (2016).
  22. Swanson, E. J., Mohan, V., Kheir, J. & Borden, M. A. Phospholipid-stabilized microbubble foam for injectable oxygen delivery. *Langmuir* **26**, 15726–15729 (2010).
  23. Sato, H. Optimazation of total liquid ventilation system with oxygen micro/nano bubble dispersion. Master thesis, Waseda University (Japanese). (2018).
  24. Kakiuchi, K. Establishment of total liquid ventilation using oxygen micro / nano bubble dispersions. Master thesis, Waseda University (2015).
  25. SHEPHERD, R. E. & GOLLNICK, P. D. Oxygen Uptake of Rats at Different Work Intensities. *Pflugers Arch* **362**, 219–222 (1976).
  26. Cavalli, R. *et al.* Preparation and characterization of dextran nanobubbles for oxygen delivery. *Int. J. Pharm.* **381**, 160–165 (2009).
  27. Khan, M. S. *et al.* Applications of Oxygen-Carrying Micro / Nanobubbles : a Potential Approach to Enhance Photodynamic Therapy and Photoacoustic Imaging. *Molecules* **23**, 1–20 (2018).
  28. Black, K. J. *et al.* Hemodynamic Effects of Lipid-Based Oxygen Microbubbles via Rapid Intravenous Injection in Rodents. *Pharm. Res.* **34**, 2156–2162 (2017).

## **Chapter 4: Efficacy of total alveolar lavage with a total liquid ventilation system using fine bubble dispersion in acute lung injury models**

### **4.1. Background of this chapter**

4.1.1. Acute respiratory distress syndrome

4.1.2. Acute respiratory distress syndrome model

4.1.3. Treatments for acute respiratory distress syndrome

### **4.2. Efficacy of total alveolar lavage with a total liquid ventilation system using oxygen fine bubble dispersion in a severe lung injury model**

4.2.1. Purpose

4.2.2. Materials and experimental procedures

4.2.3. Results and discussion

### **4.3. Efficacy of total alveolar lavage with a total liquid ventilation system using oxygen fine bubble dispersion in a lethal lung injury model**

4.3.1. Purpose

4.3.2. Materials and experimental procedures

4.3.3. Results and discussion

### **4.4. Conclusions of this chapter**

### **References**

#### **Note:**

An academic article: Total alveolar lavage with oxygen fine bubble dispersion directly improves lipopolysaccharide-induced acute respiratory distress syndrome of rats, based on the contents of this chapter have been published in Scientific Reports<sup>1</sup>. Fig. 4.3, 4.4, 4.5, 4.6, and 4.7 was referred from the article with minor modification of group names and order.

## **4.1. Background of this chapter**

### **4.1.1. Acute respiratory distress syndrome**

In 2012, the definition of acute respiratory distress syndrome (ARDS) was changed, and the concept of acute lung injury (ALI) was integrated into ARDS<sup>2</sup>. Although ARDS still has a mortality as high as 30–45%, there is currently no causative treatment<sup>3</sup>. ARDS is a rapidly progressive disease induced by several illnesses: severe pneumonia, aspiration, sepsis, or trauma. These diseases lead to ARDS by promoting inflammation responses via oversecretion of cytokines from macrophages and neutrophils. Once the permeability of the capillary vessel is increased by the primary diseases, neutrophil accumulation and plasma leakage are provoked. When these phenomena spread widely, it is confirmed as opacities in X-ray images. The exudate dilutes lung surfactants and induces alveolar collapse by increasing the surface tension of the alveoli. As a result, the functional lung area is decreased, and a respiratory disorder is induced. ARDS can be diagnosed in this state (Fig. 4.1). Under the deficiency of lung surfactant, it is necessary to perform respiratory management with positive end-expiratory pressure (PEEP). PEEP is one of the respiratory management techniques, which is controlled to leave a positive pressure at end-expiration and makes it possible to prevent the alveoli from collapse. However, PEEP is a temporary countermeasure to prevent collapse, not a causative treatment for ARDS.

Globally, approximately 3 million patients are affected by ARDS per year, and 24% of patients receive respiratory management in the ICU. Unfortunately, even if the patient recovers from ARDS, they may still suffer physical, neuropsychiatric, and neurocognitive disorders; thus, their quality of life deteriorates. In America, 200,000 patients are affected annually, and 75,000 people die (mortality is 37.5%) secondary to ARDS. The number of dead is larger than the number of people who die of breast cancer and HIV infection,

combined<sup>4</sup>. Coronavirus disease 2019 (COVID-19), which has been pandemic in recent years, is also a cause of ARDS. The COVID-19 pandemic affects more than 80 million people and causes 1.7 million deaths worldwide (survey date: 2020/12/30, COVID-19 Dashboard at Johns Hopkins University). It was reported that 20%<sup>5</sup> to 67%<sup>6</sup> of the patients admitted to hospital were diagnosed as ARDS on the basis of oxygenation criteria. Furthermore, most of mechanically ventilated patients with COVID-19 developed ARDS<sup>7</sup>. Therefore, it is clear that ARDS is a highly relevant disease for patients with severe COVID-19 and that ARDS treatment is a global medical challenge.

**Table 4.1. ARDS Berlin definition**

The Berlin definition of acute respiratory distress syndrome	
<b>Timing</b>	Within one week of a known clinical disorder or respiratory symptoms
<b>Chest imaging</b>	Bilateral opacities
<b>Origin of edema</b>	Respiratory failure is not fully explained by cardiac failure or fluid overload
<b>Oxygenation</b>	
Mild	$200 < PaO_2/FIO_2 \leq 300$ [mmHg] with PEEP or CPAP $\geq 5$ [cmH <sub>2</sub> O]
Moderate	$100 < PaO_2/FIO_2 \leq 200$ [mmHg] with PEEP $\geq 5$ [cmH <sub>2</sub> O]
Severe	$PaO_2/FIO_2 \leq 100$ [mmHg] with PEEP $\geq 5$ [cmH <sub>2</sub> O]

ARDS, acute respiratory distress syndrome; CPAP, continuous positive airway pressure;  $F_{I}O_2$ , fraction of inspired oxygen;  $PaO_2$ , arterial partial pressure of oxygen; PEEP, positive end-expiratory pressure

#### 4.1.2. Acute respiratory distress syndrome model

Although some methods induce ARDS, mechanical gas ventilation (MGV),

lipopolysaccharide (LPS), and live bacteria are the three most commonly used. LPS is a glycolipid that presents in the membrane of gram-negative bacteria. Thus, LPS- and bacteria-induced ARDS occur by a similar mechanism. LPS was chosen in this study because its biological mechanism has already been revealed, and good reproducibility was confirmed<sup>8</sup>. The value of the LPS-induced ARDS model has been reviewed to have similar conditions to those in human ARDS<sup>9</sup>, although a single symptom seldom causes ARDS in humans.

#### **4.1.3. Treatments for acute respiratory distress syndrome**

Respiratory management is the gold standard in ARDS therapy for avoiding ventilation-induced lung injury (VILI). Respiratory management is performed while confirming arterial partial pressure of oxygen ( $\text{PaO}_2/\text{F}_1\text{O}_2$ ), arterial partial pressure of carbon dioxide ( $\text{PaCO}_2$ ), and airway pressure. In general, PEEP is applied as the first choice to increase ventilation efficiency and to prevent VILI. In addition, ventilation with low tidal volume (6 mL/kg) is strongly recommended to keep the airway pressure low<sup>10</sup>. Extracorporeal membrane oxygenation (ECMO) is considered when  $\text{PaO}_2/\text{F}_1\text{O}_2$  falls below 80–100 mmHg. If respiratory acidosis progresses, extracorporeal carbon dioxide removal (ECCO<sub>2</sub>R) is considered. According to the guideline, prone positioning and high-frequency oscillatory ventilation (HFOV) are also recommended<sup>10</sup>. However, respiratory managements are only supportive treatments, not causal treatment. The physician must keep the patient breathing mechanically until the inflammation subsides, lung compliance improves, and oxygenation of blood by spontaneous breathing is achieved.

Muscle relaxants and steroids are considered as effective as drug therapy. Although muscle relaxants are used for supporting respiratory management, they are expected to

have a positive effect on respiration and blood circulation in mild to moderate ARDS patients<sup>11</sup>. There is no collective agreement on the efficacy of steroids on survival rate. Though some reports showed efficacy on the survival rate<sup>12,13</sup>, while a multicenter trial on severe ARDS showed no benefit to the survival rate<sup>3</sup>. Commonly, dosing over 14 days is not recommended in steroid treatment<sup>3,11</sup>. A neutrophil esterase inhibitor (Sivelestat; Fuji Pharma Co., Ltd. Tokyo, Japan) is widely used as a treatment for ARDS in Japan. However, a large-scale clinical trial ceased at the intermediate analysis because its efficacy was not shown. On the contrary, mortality was higher than that in the control group<sup>14</sup>.

## **4.2. Efficacy of total alveolar lavage with a total liquid ventilation system using oxygen fine bubble dispersion in a severe lung injury model**

### **4.2.1. Purpose**

Lung lavage is expected to improve patient outcomes in certain inflammatory lung diseases by direct elimination of causal substances. Indeed, it has been applied for a specific lung injury, pulmonary alveolar proteinosis, as a gold standard therapy<sup>15</sup>. However, this technique requires long therapy time which may lead to hypoxemia during lung lavage. Therefore, there are limits in extending the target disease. To overcome the issue, total alveolar lavage (TAL) with a total liquid ventilation (TLV) system using oxygen fine bubble dispersion (FB dispersion) was examined. Since the TLV system can wash both lungs simultaneously, 5 min treatment would be sufficient for lung lavage (see p117). The purposes of this study are 1) to verify the efficacy of TAL on the TLV system in ARDS model rats and 2) to confirm that postoperative rats can return to spontaneous breathing.

### **4.2.2. Materials and experimental procedures**

The protocols for the *in vivo* study were approved by the Committee of Laboratory Animals at the University of Yamanashi, and the *in vivo* studies were conducted following the institutional guidelines.

#### ***Experimental protocol***

A summary of the experimental protocol is shown in Fig. 4.1. Fifteen rats were randomly divided into three groups equally: the TAL treatment group (LPS + TLV group), whose rats received 5 min of TLV and 3 h of MGV 20 min after LPS administration; the MGV treatment group (LPS + MGV group), whose rats received 5 min and 3 h of MGV 20 min after LPS administration; and the Sham group (PBS + MGV group), whose rats received 5 min and 3 h of MGV 20 min after phosphate-buffered saline (PBS)

administration, instead of LPS.

### ***Animal Preparation***

The 15 healthy male Sprague-Dawley rats ( $401 \pm 28$  g) were anesthetized by intramuscular injection of 37.5 mg/kg ketamine hydrochloride (Ketalar; DAIICHI SANKYO COMPANY, LIMITED, Tokyo, Japan). 10 min later, 10 mg/kg propofol (Propofol; Maruishi Pharmaceutical Co., Ltd., Osaka, Japan) was intravenously administered to induce anesthesia and maintained at 30 mg/kg/h for continuous anesthesia. Oral intubation with a 30-mm-long plastic tube (Surflo IV. 14 G Catheter; TERUMO CORPORATION, Tokyo, Japan) was performed with a flexible guidewire. A mechanical gas ventilator or the TLV system was connected via the trachea tube.

### ***Respiratory management***

Respiratory management was performed with an animal ventilator (SAR-830/P ventilator; CWE Inc., PA, USA) under the following conditions;  $F_{I}O_2$ , 1.0; PEEP, 3 cm  $H_2O$ ; respiratory rate, 60/min; inspiratory/expiratory time, 0.5/0.5 s; tidal volume,  $9.2 \pm 0.3$  mL/kg. Electrocardiography and rectal temperature measurements were recorded with a biosignal acquisition recording system (PowerLab 4/26; ADInstruments, New South Wales, Australia). The airway pressure was monitored with a biological information monitor (BSM-2303; NIHON KOHDEN Co., Ltd., Tokyo, Japan).

### ***LPS administration***

Five mg/kg (5 mg/mL in PBS) of LPS was administrated into the lungs via an intubation tube by using a micro sprayer (MicroSprayer, Penn-Century, PA, USA). The rat was fixed in the supine position with its head tilted up  $45^\circ$ . Half of the dose was administered in the left lateral position, and the left chest was vibrated with an electric toothbrush (Mediclean HT-B471, OMRON, Kyoto, Japan) for 10 s. The mechanical gas ventilator was connected for 30 s in the supine position for oxygenation. The remaining

dose was administered in the right lateral position, and the right chest was vibrated with the electric toothbrush for 10 s. Finally, chest percussion and massage for both lungs were manually performed with MGV for 30 s to spread LPS homogenously into the lungs.

### ***TLV treatment***

The TLV system shown in Fig. 3.12a was constructed, and TLV was performed with the following conditions: inspiratory/expiratory pressures were set as 35/-20 cm H<sub>2</sub>O, and inspiratory/expiratory times were set as 3/6 s. The FB dispersion was prepared using a FB generator (GALF; Ultrafine GALF FZ1N-02, IDEC Corporation, Osaka, Japan) at 34±1°C with phosphate buffered saline (DPBS; FUJIFILM Wako Pure Chemical Corp., Osaka, Japan), because the buffering effect inhibits the increase of PaCO<sub>2</sub> during TLV<sup>16</sup>. Before starting the TLV, 1.25 mg/kg rocuronium bromide (Eslax, MSD K.K., Tokyo, Japan) was administered intravenously for myorelaxation. Then, TLV was performed for 5 min (V<sub>T</sub>, 21.6 ± 0.64 mL/kg). After 5 min, water aspiration was performed through the tracheal tube by repeating chest compression in the Trendelenburg position. At this time, we paid special attention not to apply negative and positive pressures to the inside of the lungs. The mechanical gas ventilator was immediately connected to the tracheal tube, and respiratory management was performed for 3 h. After 3 h, anesthesia administration was stopped, and ventilator weaning and extubation were performed after confirming that the rat had awakened from the anesthesia. Finally, the rat was returned to a cage with free access to water and feed and observed for 2 days.

### ***Hemodynamics and blood gas analyses***

After 2 days, the rats were anesthetized with ketamine hydrochloride (37.5 mg/kg), and anesthesia was sustained with propofol using the same protocol described in the *Animal Preparation* section. A tracheotomy was performed and a 14G × 15 mm plastic tube (Surflo IV. 14G Catheter; TERUMO CORPORATION, Tokyo, Japan), shorter than

the oral intubation tube, was inserted into the trachea. The mechanical gas ventilator was connected to the tracheal tube. A 24 G angiocatheter (Surflo IV. 24 G Catheter; TERUMO, Tokyo, Japan) was inserted into the carotid artery for hemodynamic measurement and blood sampling. Hemodynamic parameters were measured with the signal recording system for 10 min. Averages for 10 min of mean arterial pressure (MAP) and heart rate were used as hemodynamic parameters. Subsequently, blood sampling (0.1 mL) was conducted from the carotid artery line, and blood gas analyses were performed with a blood gas analyzer (i-STAT; Abbott, Illinois, USA). Blood gas was analyzed for the potential of hydrogen (pH), PaO<sub>2</sub> (mmHg), PaCO<sub>2</sub> (mmHg), and base excess (B.E., mmol/L).

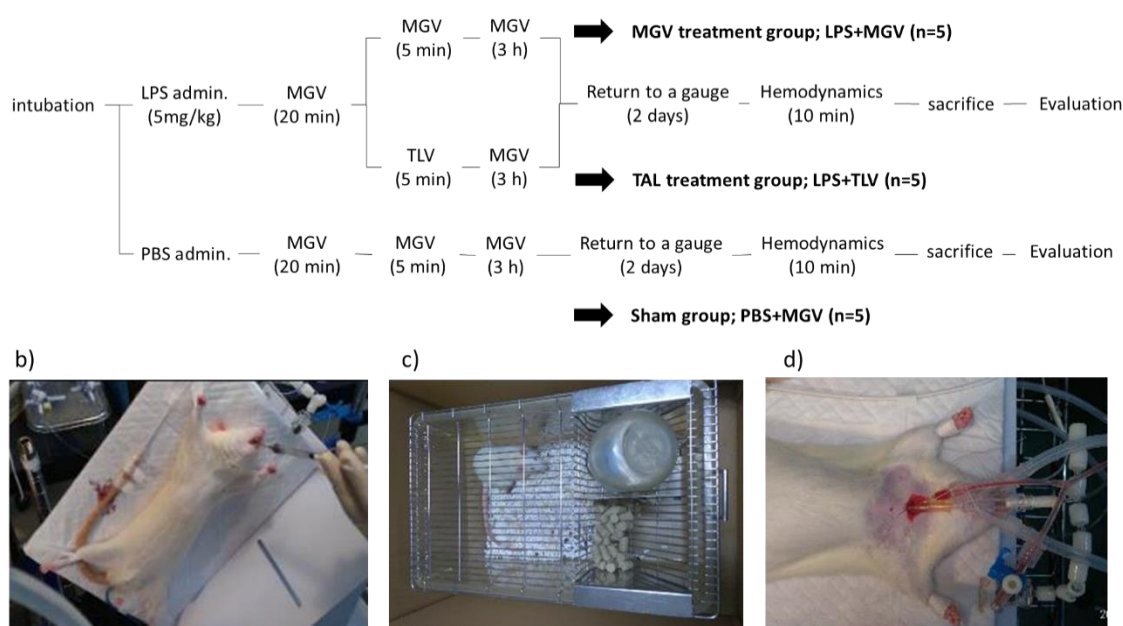


**Fig. 4.1. Protocol of the experiment.** a) Summary of the experimental protocol. Fifteen rats were divided into a TAL treatment group, an MGV treatment group, and a sham group (n = 5 each), b) an LPS (or PBS) administration step, c) an observation step after treatment, d) a hemodynamics measurement step.

***Bronchoalveolar lavage and histopathological examination (postmortem)***

The rats were sacrificed under propofol anesthesia after the final blood gas analyses.

Bronchoalveolar lavage (BAL) and histopathological examination were conducted. The lungs were removed from the chest (Fig. 4.2a), and the right main bronchus was clamped (Fig. 4.2b). BAL was performed with 5 mL of sterilized PBS for the left lung lobe through the tracheal tube (Fig.4.2c). This procedure was repeated twice so that the lavage was carried out with 10 mL of PBS in total. The corrected BAL-fluid (BALF) was centrifuged ( $400 \times g$ , 10 min,  $4^{\circ}\text{C}$ ), and the cell-free supernatant was stored at  $-70^{\circ}\text{C}$  for the enzyme-linked immunosorbent assay (ELISA kit; &D Systems, Minnesota, USA). We measured the amounts of interleukin-6 (IL-6; Rat IL-6 Quantikine ELISA Kit) and cytokine-induced neutrophil chemoattractant 1 (CINC-1; Rat CXCL1/CINC-1 Quantikine ELISA Kit). After BAL examination, the right lungs were isolated and fixed by instilling 10% formalin neutral buffered solution at lower than 25 cmH<sub>2</sub>O for 24–48 h (Fig. 4.2d and e). The posterior lobe and accessory lobe of the fixed lungs were embedded with paraffin and sectioned. Hematoxylin and eosin staining were performed according to the regular staining method, and the tissue sections were observed with a digital microscope (IX71; OLYMPUS Corporation, Tokyo, Japan). Operations after fixation were performed by the staff in the Center for Life Science Research at the University of Yamanashi School of Medicine.

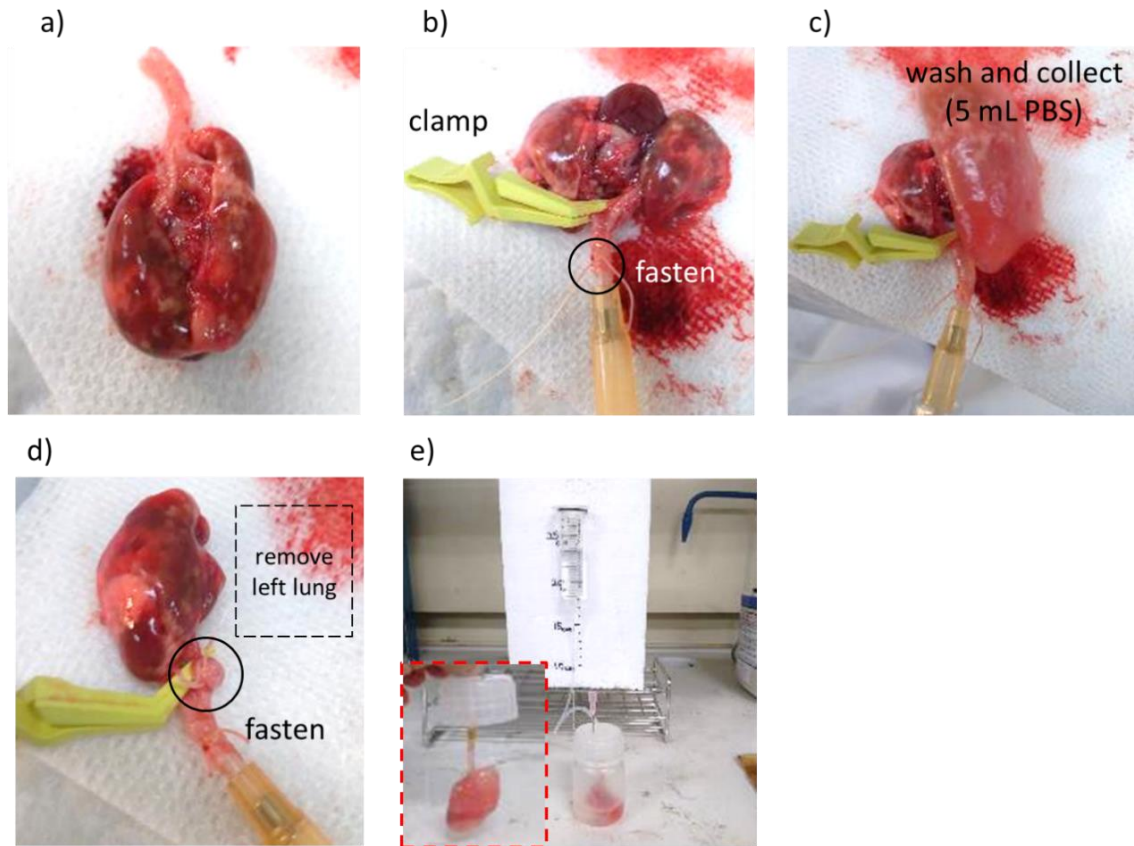


**Fig. 4.2. The procedure for evaluation of isolated lungs.** a) The first step; observation of isolated lungs. b) The second step; preparation for bronchoalveolar lavage: a trachea tube (Surflo IV. 14G Catheter) was inserted into the trachea and fastened with the suture thread, then the right bronchus was closed with a surgical clamp. c) The third step; bronchoalveolar lavage. d) The fourth step; preparation for fixation: a left lung was removed and closed to the remaining left bronchus with a suture thread. e) The fifth step; fixation. A hand-made fixation device was connected to the 14G tube

### ***Statistical analyses***

All results are expressed as mean  $\pm$  SD. Comparisons between groups were performed with the Steel-Dwass nonparametric multiple comparison test following the Kruskal-Wallis nonparametric one-way analysis of variance (ANOVA). Comparisons between the values at day 0 and day 2 in each group were examined with the Wilcoxon

signed-rank test. Statistical analyses were performed using Statcel version 3 (OMS Publishing Ltd., Tokyo, Japan), and  $p$  values  $< 0.05$  were considered statistically significant.

### **4.2.3. Results and discussion**

#### ***Physiological conditions in the three groups after 2 days***

$\text{PaO}_2/\text{F}_1\text{O}_2$  in the TAL treatment group was significantly higher than that in the MGV treatment group and significantly lower than that in the Sham group (Fig. 4.3a,  $p < 0.05$ ).  $\text{SaO}_2$  in the TAL treatment and Sham groups was 100% and significantly higher than that in the MGV treatment group (Fig. 4.3b,  $p < 0.05$ ). Blood oxygenation levels in the TAL treatment and Sham groups were within the normal range, whereas the MGV treatment group showed hypoxemia.  $\text{PaO}_2/\text{F}_1\text{O}_2$  in the MGV treatment group showed 73.2 mmHg, and it was classified into severe ARDS. Although a significant difference in  $\text{PaO}_2/\text{F}_1\text{O}_2$  was confirmed between the Sham and TAL treatment groups, these values were over 300 mmHg; there was no ventilatory impairment. There were no significant differences in  $\text{PaCO}_2$  among all groups, although a few rats in the MGV and TAL treatment groups showed a slightly acidic blood condition (Fig. 4.3c). The potential of hydrogen (pH) in the MGV treatment group was significantly lower than that in the Sham group (Fig. 4.3d,  $p < 0.05$ ). However, the value was within the normal range. Therefore, no group had a disorder in blood acid-base balance.

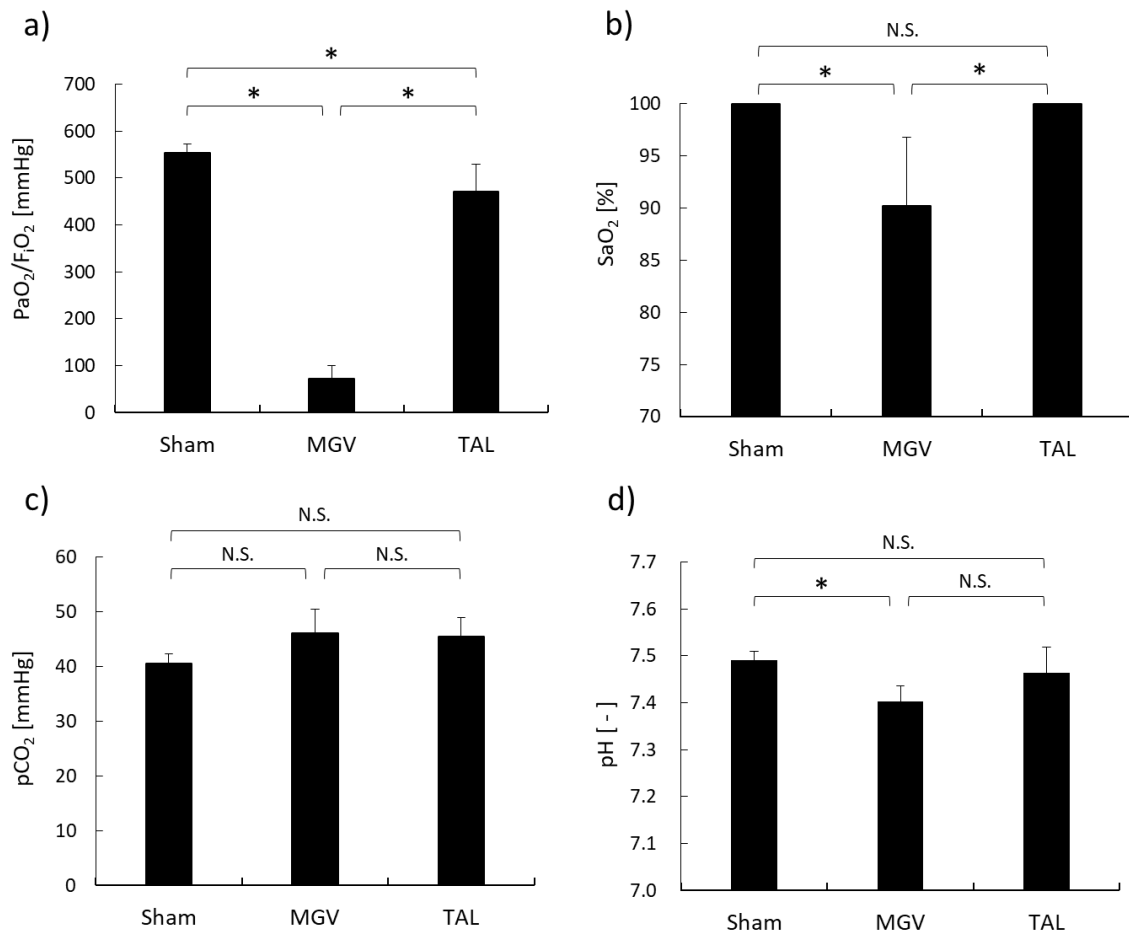


**Fig. 4.3. Blood gas analyses of the rats 2 days after each treatment<sup>1</sup>.** a) Arterial partial pressure of oxygen ( $\text{PaO}_2/\text{F}_i\text{O}_2$ ), b) arterial oxygen saturation ( $\text{SaO}_2$ ), c) arterial partial pressure of carbon dioxide ( $\text{PaCO}_2$ ), and d) potential of hydrogen (pH) were measured in blood gas analyses 2 days after each treatment ( $n = 5$ ). Sham, MGV, and TAL mean Sham treatment group, MGV treatment group, and TAL treatment group, respectively.

MAP in the TAL treatment group was significantly higher than that in the MGV treatment group (Fig. 4.4a,  $p < 0.05$ ), and there were no significant differences between the other groups (Fig. 4.4a). However, 120 mmHg in the MGV treatment group was a low value compared to the normal range (150–180 mmHg). There were no significant differences in heart rate among all groups (Fig. 4.4b). Since the body weight decreased in the MGV treatment group (Fig. 4.5c), it was suspected that circulating blood volume

decreased due to dehydration. As a result, the heart rate was increased to maintain oxygenation and showed a normal range. However, pneumonia-induced sepsis may have caused the cardiac disorder. It is necessary to examine the amount of drinking water or cytokines level in the blood to determine the cause of cardiac disorder.

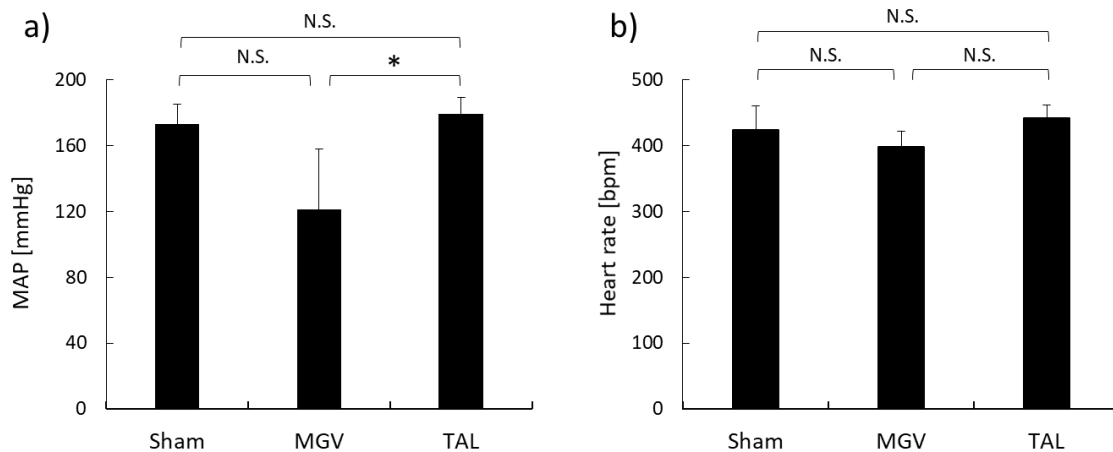


**Fig. 4.4. Hemodynamics of the rats 2 days after each treatment<sup>1</sup>.** Average of a) Mean arterial pressure (MAP) and b) Heart rate for 10 min in the MGV treatment, TAL treatment, and Sham groups 2 days after each treatment (n = 5).

The changes in peak inspiratory pressure (PIP) and body weight between day 0 and day 2 in the three groups are shown in Fig. 4.5. PIP at day 0 (after each treatment) in the TAL treatment group was significantly higher than those in the MGV treatment and Sham groups, which were not significantly different from each other (Fig. 4.5a gray bars,  $p < 0.05$ ). The increment of PIP in the TAL treatment was induced by the remaining FB dispersion inside the lungs after TLV; TLV did not harm lung structure. Therefore, there was no difference between the Sham and MGV treatment groups: without lung washing groups. However, it is not a severe side effect since a value of 16 mmHg (21.8 cmH<sub>2</sub>O) is not considered to be high enough to damage alveolar structures<sup>17</sup>. PIP at day 2 in the Sham group was significantly lower than that in the TAL and MGV treatment groups (Fig. 4.5a, black bars,  $p < 0.05$ ). There was no significant difference in PIP between day 0 and

day 2 in all groups. Moreover, although PIP in the MGV treatment group showed the highest value among the three groups at day 2, the value of 16 mmHg was not serious. However, focusing on the change between day 0 and day 2 ( $\Delta$ PIP), the  $\Delta$ PIP in the MGV treatment group showed a positive value, and the  $\Delta$ PIP in the TAL treatment and Sham groups showed negative values. There were significant differences between the  $\Delta$ PIP in the MGV treatment group and the other two groups (Fig. 4.5b,  $p < 0.05$ ). Only in the MGV treatment group, the condition inside the lungs deteriorated within 2 days with inflammation; thus, the airway pressure increased. It means complications of ventilator associated lung injury is induced if inflammation is not suppressed. Meanwhile, the PIP in the TAL treatment group decreased from day 0 to day 2. It indicated that lung obstruction due to inflammation did not occur, and it is expected the capillary absorption and vaporization of the remnant FB dispersion occur.

The body weights of all rats significantly decreased 2 days after each treatment (Fig 4.5c,  $p < 0.05$ ). Although all rats lost their weight, the percentage of weight loss in the MGV treatment group was significantly higher than those in the TAL treatment and Sham groups (Fig. 4.5d,  $p < 0.05$ ). It is considered that rats with severe inflammation lost much weight because they might not take food and water. Probably, there was a difference in the exercise intensity of the rats, and it is expected that the rats in the MGV treatment group were significantly less active than those in the other two groups.

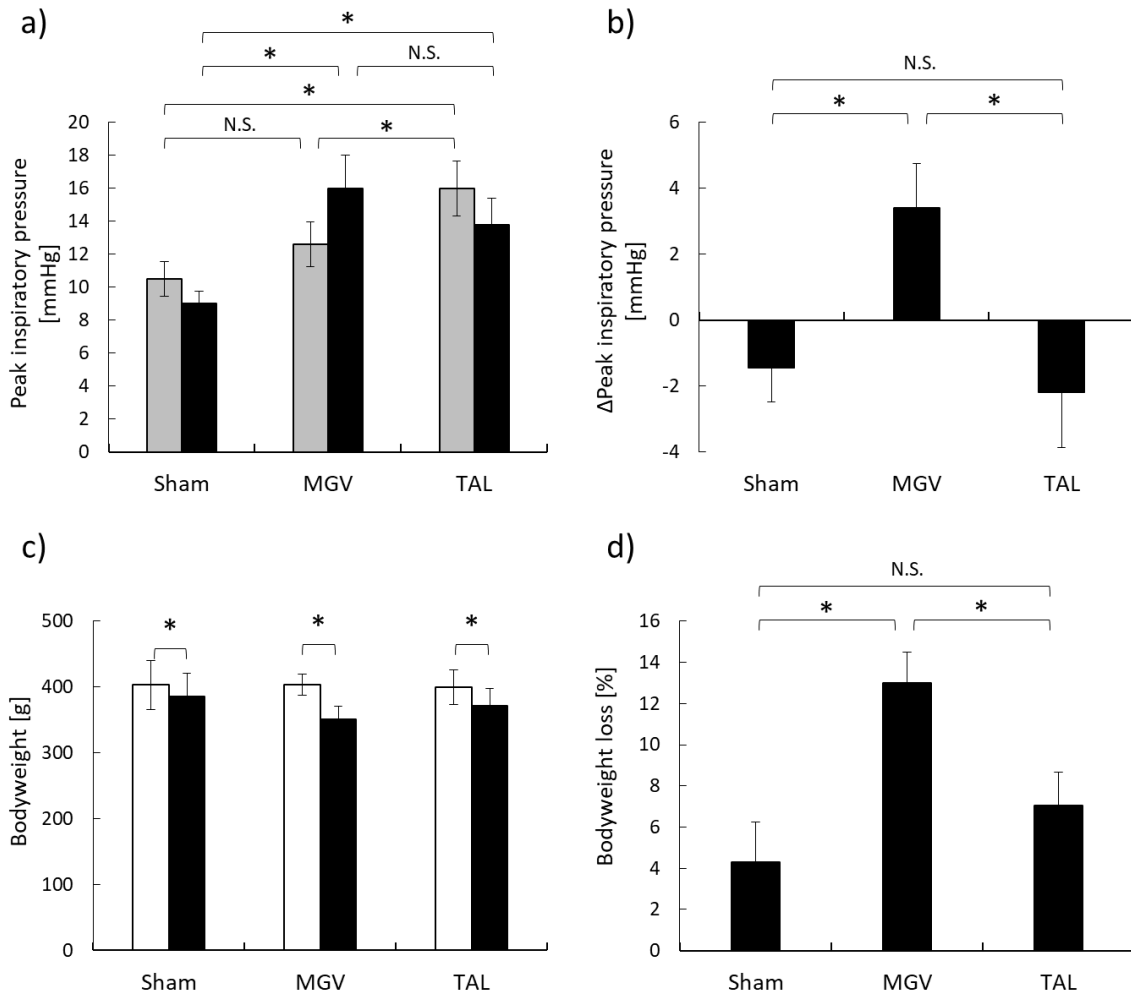


**Fig. 4.5. The changes in peak inspiratory pressure and body weight between day 0 and day 2<sup>1</sup>.** a) Peak inspiratory pressure at day 0 and day 2 (gray bar: day 0 [after treatment], black bar: day 2) and b) The degree of change in the peak inspiratory pressure ( $\Delta$ peak inspiratory pressure = PIP at day 0 – PIP at day 2) in the MGJV treatment, TAL treatment, and Sham groups (n = 5). c) The body weight of the rats at day 0 and day 2 (white bar: day 0 [before treatment], black bar: day 2) and d) The percentage of body weight loss in the MGJV treatment, TAL treatment, and Sham groups (n = 5), \*p < 0.05.

Fig. 4.6 shows the macroscopic findings of the lungs and the histopathological findings for each lung tissue. Homogenously severe inflammation was confirmed in the

MGV treatment group (Fig. 4.6b). However, mild inflammation was observed in the TLV treatment group, and healthy features were observed in the Sham group (Fig. 4.6a and c). At the tissue level, the MGV treatment group showed the typical signs of inflammation: accumulation of neutrophils in the interalveolar spaces, thickened alveolar walls, and interstitial congestion (Fig. 4.6e). These findings were suppressed in the TAL treatment group, which showed only mild inflammatory features (Fig. 4.6f). The Sham group showed normal findings (Fig. 4.6d).

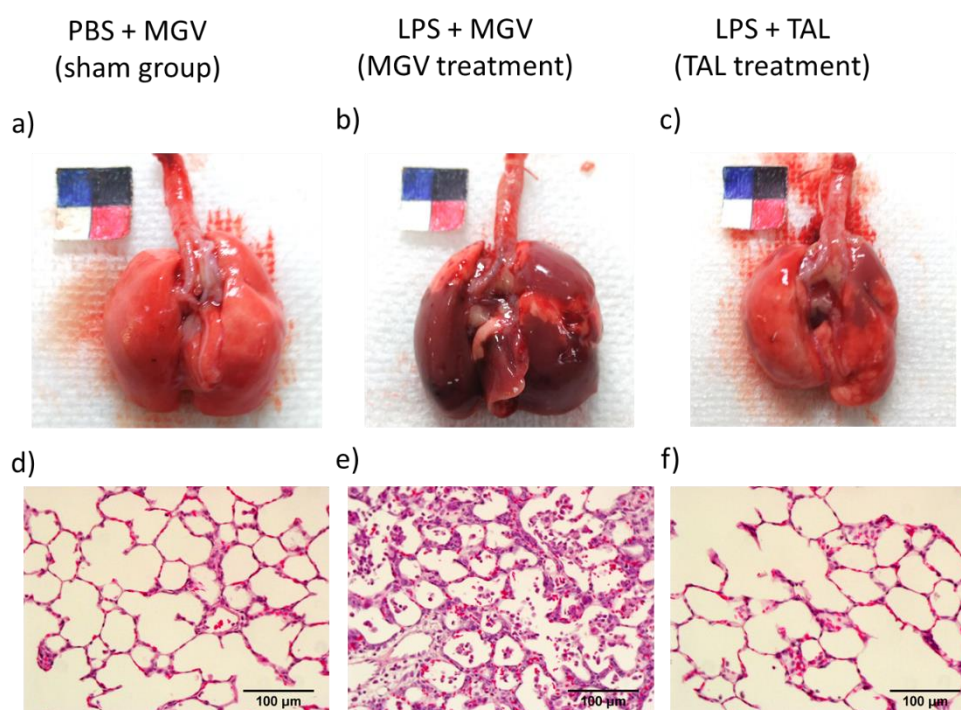


**Fig. 4.6.** The macroscopic and histopathological findings of the lungs 2 days after each treatment<sup>1</sup>. The representative pictures of the lungs in the a) Sham group, b) MGV treatment group, and c) TAL treatment group. The left top sheet is a color and length scale with a 10-mm square (5-mm square in four colors). Representative microscopic images of the lung tissue section (posterior lobe) stained with hematoxylin and eosin (H&E) in the d) Sham group, e) MGV treatment group, and f) TAL treatment group. Scale bar, 100 µm.

Inflammatory cytokine levels in the BALF, expressed as natural logarithmic values, are shown in Fig. 4.7. The IL-6 level in the MGV treatment group was significantly higher than that in the Sham group (Fig. 4.8a,  $p < 0.05$ ) and the IL-6 level in the TLV treatment group tended to be placed in between those in the Sham and MGV treatment groups (Fig. 4.7a). The concentration of cytokine-induced neutrophil chemoattractant 1 (CINC-1), which induced the accumulation of neutrophils in the MGV treatment group, was significantly higher than those in the TAL treatment and Sham groups (Fig. 4.7b,  $p < 0.05$ ). Levels of inflammatory cytokines were increased in the MGV treatment group and suppressed in the TAL treatment group. These results showed the same tendency as the macroscopic and microscopic findings in Fig. 4.6. IL-6 is one of the most active proinflammatory cytokines and shows elevated levels associated with pathological disorders such as ARDS<sup>18</sup>. CINC-1 and CINC-3, are chemokines that contribute to the accumulation of neutrophils and are known to be increased in LPS-induced pulmonary inflammation<sup>9</sup>. CINC-1 in rodents play a role as the same as IL-8 in humans.

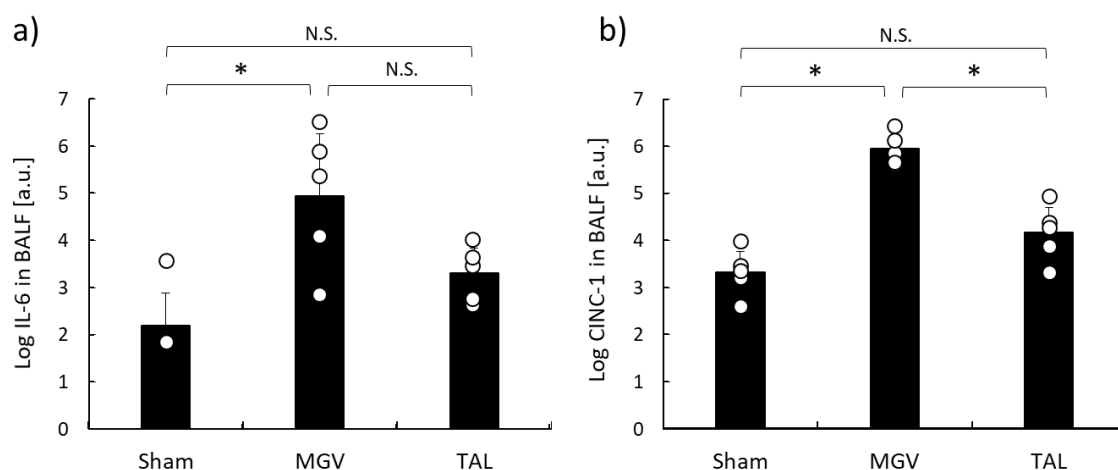


**Fig. 4.7. The concentrations of inflammatory cytokines and chemokines 2 days after each treatment<sup>1</sup>.** The concentrations of a) IL-6 and b) CINC-1 in the BALF in the Sham, MGV treatment, and TAL treatment groups ( $n = 5$ ). The results are shown as natural

logarithmic values. The opened circle represents each measurement value in a group. \* $p < 0.05$ .

The inflammatory responses induced by LPS are summarized in Fig. 4.8. LPS binds to TLR-4 and CD-14 on the cell surface of Type I pneumocytes and alveolar macrophages. The activated cells release tumor necrosis factor  $\alpha$  (TNF- $\alpha$ ) and IL-1 $\beta$  and subsequently secrete IL-6 and IL-8 (CINC-1). IL-8 (CINC-1) induces neutrophil infiltration,

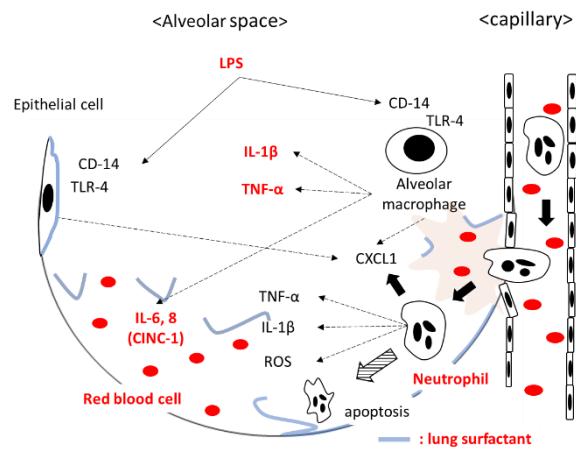


**Fig. 4.8. inflammatory responses induced by lipopolysaccharide.**

which further secretes inflammatory cytokines. These inflammatory responses weaken the adhesion of the vascular endothelium and provoke alveolar hemorrhage and pulmonary edema. In this experiment, the characteristics of the inflammatory response were confirmed in the MGV treatment group from the ELISA results, the appearance of the isolated lungs, and the features of the tissue sections. Meanwhile, in the TAL treatment group, it was significantly suppressed. Although I did not conduct this in the experiment, the therapeutic effect can be specifically shown by measuring the amount of cytokines and LPS contained in the drained solution (FB dispersion) during TAL treatment.

The 5-min TAL with the TLV system using the FB dispersion prevented the rats from pulmonary inflammation. However, it is also interesting that the rats recovered from TLV to spontaneous breathing without supplementation of lung surfactants or alternative drugs. In general, lung lavage with normal saline is used to prepare a lung surfactant-deficient model<sup>19-21</sup>. Therefore, we thought that lung surfactants were necessary to return

to spontaneous breathing. However, the rats recovered to MGV from TLV, and ventilation weaning was performed after respiratory management for 3 h. Since there was no pneumonocyte in BALF 2 days after TLV (Fig. 4.9), the type II alveolar epithelial cells were believed not to be washed away. However, it is necessary to repeat and verify this experiment because this is a result of a preliminary examination. If lung

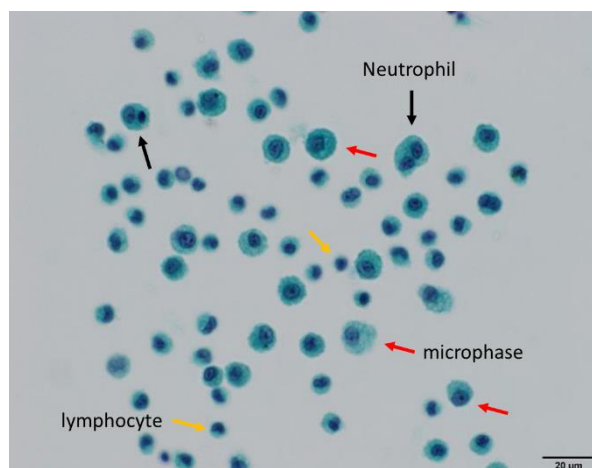


**Fig. 4.9. Inflammatory cells in BALF 2 days after TAL treatment.** Black arrows, neutrophils; red arrows, alveolar microphases; yellow arrows, lymphocytes. Scale bar, 20 $\mu$ m. Stain, Papanicolaou stain.

surfactants were washed out during the TAL treatment, some biological events would be necessary to regenerate lung surfactants during the respiratory management for 3 h. However, it is already confirmed that the sufficient drainage of the FB dispersion from the lungs was essential for this returning operation. If drainage were insufficient, the rats would die within 3 h. Therefore, drainage is the most important process for management after lung lavage. In this study, I established a returning operation after many attempts (see section: *TAL treatment*) to remove the FB dispersion from the rat's lungs efficiently.

### **4.3. Efficacy of total alveolar lavage with a total liquid ventilation system using oxygen fine bubble dispersion in a lethal lung injury model**

#### **4.3.1. Purpose**

The efficacy of TAL with the TLV system was confirmed in the severe lung injury model. The results showed that TAL prevented the rats from severe lung inflammation by removing the causative substances. However, the rats receiving the MGV treatment survived for 7 days, even when they had severe respiratory failure on day 2. Therefore, it is necessary to show the efficacy of TAL in more severe conditions. Moreover, the necessity of FBs was still unknown from the previous experiment. The purposes of this experiment are 1) to examine the efficacy of TAL treatment in a lethal lung injury model and 2) to examine the efficacy of a TAL treatment with oxygenated PBS.

#### **4.3.2. Materials and experimental procedures**

##### ***Experimental protocol***

Thirteen rats were randomly divided into three groups: the TAL treatment with FB dispersion group (n = 5), in which the rats received 5 min of TLV with FB dispersion and 3 h of MGV 20 min after LPS administration; the TAL treatment with oxygenated PBS group (n = 3), in which the rats received 5 min of TLV with oxygenated PBS and 3 h of MGV 20 min after LPS administration; the MGV treatment group (n = 5), in which the rats received 5 min and 3 h of MGV 20 min after LPS administration.

##### ***Animal preparation***

The 13 healthy male Sprague-Dawley rats ( $392 \pm 27.7$  g) were anesthetized by intramuscular injection of 37.5 mg/kg ketamine hydrochloride. Ten min later, 10 mg/kg propofol was intravenously administered for induction of anesthesia and maintained at 30 mg/kg/h for continuous anesthesia. Oral intubation with a 30-mm-long plastic tube was

performed with a flexible guidewire. The mechanical gas ventilator or TLV system was connected via the tube.

### ***Respiratory management***

Respiratory management was performed with the animal ventilator under the following conditions:  $F_{I}O_2$ , 1.0; PEEP, 3 cm  $H_2O$ ; respiratory rate, 60/min; inspiratory time/expiratory time, 0.5/0.5 s; tidal volume,  $9.38 \pm 0.12$  mL/kg. Electrocardiography and rectal temperature were measured and recorded with the Power lab system for monitoring the physiological condition of the rats. The airway pressure was monitored with a biological information monitor.

### ***LPS administration***

A 10 mg/kg (5 mg/mL in PBS) of LPS, double volume as the previous experiment, was administered into the lungs via the intubation tube using a micro sprayer. The LPS administration method was the same as in the previous experiment (Chapter 4.2).

### ***Oxygenated phosphate-buffered saline***

Oxygenated PBS was prepared by an air stone (Soft-tube air bubble; Faburo jp, Shenzhen, China) at the middle reservoir in the TLV system shown in Fig. 3.12a. 100% oxygen gas was fed at a rate of 0.5 L/min to generate macro oxygen bubbles at  $34 \pm 1^\circ C$ . PBS was continuously supplied from the upper reservoir so that the overflow system worked. Thus, the water head pressure was kept stable at 35 cm $H_2O$ .

### ***TAL treatment***

The TLV system shown in Fig. 3.12a was constructed and performed with the following conditions: inspiratory/expiratory pressures were set as 35/-20 cm  $H_2O$ , and the inspiratory/expiratory time was set at 3/6 s. The FB dispersion was prepared in the same way as the previous experiment (Chapter 4.2)

Before starting the TAL treatment, 1.25 mg/kg rocuronium bromide was

administered intravenously for myorelaxation. Then, TAL was performed for 5 min ( $V_T$ ,  $22.8 \pm 0.57$  and  $21.7 \pm 0.41$  mL/kg in the TAL treatment with FB dispersion and oxygenated PBS, respectively). After 5 min, water aspiration was performed through the tracheal tube by repeating chest compression in the Trendelenburg position. The mechanical gas ventilator was immediately connected to the tracheal tube, and gas ventilation was performed for 3 h. Ventilator weaning and extubation were performed after confirming that the rat had awakened from anesthesia. Finally, the rat was returned to a cage with free access to water and feed and observed for 7 days.

#### ***Hemodynamics and blood gas analyses***

After 7 days, the surviving rats were anesthetized with ketamine hydrochloride (37.5 mg/kg), and anesthesia was sustained with propofol (10 mg/kg and 30 mg/kg/h) with the same protocol as that described in the *Animal Preparation*. The procedures of hemodynamics and blood gas analyses were the same as those in the previous experiment.

#### ***Statistical analyses***

All results are expressed as mean  $\pm$  SD. Comparisons between the two groups were examined with the student t-test. The survival curves were constructed by the Kaplan–Meier method, and differences between the curves were tested with the log-rank statistic. Statistical analyses were performed using Statcel version 3 (OMS Publishing Ltd., Tokyo, Japan), and p values  $< 0.05$  were considered statistically significant.

#### **4.3.3. Results and discussion**

Fig. 4.10 shows the survival rate of the lethal lung injury model rats after each treatment. All rats in the MGJV treatment group died within 2 days after administration of 10 mg/kg LPS. Meanwhile, the survival rate of the rats significantly improved to 80% in the TAL with FB dispersion group (vs. MGJV treatment:  $p = 0.0079$ ) and 100% in the TAL

treatment with oxygenated PBS group (vs. MGV treatment:  $p = 0.027$ ). There was no difference between TAL treatment groups ( $p = 0.44$ ). A rat in the TAL with FB dispersion group died 3 days after the treatment, and its lungs showed severe inflammation and hemorrhage. It is thought that the lung lavage was inadequate. Concerning the TAL treatment time, according to the report on whole lung lavage (WLL) for protein alveolar proteinosis (PAP), 10–23 washes should be enough to remove the surfactant-like substance from the lungs<sup>22–24</sup>. Since the TLV system can wash both lungs 33 times within 5 min, the TAL treatment was conducted only for 5 min in this experiment. However, a target symptom was different from PAP; thus, it is necessary to examine with increasing the frequency of lung lavage. If there is a method for quickly measuring a substance contained in the drained solution, a more appropriate operation time can be determined at an operating site. Although it is difficult to discuss the necessity of FB on the lavage effect from these results, the efficacy of the TAL with the TLV system on pulmonary inflammation was confirmed, even without FBs.

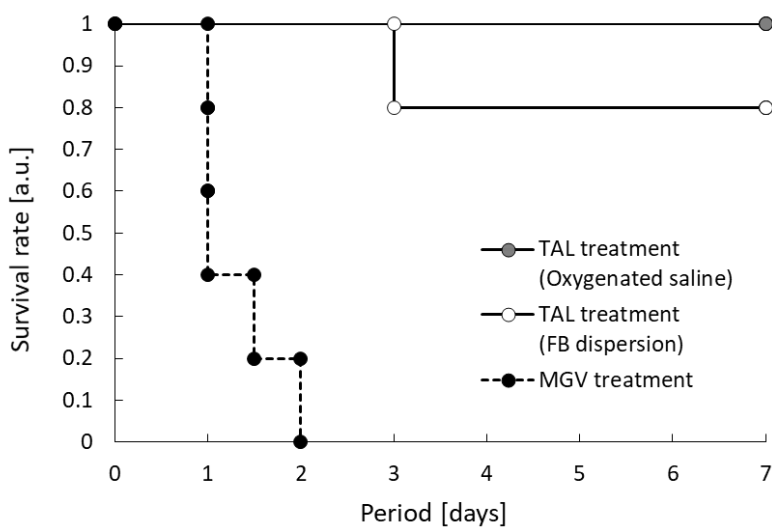


**Fig. 4.10. The survival rate of lethal lung injury model rats.** a) The Kaplan-Meier curve of the rats in the TAL with FB dispersion group, the TAL with oxygenated PBS group, and MGV treatment group. (gray circle; TAL with oxygenated PBS group [ $n = 3$

rats]; opened circle, the TAL with FB dispersion group [n = 5]; closed circle, MGV treatment group [n = 5]).

Fig. 4.11 shows the representative pictures of the isolated lungs and their tissue section at the posterior lobe. The lung in the MGV treatment group 2 days after the treatment showed homogenous severe congestion and hypertrophy (Fig. 4.11a, upper). The histopathological findings in the MGV treatment group showed accumulation of neutrophils with severe alveolar hemorrhage (Fig. 4.11a, bottom). Both macroscopic and microscopic findings in the TAL with FB dispersion group indicated almost healthy and well-preserved alveolar structures (Fig. 4.11b). The same results were obtained in the TAL with oxygenated PBS group (Fig. 4.11c). However, TAL treatment just reduced the degree of inflammation by eliminating inflammatory substances. The rats in the TAL group might get inflammation, which was induced by the remaining LPS. Then they recovered from the inflammation thanks to their immune response. Indeed, the rats in the TAL groups appeared weak and showed low activity until 2 days after the TAL treatments, gradually recovered beginning on the 3<sup>rd</sup> day. Finally, they were almost completely healthy after 7 days.

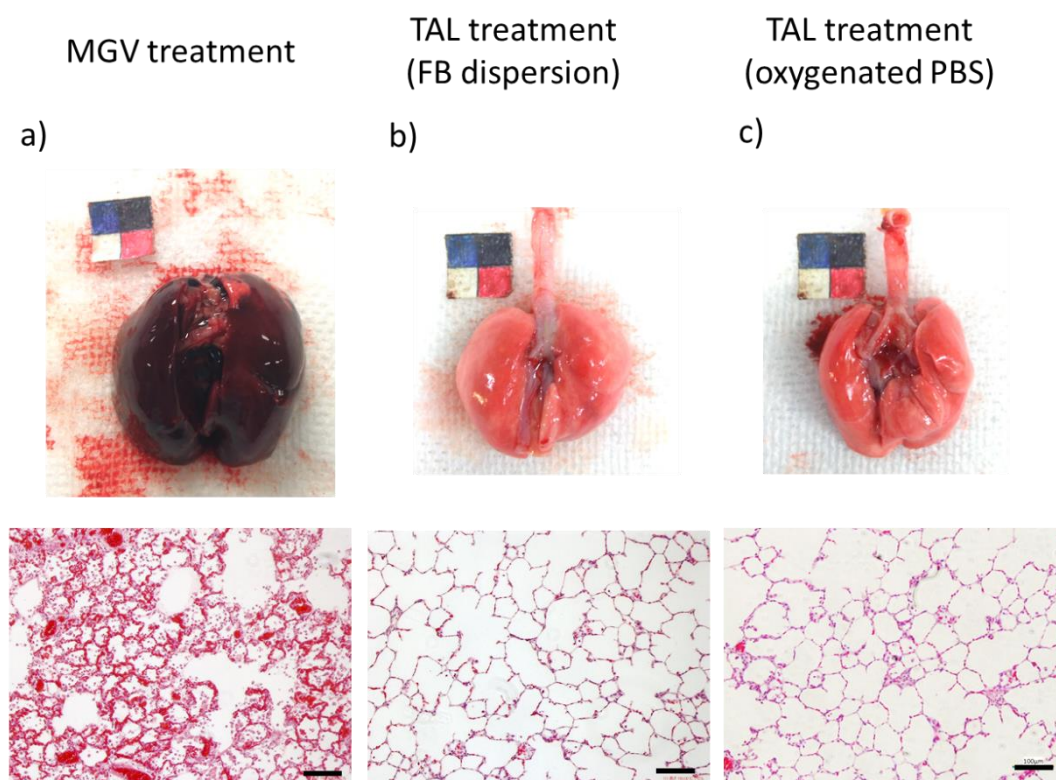


**Fig. 4.11. Representative pictures of the lungs and histopathological findings.** Isolated lung and its tissue sections were stained with hematoxylin and eosin (H&E) in a) the MGV treatment group, b) the TAL treatment with FB dispersion group, and c) the TAL treatment with oxygenated PBS group. The left top sheet is a color and length scale with a 10-mm square (5-mm square in four colors). Scale bar, 100  $\mu\text{m}$ .

Table 4.2 shows the summary of the physiological conditions of the surviving rats 7 days after the TAL treatments and the rats in the Sham group in the previous experiment (Chapter 4.2).  $\text{PaCO}_2$  in the TAL with FB dispersion group was significantly higher than that in the TAL with oxygenated PBS group ( $p < 0.05$ ); however, the value showed a mild disorder. Since pH in blood was within the normal range and B.E. and  $\text{HCO}_3^-$  were higher than the normal range in the TAL with FB dispersion group, metabolic alkalosis was suspected. Focusing on the body weight loss 7 days after the treatment, the rats in the TAL with FB dispersion group lost more weight than those in the TAL with oxygenated

PBS group (-5.9% vs. -2.4%). Thus, it is considered that the decrease of fluid volume due to dehydration induced metabolic alkalosis, and PaCO<sub>2</sub> increased due to respiratory compensation. Since similar symptoms were observed in the rats of the Sham group in the previous experiment (Chapter 4.2), it is believed that the cause is not the influence of inflammation or the FB dispersion, but postoperative feeding behavior. If the cause is dehydration, this problem can be resolved by infusion management. However, it is not considered a severe problem because symptoms were mild, and there were no abnormalities in hemodynamics (MAP: 173 ± 15.6 mm Hg, HR: 431 ± 46.6 bpm) and blood oxygenation (PaO<sub>2</sub>/FiO<sub>2</sub>: 505 ± 50.9, SaO<sub>2</sub>: 100%) in the surviving rats in the TAL treatment with FB dispersion group. The PIP in the TAL group at 7 days after treatment was 10.5 ± 1.7 mmHg (with FB dispersion) and 9.3 ± 0.6 mmHg (with oxygenated PBS), respectively. These were similar to the values in the Sham group in the previous experiment. It is suggested that FB dispersion and PBS can be safely absorbed into the body or vaporized.

**Table 4.2. Physiological conditions of the survived rats after 7 days.**

	pH	PaCO <sub>2</sub>	PaO <sub>2</sub> /F <sub>I</sub> O <sub>2</sub>	B.E.	HCO <sub>3</sub> <sup>-</sup>	PIP
	[ - ]	[mmHg]	[mmHg]	[mmol/L]	[mmol/L]	[mmHg]
FB dispersion	7.44 ± 0.05	47.4 ± 2.02*	506 ± 50.9	8.3 ± 3.9	32.2 ± 2.52	10.5 ± 1.73
Oxygenated PBS	7.45 ± 0.04	40.2 ± 3.70	491 ± 40.4	3.7 ± 2.1	27.9 ± 1.43	9.3 ± 0.6
Sham	7.49 ± 0.02	40.5 ± 1.90	554 ± 18.0	7.6 ± 1.0	30.9 ± 1.16	9.0 ± 0.7
Normal range	7.4 ± 0.05 <sup>25</sup>	40 ± 5 <sup>25</sup>	300< <sup>2</sup>	±2 <sup>25</sup>	24 ± 2 <sup>25</sup>	<22.1 <sup>26</sup>

FB: fine bubble; O<sub>2</sub>-PBS: oxygenated phosphate-buffered saline; pH: potential of hydrogen; PaCO<sub>2</sub>: arterial partial pressure of carbon dioxide; PaO<sub>2</sub>: arterial partial pressure of oxygen; F<sub>I</sub>O<sub>2</sub>, F<sub>I</sub>O<sub>2</sub>: fraction of inspired oxygen; B.E.: base excess; HCO<sub>3</sub><sup>-</sup>: hydrogen carbonate; PIP: peak inspiratory pressure. \*p < 0.05.

I hypothesized that the TAL with FB dispersion showed a greater lavage effect than the TAL with oxygenated PBS; however, there was no difference. This means that the TAL with oxygenated PBS was enough to remove inflammatory substances, such as LPS and cytokines, considering only the effect of lung lavage. An advantage of FB dispersion compared to oxygenated PBS was seen in the

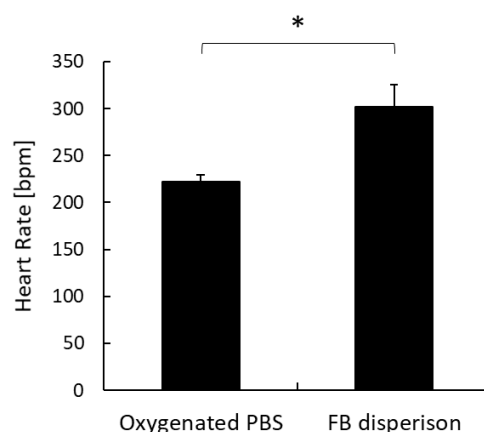


**Fig. 4.12. Heart rate during the total alveolar lavage treatment.**

heart rate during the TAL treatments. Only electrocardiogram and body temperature were measured during the TAL treatments to evaluate the physiological condition of the rats. However, the heart rate in the TAL with oxygenated PBS group was significantly lower than that in the TAL with FB dispersion group (Fig. 4.12,  $p < 0.05$ ). The frequency of arrhythmias was also increased in the TAL with oxygenated PBS group. Since the oxygen content in the liquid is important to maintain cardiac function during TAL treatments, FB dispersion ( $41.4 \pm 1.51$  mg/L) is more suitable for TLV than oxygenated PBS ( $23.9 \pm 0.31$  mg/L) in terms of dissolved oxygen.

Since FB dispersion is composed of only PBS and oxygen, it is possible to evaluate biomarkers in the drained liquid during TAL treatment with a conventional BALF evaluation. This means that our TLV system can be used as not only a TAL treatment but also an inspection method for severe respiratory failure. Moreover, it is expected that an advanced effect would be obtained by combining the TLV treatment with some drugs like anti-inflammatory drugs. However, the TLV experiment with gas liposome dispersion, which is summarized in chapter 3, suggests that it is necessary to consider the foamability and the influence on fluid flow in the lungs.

Recently, the pneumonia-like disease caused by a new coronavirus (COVID-19) is spread all over the world<sup>27</sup>. For such lung diseases, lung lavage may be capable of direct removal of causative substances from the lungs. There is a report that claims that BAL can collect the virus from the lower respiratory tract<sup>28,29</sup>. It is possible to wash out a part of the propagated virus from the lungs. When the immune system fights the virus in the body, reducing the absolute number of the virus is considered to provide some value. However, since the virus infecting the host cell cannot be washed out, it is difficult to completely cure only with the TAL treatment. I hope that the efficacy of TAL treatment will improve when combined with drugs.

#### **4.4. Conclusions of this chapter**

This chapter includes two experiments: Efficacy of the TAL with the TLV system on 1) a severe lung injury model and 2) a lethal lung injury model. The important findings for each experiment are summarized below.

##### ***1) Efficacy of TAL with a TLV system using oxygen fine bubble dispersion in a severe lung injury model***

The 5-min TAL treatment with the TLV system prevented the rats from severe lung injury. TAL treatment preventively improved the LPS-induced inflammatory responses compared to MGIV treatment. Furthermore, the rats receiving TAL treatment could recover to spontaneous respiration without lung surfactant administration.

##### ***2) Efficacy of TAL with a TLV system using oxygen fine bubble dispersion in a lethal lung injury model***

The 5-min TAL treatment with the TLV system prevented severe pulmonary inflammation and dramatically improved the survival rates of the ALI model rats. Moreover, blood oxygen level and cardiac functions were recovered to healthy conditions 7 days after TAL treatment, although tendency of alkalosis was suggested. Lung lavage was achieved with oxygenated PBS; therefore, FBs are not necessary for this purpose. However, the FB dispersion (supersaturated solution) was superior to oxygenated PBS in terms of oxygen supply during the TAL treatment.

## References

1. Kakiuchi, K., Miyasaka, T., Takeoka, S., Matsuda, K. & Harii, N. Total alveolar lavage with oxygen fine bubble dispersion directly improves lipopolysaccharide-induced acute respiratory distress syndrome of rats. *Sci. Rep.* **10**, (2020).
2. Ranieri, V. M. *et al.* Acute respiratory distress syndrome: The Berlin definition. *JAMA* **307**, 2526–2533 (2012).
3. Matthay, M. A. *et al.* Acute respiratory distress syndrome. *Nat. Rev. Dis. Prim.* **5**, 1–22 (2019).
4. Fan, E., Brodie, D. & Slutsky, A. S. Acute respiratory distress syndrome advances in diagnosis and treatment. *JAMA* **319**, 698–710 (2018).
5. Wang, D. *et al.* Clinical Characteristics of 138 Hospitalized Patients with 2019 Novel Coronavirus-Infected Pneumonia in Wuhan, China. *JAMA - J. Am. Med. Assoc.* **323**, 1061–1069 (2020).
6. Yang, X. *et al.* Clinical course and outcomes of critically ill patients with SARS-CoV-2 pneumonia in Wuhan, China: a single-centered, retrospective, observational study. *Lancet Respir. Med.* **8**, 475–481 (2020).
7. Arentz, M. *et al.* Characteristics and Outcomes of 21 Critically Ill Patients With COVID-19 in Washington State. *JAMA* **323**, 1612–1614 (2020).
8. Matute-Bello, G., Frevert, C. W. & Martin, T. R. Animal models of acute lung injury. *Am. J. Physiol. Cell. Mol. Physiol.* **295**, L379–L399 (2008).
9. Chen, H., Bai, C. & Wang, X. The value of the lipopolysaccharide-induced acute lung injury model in respiratory medicine. *Expert Rev. Resp. Med* **4**, 773–783 (2010).
10. Fan, E. *et al.* An official American Thoracic Society/European Society of intensive care medicine/society of critical care medicine clinical practice

- guideline: Mechanical ventilation in adult patients with acute respiratory distress syndrome. *Am. J. Respir. Crit. Care Med.* **195**, 1253–1263 (2017).
11. Otsuka, M. *ARDS (Japanese). kyukyu, shuchu chiryo* **29**, (2017).
  12. Meduri, G. U. *et al.* Effect of prolonged methylprednisolone therapy in unresolving acute respiratory distress syndrome: A randomized controlled trial. *J. Am. Med. Assoc.* **280**, 159–165 (1998).
  13. Meduri, G. U. *et al.* Methylprednisolone infusion in early severe ards: Results of a randomized controlled trial. *Chest* **131**, 954–963 (2007).
  14. Zeiher, B. G. *et al.* Neutrophil elastase inhibition in acute lung injury: Results of the STRIVE study. *Crit. Care Med.* **32**, 1695–1702 (2004).
  15. Campo, I. *et al.* Whole lung lavage therapy for pulmonary alveolar proteinosis : a global survey of current practices and procedures. *Orphanet J. Rare Dis.* **11**, 115–125 (2016).
  16. Oue, A. Improvement of total liquid ventiation with oxygen micro/nano bubble dispersion. Master thesis, Waseda University (Japanese). (2016).
  17. Webb, H. H. & Tierney, D. F. Experimental pulmonary edema due to intermittent positive pressure ventilation with high inflation pressures. Protection by positive end-expiratory pressure. *Am. Rev. Respir. Dis.* **110**, 556–565 (1974).
  18. Chepurnova, D. A., Samoilova, E. V., Anisimov, A. A., Verin, A. D. & Korotaeva, A. A. Compounds of IL-6 Receptor Complex during Acute Lung Injury. *Bull. Exp. Biol. Med.* **164**, 609–611 (2018).
  19. Lachmann, B., Robertson, B. & Vogel, J. In Vivo Lung Lavage as an Experimental Model of the Respiratory Distress Syndrome. *Acta Anaesthesiol. Scand.* **24**, 231–236 (1980).
  20. Nakazawa, K., Yokoyama, K., Yamakawa, N. & Makita, K. Effect of positive

- end-expiratory pressure on inflammatory response in oleic acid-induced lung injury and whole-lung lavage-induced lung injury. *J. Anesth.* **21**, 47–54 (2007).
21. van Zyl, J. M., Smith, J. & Hawtrey, A. The effect of a peptide-containing synthetic lung surfactant on gas exchange and lung mechanics in a rabbit model of surfactant depletion. *Drug Des. Devel. Ther.* **7**, 139–148 (2013).
  22. Bussieres, J. S. Whole-lung lavage. *Thorac. Anesth.* **19**, 543–558 (2001).
  23. Michaud, G., Reddy, C. & Ernst, A. Whole-lung lavage for pulmonary alveolar proteinosis. *Chest* **136**, 1678–1681 (2009).
  24. Sugimoto, C. *et al.* Multidisciplinary assessment of effects, safety and procedure of whole lung lavage for 8 patients with autoimmune pulmonary alveolar proteinosis (Japanese). *Ann. Japanese Respir. Soc.* **49**, 569–576 (2011).
  25. Otsuka, M. *Ketsuekigasū no naze ga wakaru (Japanese)*. (Gakken Medical Shujunsha Co.,Ltd., 2012).
  26. Gajic, O., Frutos-Vivar, F., Esteban, A., Hubmayr, R. D. & Anzueto, A. Ventilator settings as a risk factor for acute respiratory distress syndrome in mechanically ventilated patients. *Intensive Care Med.* **31**, 922–926 (2005).
  27. Huang, C. *et al.* Clinical features of patients infected with 2019 novel coronavirus in Wuhan, China. *Lancet* **S0140-6736**, 1–10 (2020).
  28. Garbino, J. *et al.* Respiratory viruses in bronchoalveolar lavage : a hospital-based cohort study in adults. *Thorax.* **64**, 399–404 (2009).
  29. Yao, X. *et al.* Pathological evidence for residual SARS-CoV-2 in pulmonary tissues of a ready-for-discharge patient. *Cell Res.* 2–4 (2020).
- doi:10.1038/s41422-020-0318-5

## **Chapter 5: Conclusions and Prospects**

### **5.1. Conclusions**

### **5.2. Prospects**

## 5.1. Conclusions

This thesis contains three research topics: 1) Studies on fine bubble (FB) dispersion as an oxygen carrier with a novel oxygen measurement method, 2) Evaluation and improvement of the total liquid ventilation (TLV) system with FB dispersion, and 3) Examination of the efficacy of total alveolar lavage (TAL) with the TLV system on acute lung injury models. Below, I have summarized the findings in each research topic.

### ***1) Studies on FB dispersion as an oxygen carrier with a novel oxygen measurement method***

A novel oxygen content measurement method with a conventional oxygen electrode device to measure the oxygen content in FB dispersion has been developed. The measurement error of this method is within 5% and the measurement range is theoretically 0–320 mg/L, which is six times larger than a high spec dissolve oxygen (DO) meter. Moreover, the results can be obtained within 8 min with four steps. This method requires only a small amount of sample (50–500  $\mu\text{L}$ ), which is also an advantage of this method. In general, titration methods and DO meters are used for measuring oxygen content in liquids. However, there are some issues when using for FB dispersion, and no method is authorized for measuring oxygen content in FB dispersion. This method has the potential to become the standard method to measure oxygen content in FB dispersion.

I evaluated the fundamental properties of FB dispersion as an oxygen carrier by using the novel oxygen measurement method. Few reports mention the property of FB dispersion as an oxygen carrier because there is no standard method to measure the oxygen content in FB dispersion. Thus, this is the first report to comprehensively examine the properties of FB dispersion as an oxygen carrier, although fragments of the phenomenon have already been confirmed by other researchers. I reveal the relationship between oxygen content and ultra FB (UFB) concentration as follows: 1) there is no relationship between UFB concentration and oxygen content in FB dispersion when UFB concentration is within the range of  $10^8$ - $10^9$  particles/mL; 2) apparent UFB concentration

does not change as a result of ambient oxygen level, but UFB disappears in degassed water. It means gas diffusion between the inside and outside of UFB may occur; 3) UFB concentration does not change under the temperature range of 20–40°C for 60 min, but the oxygen content in FB dispersion is temperature-dependent, as in general dissolved oxygen; 4) gas equilibrium at the air-water interface does not affect the stability of UFB concentration but affects the oxygen content in FB dispersion. Moreover, I also found that there is no positive correlation between the oxygen content and the amount of MBs. Under the current FB concentration, the oxygen content in FB dispersions is due to supersaturated dissolved oxygen, and bubbles do not contribute to the oxygen content.

## ***2) Evaluation and improvement of the TLV system with fine bubble dispersion***

Firstly, I evaluated the physiological conditions of the rats in the short-time TLV test. The results show that the rats got severe hypoxemia within 5 min. This means the oxygen content in the FB dispersion is insufficient to supply oxygen demand in rats. However, it is also suggested that the rats can return to mechanical gas ventilation after 5 min of TLV.

Secondly, I examined the feasibility of combining FB and gas liposome (GL) dispersions to increase the oxygen supply capacity during TLV. GL dispersion is known to be able to deliver high oxygen content (50–90 vol%) to the blood by injection. However, the combination dispersion does not improve the oxygen supply because the coalesced GL is clogged inside the lungs and disturbs the liquid ventilation. It is a negative result; however, it is an important finding for using drug combinations in the future.

Thirdly, I improved the TLV system from the viewpoint of the components of the system and expiratory conditions to increase the oxygen supply capacity during TLV. I showed that the tidal volume per minute is improved by changing the components to reduce the pressure loss in the system. Finally, the tidal volume was improved by approximately 19% from the previous TLV system.

### ***3) Examination of the efficacy of TAL with the TLV system in acute lung injury models***

I examined the efficacy of TAL treatment on two injury models with different severity. In the severe lung injury model, TAL treatment washes out causative substances from the lungs, and the degree of inflammation is critically suppressed, whereas the rats in the conventional treatment group get severe lung injury. In lethal lung injury models, TAL treatment prevents rats from severe lung injury, resulting in improving the survival rate from 0% to 80%. Furthermore, rats receiving TAL treatment returned to spontaneous breathing only with 3-h respiratory management, and they became healthy 7 days after treatment. These results show that TAL treatment with the TLV system can cure acute respiratory distress syndrome as a preventive treatment. While the FB dispersion is useful as oxygen supersaturated water to supply oxygen during the TAL treatment, it does not contribute to the improvement of the effect of lung lavage in these models.

## **5.2. Prospects**

### ***1) Development of a new measurement method for the oxygen content in liquids***

This novel measurement method can measure high oxygen content ( $> 50$  mg/L) in a brief time with a small sample volume. High oxygen content in liquids is often required in the biomedical fields, for example, in regenerative medicine and transplantation. A disadvantage of this method is the requirement of nitrogen bubbling; thus, there are limits in the experiment location. Therefore, I would like to develop a portable device to measure high oxygen content by using the same principles that I developed here.

### ***2) Studies on FB dispersion as an oxygen carrier***

The relationship between the concentration of FBs and oxygen content was evaluated, and it was found that UFBs did not contribute to increasing oxygen content at concentrations  $10^8$ – $10^9$  particles/mL. I believe that  $10^{10}$  particles/mL FBs of 1-5  $\mu\text{m}$  are necessary for functional oxygen carriers. Recently, a novel method for generating  $1.92 \times 10^{10}$  particles/mL of 175 nm UFB was reported<sup>1</sup>. When converted to the oxygen

content, the amount of oxygen, which is 1.34 mg/mL, is still low. However, if the particle size can be increased to 1000 nm, the oxygen content inside the UFBs will increase to 55 mg/L, and the total oxygen content in the dispersion will be > 90 mg/L, including the DO. The target value of oxygen-enriched water for total liquid ventilation (TLV) is 100–150 mg/L, and it may not be impossible to achieve this with a FB dispersion. Hence, there are two approaches to prepare the oxygen-enriched water for TLV. The first approach is to develop a device that generates more than  $1.0 \times 10^{10}$  particles/mL UFB of about 1  $\mu\text{m}$  (< 5  $\mu\text{m}$ ). The second approach is the development of a pressure container that can reduce the pressure while minimizing the disappearance of oxygen as bubble. In addition, there is little knowledge about oxygen diffusion from UFBs. First, it is necessary to establish the method to confirm whether the enclosed oxygen in UFBs diffuses to the dispersion medium. Furthermore, the effects of temperature, oxygen partial pressure difference, and salt concentration on diffusion will be examined.

### ***3) Evaluation and improvement of the TLV system with FB dispersion***

Although eight years have passed since the TLV research with the FB dispersion started, the deficiency of oxygen supply has not yet been resolved. The experiments in Chapter 2 suggests that most of the oxygen in the FB dispersion is in the dissolved state. Thus, it is speculated that the oxygen supply during TLV is caused by the difference in partial oxygen pressure between the FB dispersion and blood. There are two approaches to overcome the deficiency of oxygen supply; to develop a method of generating large amounts of FBs whose size is less than 5 $\mu\text{m}$ , or to develop a system for supplying supersaturated water to the lungs without using FBs. Recently, I found an interesting phenomenon that supersaturated water maintains a high oxygen state even at atmospheric pressure unless there is physical stimulation. Currently, I have constructed a new TLV system based on the findings, and I obtained data suggesting the physical condition of rats during TLV improved in the preliminary experiment. If a material which satisfies the oxygen demand of rats is developed, it would be useful for larger animals, including

humans. In addition, the material is expected to be applied not only to other medical applications, but also biological and chemical applications.

#### ***4) Examine the efficacy of TAL with the TLV system***

It was found that inflammatory substances inside the lungs could be removed by washing for only 5 min by using the TLV system. However, I have not confirmed the effect on the progress symptoms. Therefore, I would like to confirm whether the TAL treatment can be performed safely and effectively after developing acute respiratory distress syndrome (ARDS). ARDS is classified into three phases: acute (first 1–6 days), subacute (next 7–14 days), and chronic (after 14 days)<sup>2</sup>. The effects of TAL are expected in the acute and subacute periods, which are reversible states. Meanwhile, reversal is difficult in the chronic phase because fibrosis has already begun. Furthermore, since advantages of TLV are limited to lung lavage, oxygen supply to alveolar, and re-expansion of collapsed alveolar, it is not considered effective for hypoxemia associated with abnormal pulmonary circulation. Furthermore, it is not expected to directly improve multiple organ failures and cardiac disorders associated with the progression of ARDS. Thus, for clinical use, target symptoms of TLV should be specified, and combination with other therapies is important.

In this study, I could not show the advantages of the FB dispersion in the washing effect. However, it is expected that a high washing effect with FB dispersion can be obtained in cases of removing sticky substances such as sputum from the lungs. Fig. 5.1 shows the hypothesis of the mechanisms of the cleaning effect of ultrafine bubbles (UFB)<sup>3</sup>. UFBs enter the gap between the substances, and the collision of UFBs causes coalescence. Adhering bubbles gradually lift the substance, and finally, remove it from the solid surface. Referring to the theory, the TAL with FB dispersion may be more effective in models that require removal of strong adhesive substances such as sticky sputum.

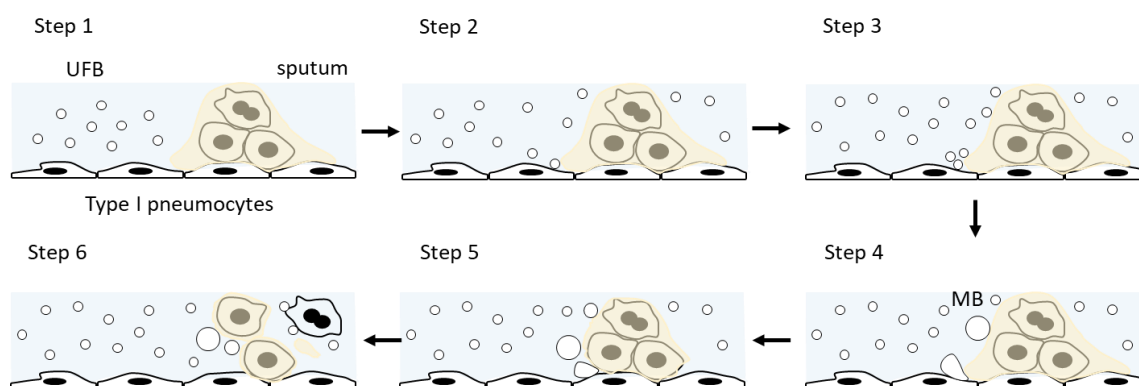


**Fig. 5.1 Hypothesis of a cleaning mechanism with fine bubbles<sup>3</sup>**

The TAL treatment is expected to remove pathogens, such as viruses and bacteria. Therefore, I will expand the target primary disease and evaluate the efficacy of TAL treatment. By only focusing on lung lavage, we can apply the TAL treatment with the TLV system in combination with extracorporeal membrane oxygenation (ECMO). Since ECMO is employed for suitable patients removing the causative substances of inflammation is valuable. Technical issues and the burden of the patient and medical staffs are concerns when operating both TLV and ECMO systems for a patient with severe respiratory disease. However, recently, whole-lung lavage with ECMO was performed on a patient with severe hypoxemic respiratory failure, which revealed benefit<sup>4</sup>.

Since the TAL efficacy was assessed in an animal model, the results may not be generalizable to humans. However, the effect of physically removing pathogens may not change when applying to different animal species. In the future, the TAL treatment will be performed in larger animals and humans. Since the structures of lungs are totally different among species, ventilation conditions will be the primary consideration for adaptation. Since this is a study on hydromechanics, it is expected that fluid simulation will be useful. Meanwhile, rodents are the most difficult animals, from the viewpoint of oxygen consumption; oxygen consumption while sleeping in rats and humans are 12–15 (mL/min/kg)<sup>5</sup> and 3.21 (mL/min/kg)<sup>6</sup>, respectively. If I can construct a TLV system that can supply sufficient oxygen to rats, I can proceed to further studies with optimism. For application to humans, first, the tidal volume is calculated from the bodyweight of the

patient. Thereafter, the adjustments can be performed according to the peak inspiratory pressure (PIP) and oxygen saturation level during TLV operation. Because PIP cannot be increased from the perspective of safety, adjusting the operation mainly by the respiratory time (inspiratory time and expiratory time) is considered.

Recently, a TLV system with perfluorocarbon liquids (PFCs) was developed, and an experiment with monkeys and large pigs was conducted. However, it is hard to use in the medical field because of “cost” and “environmental problems.” Some researchers claimed issues in their reports<sup>7,8</sup>. If TLV is performed on a 60 kg adult human with 10 mL/kg PFCs, it would cost 1.1 million yen, despite only filling the lungs with PFCs once, without considering the capacity of the external TLV system and any other loss. It is not financially practical to perform TLV using such materials.

In developing medical engineering, I emphasize that it is important that the technology can be used at medical sites around the world, not only in developed countries. Therefore, I focus on a modest device with inexpensive and safe materials.

## References

1. Jin, J., Feng, Z., Yang, F. & Gu, N. Bulk Nanobubbles Fabricated by Repeated Compression of Microbubbles. *Langmuir* **35**, 4238–4245 (2019).
2. Matthay, M. A. & Zemans, R. L. The Acute Respiratory Distress Syndrome: Pathogenesis and Treatment. *Annu Rev Pathol.* **28**, 147–163 (2011).
3. Hata, T. *et al.* Research on Cleaning and Purification Using Fine Bubbles (Japanese). *Japanese J. Multiph. Flow* **32**, 4–11 (2018).
4. Moreira, joao P. *et al.* Whole-lung lavage for severe pulmonary alveolar proteinosis assisted by veno-venous extracorporeal membrane oxygenation : a case report. *Can J Respir Ther.* **55**, 9–12 (2019).
5. SHEPHERD, R. E. & GOLLNICK, P. D. Oxygen Uptake of Rats at Different Work Intensities. *Pflugers Arch* **362**, 219–222 (1976).
6. Tanaka, Y. standard knowledge for management of safety anesthesia (Japanese). *J. Kyoto Prefect. Univ. Med.* **119**, 313–338 (2010).
7. Shine, K. P. *et al.* Perfluorodecalin : global warming potential and first detection in the atmosphere. *Atmos. Environ.* **39**, 1759–1763 (2005).
8. Dunster, K. R. & Davies, M. W. A novel expiratory circuit for recovery of perfluorocarbon liquid during partial liquid ventilation. *Intensive Care Med.* **30**, 514–516 (2004).

## *Academic achievement*

### **(List of publications)**

- (1) Kenta Kakiuchi, Takehiro Miyasaka, Shinji Takeoka, Kenichi Matsuda, Norikazu Harii. “Total alveolar lavage with oxygen fine bubble dispersion directly improves Lipopolysaccharide-induced acute respiratory distress syndrome of rats”, *Scientific Reports*, 10, Article number 16597 (2020)
- (2) Tomohisa Ichiba, Kenta Kakiuchi, Masahiro Suzuki, and Makoto Uchiyama. “Warm Steam Inhalation before Bedtime Improved Sleep Quality in Adult Men”, *Evid. Based Complementary Altern. Med.*, Article number 2453483 (2019).
- (3) Kenta Kakiuchi, Kenichi Matsuda, Norikazu Harii, Keitaro Sou, Junko Aoki and Shinji Takeoka. “Establishment of total liquid ventilation using oxygen micro/nano bubble dispersion in rats”, *Journal of Artificial Organs*, 18(3), 220-227 (2015).

### **(International conference and symposium: poster presentations)**

- (1) Kenta Kakiuchi, Norikazu Harii, Takehiro Miyasaka, Shinji Takeoka, Kenichi Matsuda. “Total liquid ventilation with oxygen fine bubbles for acute lung injury”, The 17th International Symposium on Blood Substitutes and Oxygen Therapeutics, 2019.11
- (2) Kenta Kakiuchi, Norikazu Harii, Takehiro Miyasaka, Shinji Takeoka, Kenichi Matsuda. “Total Liquid Ventilation with Oxygen Fine Bubble Dispersion Prevents from Acute Lung Injury in Rats”, 8th Meeting of the International Federation for Artificial Organs, 2019.11
- (3) Kenta Kakiuchi, Shinji Takeoka, Norikazu Harii, Takehiro Miyasaka, Kenichi Matsuda. “TOTAL LIQUID VENTILATION WITH OXYGEN MICRO/NANO BUBBLE DISPERSED SALINE PREVENTS FROM LIPOPOLYSACCHARIDE-INDUCED ACUTE LUNG INJURY IN RATS”, 46th European Society for Artificial Organs, 2019.9

**(Domestic conference: oral presentations)**

- (1) 垣内健太, 針井則一, 宮坂武寛, 武岡真司 “酸素ファインバブル分散液を用いた完全液体換気技術の開発”, 第 24 回 酸素ダイナミクス研究会, 2020.10
- (2) 垣内健太, 松田兼一, 針井則一, 宮坂武寛, 武岡真司 “酸素マイクロ・ナノバブル分散酸素富化液を用いた完全液体換気法の確立”, 第 2 回稲門医学会, 2019.02
- (3) 垣内健太, 青木順子, 針井則一, 松田兼一, 武岡真司 “酸素マイクロ・ナノバブル分散液を用いた完全液体換気への応用”, 第 21 回日本血液代替物学会年次大会, 2014.12
- (4) 垣内健太, 青木順子, 針井則一, 松田兼一, 武岡真司 “マイクロ・ナノバブル分散酸素富化液を用いた液体換気への応用”, 第 20 回日本血液代替物学会年次大会, 2013.11

**(Domestic conference: poster presentations)**

- (1) 垣内健太, 青木順子, 松田兼一, 針井則一, 宗慶太郎, 武岡真司 “酸素マイクロ・ナノバブル分散酸素富化液を用いた完全液体換気への応用”, 第 52 回日本人工臓器学会大会, 2014.10,
- (2) 垣内健太, 青木順子, 針井則一, 松田兼一, 武岡真司 “マイクロ・ナノバブル分散酸素富化液を用いた液体換気への応用”, 第 35 回日本バイオマテリアル学会大会, 2013.12

**(Prizes)**

- (1) Young researcher abstract award, The 17th International Symposium on Blood Substitutes and Oxygen Therapeutics, 2019.11
- (2) 優秀賞, 2018 年度アーリーボードプログラム, 2019.3
- (3) 優秀演題賞, 第 2 回稲門医学会, 2019.2
- (4) 萌芽研究ポスター発表優秀賞, 第 52 回日本人工臓器学会大会, 2015.6

**(Column)**

- (1) 武岡真司, 垣内健太 “TWIns -医学・理学・工学の融合拠点として-”, 人工臓器, 49(1), 66-67 (2020).

**(Award report)**

- (1) 垣内健太, 青木順子, 松田兼一, 針井則一, 宗慶太郎, 武岡真司 “酸素マイクロ・ナノバブル分散酸素富化液を用いた完全液体換気への応用”, 日本人工臓器, 44(1), 27 (2015).

## *Acknowledgements*

The presented thesis is the collection of the studies which have been carried out under the direction of Prof. Dr. Shinji Takeoka, Department of Life Science and Medical Bioscience in Waseda University, during 2017–2020. I express the greatest acknowledgement to Prof. Dr. Shinji Takeoka for his valuable suggestions, helpful discussions, and continuous encouragement throughout this work. I also express my sincere gratitude to Prof. Dr. Nobuhito Goda and Prof. Dr. Haruko Takeyama for the efforts as members of the judging committee for the doctoral thesis.

I gratefully acknowledge to Prof. Dr. Kenichi Matsuda for his valuable advices and encouragement. His professional attitude to science and works always inspired me.

I would like to express special thanks to Associate Prof. Dr. Norikazu Harii, Prof. Dr. Takehiro Miyasaka, and Prof. Dr. Nobuyuki Mase for their constructive comments, technical advice, and fruitful discussions through the experiments.

I acknowledge Dr. Tianshu Li and Dr. Keitaro Sou for constructive comments and fruitful discussions.

I express remarkable thanks to Mr. Kon Son, Mr. Tomoki Kozuka, and my colleagues in doctor course: Mr. Sho Mihara, Mr. Masato Takikawa, Mr. Yuma Tetsu, Mr. Morihiro Hotta, and Mr. Hu Runkai for their helpful and valuable advices on experiments.

All members in the Laboratory of Biomolecular-Assembly offered kind assistance for which I would like to thank deeply.

Finally, my deepest appreciation goes to my family, Mr. Yasunobu and Mrs. Junko Kakiuchi, Mrs. Yui and Mr. Daiki Taniguchi, Mrs. Sayuri and Mr. Kenju Wagatsuma, and Ao and Hudson. This assignment would not be possible without their constant encouragement and healing.

February 2021

Kenta KAKIUCHI